TECHNISCHE UNIVERSITÄT MÜNCHEN

Lehrstuhl für Entwicklungsgenetik

Analysis of Tau Phosphorylation in Transgenic ES and iPS Cell-Derived Neurons

Aljoscha Kleinhammer

Vollständiger Abdruck der von der Fakultät Wissenschaftszentrum Weihenstephan für Ernährung, Landnutzung und Umwelt der Technischen Universität München zur Erlangung des akademischen Grades eines

Doktors der Naturwissenschaften

genehmigten Dissertation.

Vorsitzender: Univ.-Prof. Dr.rer.nat Erwin Grill

Prüfer der Dissertation:
1. Univ.-Prof. Dr.rer.nat Wolfgang Wurst
2. Univ.-Prof. Angelika Schnieke, Ph.D. (Univ. of Edinburgh/UK)

Die Dissertation wurde am 10.07.2012 bei der Technischen Universität München eingereicht und durch die Fakultät Wissenschaftszentrum Weihenstephan für Ernährung, Landnutzung und Umwelt am 05.11.2012 angenommen.

Content

1 Abstract

The understanding of neurodegenerative diseases and the development of therapies is at present hampered by the inaccessibility of live neurons from patients and the lack of research models that fully recapitulate the sporadic form of the disease. It might be possible to overcome these issues by using iPSC from patients for the unlimited generation of analyzable neurons. However, in the published studies, not all aspects of the diseases could be fully recapitulated and it is not clear if a late-onset phenotype can be modeled in 'young' iPSC-derived neurons.

In order to analyze if the late-onset phenotype of Tau pathology can be modeled in PSC-derived neurons, I generated iPSC lines from the Tau pathology mouse models 3xTg AD, Tau^{P301S} and hTau (Andorfer *et al.* 2003; Oddo *et al.* 2003; Yoshiyama *et al.* 2007) and derived a transgenic Tau^{P301S}/APP^{Swe}/Venus ESC line. All four PSC lines were used for the generation of neurons according to the Bibel & Barde protocol (Bibel *et al.* 2007). Although the protocol reportedly produces a homogeneous population of fully mature cortical glutamatergic neurons, a detailed analysis revealed surprisingly that the PSC-derived neurons in this work were immature and very heterogeneous regarding their neuronal identities. The four promoter systems proved to be strongly influenced in their activity by the neuronal characteristics and were accordingly differently well suitable for driving transgene overexpression in the PSC-derived neurons. Human MAPT promoter generated strong and Prion promoter mild to weak transgene expression. Thy1.2 promoter was inactive and the CAG promoter was unsuited due to strong positional effects. In the neurons derived from Tau^{P301S} and hTau iPSC no Tau hyperphosphorylation was detectable under standard and oxidative stress conditions and they did not show an increased sensitivity to phosphatase inhibition. Thus, the *in vitro* neurons did not recapitulate the Tau pathology that is observed in their *in vivo* counterparts in the brains of the Tau^{P301S} and hTau mouse models.

In conclusion, I could demonstrate in this work that Tau pathology can be studied in PSC-derived neurons, but the neurons derived from Tau pathology mouse model iPSC differed so much from their *in vivo* counterparts that they did no reproduce the Tau pathology under standard conditions. Thus, this work generated valuable insights about the modeling of neurodegenerative diseases in PSC-derived neurons and which hurdles have to be overcome in future. The findings represent a stepping stone for improving the analysis of neurodegenerative diseases in neurons derived from patients' iPSC and in this way may contribute to the understanding of neurodegenerative diseases and the development of causal therapies.

2 Introduction

2.1 Significance and Challenges of Neurodegenerative Disease Research

Neurodegenerative diseases represent a major burden for society and public health systems and are expected to increase in their significance as mostly elderly people are affected and the society is aging. One of the most important neurodegenerative diseases (NDDs) is Alzheimer's disease which encompasses Tau pathology. Alzheimer's disease was estimated to be affecting 35.6 million people by 2010 and is predicted to affect 115.4 million by 2050 (ADI 2010). These numbers in combination with the unavailability of causal therapies demonstrate the significance of neurodegenerative disease research.

Neurodegenerative diseases are characterized by a progressive loss of neurons with a disease-specific affection of a defined subset of neurons. This results predominantly in dementia and movement disorders as for example Alzheimer's disease (AD), frontotemporal dementia (FTD), Parkinson's disease (PD) and amyotrophic lateral sclerosis (ALS) (Przedborski *et al.* 2003). In contrast to their different clinical symptoms, NDDs share major characteristics on the molecular level. The accumulation of misfolded, disease-specific proteins in insoluble deposits is a hallmark of each NDD (Taylor *et al.* 2002; Haass & Selkoe 2007). Additionally, comparable patterns of disturbed proteostasis, signaling pathways and organelle function are observed (Saxena & Caroni 2011). The fact that the affected proteins and cellular elements are ubiquitously present is contrasted by specific protein deposits and confined neuronal populations for each NDD. This specificity is considered to be the result of an individual combination of selective neuronal vulnerability, genetic predisposition and environmental factors as e.g. nutrition, toxic exposures, stress and physical activity (Mattson & Magnus 2006). Therefore NDDs are described as multifactorial diseases.

In addition to this already complex etiology, there are more characteristics which make neurodegeneration research challenging and explain for our currently limited understanding of NDDs. A major obstacle for the analysis of NDDs is the inaccessibility of live neurons from patients. Postmortem samples already allowed for the identification of key characteristics and pathway alterations for most of the neurodegenerative diseases. But the researcher is mostly confronted with sample tissues that are destroyed by end-stage manifestations of a degenerative process that has been going on for years or decades (Han *et al.* 2011). Needless to say, by

postmortem analysis alone it is difficult or impossible to identify early events that actually cause the disease.

A solution for this problem was found when gene mutations responsible for familial forms of NDDs were identified. In contrast to the sporadic form of a neurodegenerative disease, its familial (or Mendelian) form has a traceable heredity pattern and an earlier age of onset. Because of their phenotypic similarities, the sporadic and the familial form are considered to share pathogenic mechanisms and biochemical pathways (Wichterle & Przedborski 2010). According to this rationale, gene mutations from familial forms of NDDs are used for the generation of transgenic animal models which phenocopy aspects of the human condition. This allows for the observation and manipulation of a NDD causing process as it takes place in an organism and has greatly contributed to the dissection of disease mechanisms. However, the relevance of findings in familial NDD animal models for the sporadic form remains unclear. This is a very important shortcoming as most patients of neurodegenerative diseases suffer from the sporadic form. In fact, successful preclinical treatment of familial NDD animal models has not translated into successful therapies in patients (Han *et al.* 2011). Another aspect that has hampered the identification of causative elements in sporadic forms of neurodegenerative diseases is the complex interaction network between genetic and environmental risk factors. At the moment it seems impossible to fully rebuild these interactions in a model because: First, not all factors or their interactions are known as demonstrated by our inability to fully explain the observed phenomena (Han *et al.* 2011). Second, genetic animal models exist only for a part of the many candidate risk gene variants (e.g. http://www.alzgene.org/, http://www.pdgene.org/) because their construction is laborious and time consuming. Testing multiple combinations of risk gene variants in animal models is of highest interest for the analysis of a multifactorial disease but takes even more time and is therefore not realizable via the classic transgenic animal approach. In addition to these difficulties, it can take more than one year until a clear phenotype is observable in a transgenic mouse model as experiences with familial NDD mutations have shown (McGowan *et al.* 2006; Götz & Ittner 2008).

Taken together, the analysis of neurodegenerative diseases in transgenic animal models with familial mutations has greatly enhanced our understanding of pathologic mechanisms but the thus achieved insights mostly concern *how* and not *why* the disease develops in the human sporadic condition. Consequently, the existing therapies can only alleviate the symptoms but do not counteract the processes that are causative for the disease (Citron 2010; Han *et al.* 2011). For Alzheimer's disease therapies are most urgently needed and as several late-phase clinical trials have failed and important pathogenic mechanisms remain unclear, the research field demands

strongly for research models that better recapitulate the human sporadic condition (Selkoe 2011; Israel *et al.* 2012).

A promising approach for meeting this requirement is the generation of induced pluripotent stem cells (iPSC) from patients with sporadic forms of neurodegenerative diseases and their differentiation into neurons (Han *et al.* 2011). However, it is unclear whether iPSC-derived neurons can be used to study late-onset sporadic forms of neurodegenerative diseases (Israel *et al.* 2012). For elucidation of this situation, in this work I used transgenic mouse iPSC and ESC to analyze if and how the correspondent *in vitro* generated neurons can be used to study the neurodegenerative late-onset symptom Tau pathology. After giving an introduction to Tau pathology and neurodegenerative disease research with *in vitro* generated neurons (sections 2.2 and 2.3), I will describe in detail focus and aims of this project (section 2.4).

2.2 Tau Pathology

The intracellular deposition of Tau protein aggregates in brain neurons is a hallmark of Alzheimer's disease and several other neurodegenerative diseases and is thus one of the most important neurodegenerative pathologies. Tau pathology was chosen as subject of this study due to its significance and because its intracellular phenotype is well suited for analysis in a cell culture model. Tau Protein, also known as MAPT (microtubule-associated protein Tau), is almost exclusively expressed in the central and peripheral nervous system (Buee *et al.* 2000). Alternative mRNA splicing of exons 2, 3 and 10 results in the production of 6 Tau isoforms in humans (Fig. 3.17). The isoforms have two, one or no N-terminal insert (2N, 1N, 0N) and four or three microtubule-binding repeat motifs (3R, 4R) in the C-terminal half (Goedert & Jakes 1990). The smallest isoform (0N/3R) predominates in fetal human brain while all six isoforms are expressed in the adult brain. In fetal rodent brain only the 0N/3R Tau isoform is expressed. In contrast to the human brain in which a mixture of 3R and 4R Tau isoforms is expressed, the adult rodent brain contains only 4R Tau isoforms (0N/4R, 1N/4R, 2N/4R) (Kampers *et al.* 1999). Under normal conditions the majority of Tau protein in the cell is bound to the microtubules. Stabilization of microtubules is the function which has been mostly assigned to Tau, but this view has been questioned in the last years. On the one hand, ablation of Tau has no significant impact on microtubule stability, survival or brain function. On the other hand, Tau interacts with many binding partners including lipids and signaling molecules which suggests various roles (Morris *et al.* 2011).

Under pathological conditions, Tau becomes hyperphosphorylated which means that it is phosphorylated to a higher degree at physiological sites, but also gets

phosphorylated at pathological sites (Götz *et al.* 2010). As a consequence of the altered charge distribution, hyperphosphorylated Tau has a lower affinity to microtubules which increases its cytosolic concentration. In addition, hyperphosphorylation results in a conformation of Tau protein in which the regions with a beta-structure propensity are exposed and can interact (Iqbal *et al.* 2009). High cytosolic Tau concentration and exposure of critical regions both promote the aggregation of Tau protein to PHFs (paired helical filaments) and NFTs (neurofibrillary tangles) which form the insoluble deposits (Mandelkow *et al.* 2007). The ultimate consequence of this process is considered to be synapse loss and neuronal cell death (Spires-Jones *et al.* 2009) but how Tau toxicity is exerted is a matter of debate. Because of the association with pathological processes, Tau hyperphosphorylation is regarded as early-stage indicator and Tau deposition as advanced-stage indicator of Tau pathology (Brandt *et al.* 2005). In contrast to the end-stage of Tau pathology which is described in great detail, the knowledge about causative events in the beginning of the process is far less substantiated. The pathologic condition of hyperphosphorylated Tau is definitively caused by an imbalance in the activities of Tau kinases and phosphatases (Ballatore *et al.* 2007), but upstream events causing this imbalance in different disease conditions remain elusive. Discussed upstream factors of Tau pathology are for example oxidative stress, beta-amyloid and inflammation (Ballatore *et al.* 2007). Another hypothesis proposes a yet unknown toxic function for Tau which causes hyperphosphorylation of Tau to decrease its interaction with non-microtubuli binding partners (Morris *et al.* 2011).

The upstream factor of Tau pathology that is probably best analyzed and understood is the factor of Tau gene mutations that were identified in familial forms of neurodegenerative diseases with Tau pathology (e.g. FTDP-17, frontotemporal dementia and parkinsonism linked to chromosome 17) (Götz *et al.* 2007). Several of the transgenic animal models that overexpress Tau with familial mutations recapitulate Tau hyperphosphorylation and Tau deposition. Some of the Tau versions (e.g. P301L) promote Tau pathology because they become faster hyperphosphorylated, have a higher propensity for aggregation and self-aggregate to filaments at a lower phosphorylation stoichiometry compared to wild type Tau (Alonso *et al.* 2004; Iqbal *et al.* 2009). On the one hand, these characteristics can be regarded as an advantage for the analysis of Tau pathology upstream factors based on the assumption, that the same factors cause Tau pathology in the mutant and in the wild type condition. This implies that in both the familial and the sporadic form of the disease Tau pathology is caused by the same pathway alterations but their critical threshold values are lower in the case of Tau with familial mutations due to its higher susceptibility. On the other

hand, the relevance of models overexpressing familial Tau mutations for understanding the sporadic forms of Tau pathology has been questioned. Overexpressing Tau could result in Tau hyperphosphorylation that is due to the effort of the neuron to remove excess Tau from the microtubules where it blocks transport (Baas & Qiang 2005). The increase of cytosolic Tau concentration, resulting from its up to 8 fold overexpression, facilitates Tau aggregation (Mandelkow *et al.* 2007). Recent findings further support the idea that overexpressing familial Tau mutations results in a 'fast forward' course to Tau pathology. Thereby sporadic disease relevant mechanisms and therapeutic opportunities might be overridden (Morris *et al.* 2011).

In general for neurodegenerative diseases (section 2.1) and in particular for Tau pathology as exemplified in this section, it is an unresolved issue how relevant transgenic animal models with familial mutations are for understanding the human sporadic form of the disease. In the case of Tau pathology the use of such familial models has allowed for unraveling in detail the molecular mechanisms by which the highly soluble Tau protein becomes hyperphosphorylated and forms insoluble aggregates. However, the identification of causative factors as well as the development of disease-modifying therapies has so far not been successful. This is possibly due to discrepancies between familial animal models and the sporadic human condition (Morris *et al.* 2011). How the analysis of Tau pathology in transgenic mouse iPSC- and ESC-derived neurons can contribute to overcome this problem is part of this work and conceptualized in section 2.4.

2.3 Neuronal Differentiation of Pluripotent Stem Cells as a Tool for Neurodegenerative Disease Research

ESC and induced iPSC (together termed PSC or pluripotent stem cells) are characterized by their unlimited self-renewal and the capacity to give rise to all cell types of the organism including neurons. *In vivo*, the development from an ES cell in the embryonic blastocyst stage to a neuron in the adult brain passes through various stages and is the result of an interplay between the genetic developmental program and inputs from extrinsic factors (Gaulden & Reiter 2008). The *in vitro* generation of neurons from ESC and iPSC is based on a selective recapitulation of the *in vivo* process by controlled culture conditions. Most of the protocols accomplish this by using either an embryoid body-based or a monolayer-based approach (Germain *et al.* 2010). As in this work the embryoid body-based protocol as published by Bibel & Barde (Bibel *et al.* 2007) and the monolayer-based protocol as published by Gaspard & Vanderhaeghen (Gaspard *et al.* 2009) were used, these protocols are presented for exemplifying the two general differentiation principles. Both strategies allow for

directing the aquisition of different neuronal identities, but the presented examples focus on cortical glutamatergic neurons.

The embryoid body-based approach mimics conditions of the embryo that produce neurectoderm by appropriate cell-cell interactions and signals. Embryoid bodies (EBs) are formed when PSC are cultured in suspension and under conditions allowing for differentiation. Within 2-4 days the aggregates consist of an outer layer of hypoblast-like cells (extra-embryonic endoderm) and a core of epiblast-like cells with the potential to generate cells of all three germ layers (ecto-, endo- and mesoderm) (Cai & Grabel 2007). At this stage, the EB core cells can be directed toward neurectoderm by neural induction conditions (Gaulden & Reiter 2008). Retinoic acid strongly induces neural differentiation *in vitro* despite the fact that in embryonic development its reported role is restricted to neural tube patterning (Glaser & Brüstle 2005). Induction in EBs with retinoic acid resulted in up to 90% neuronal progenitors which have been characterized as Pax6-positive-radial glia cells giving rise to cortical glutamatergic neurons. The thus generated neuronal progenitors are plated as single cells which induces the transition to terminal differentiation and to the postmitotic state (Bibel *et al.* 2004; Bibel *et al.* 2007). The monolayer-based approach takes advantages of the 'default pathway' of neural differentiation. When deprived of extrinsic signals and cell-cell interactions, PSC differentiate into neural progenitors due to induction of the default pathway. What *in vivo* is the result of the inhibition of non-neural inducers is achieved *in vitro* by culturing the PSC at low density in serum-free medium (Cai & Grabel 2007). The cells recapitulate stages of neural development until they reach the state of neural progenitors. The default neural identity is the forebrain identity, but as the cells can produce the ventralizing morphogen sonic hedgehog (shh) the usage of shh-inhibitor cyclopamine is necessary for the generation of cortical (dorsal forebrain) progenitors. The progenitors differentiate into cortical glutamatergic neurons after being replated as single cells (Gaspard *et al.* 2009).

The high efficiency of the *in vitro* generation of neurons as described above allows for two basic principles how PSC can be used for the modeling of neurodegenerative diseases: First, genetically modified ESC (e.g. transgenic for a familial Tau mutation) and second, iPSC from neurodegenerative disease patients can be differentiated into neurons which are analyzed for the relevant phenotype.

Both principles open novel promising possibilities to fill the research gaps that have been elaborated on in section 2.1. Neuronal *in vitro* differentiation of PSC represents a very fast method to obtain live neurons which are genetically modified, because after their genetic modification PSC are directly differentiated into neurons. Classical approaches are laborious and time consuming as for example the generation

of genetically modified mouse primary neurons can take years as it requires production of chimeric mice and further matings. In contrast, as the *in vitro* differentiation from PSC to neurons takes several weeks, it takes only few months from genetic modification of PSC to phenotype analysis in PSC-derived neurons. At the moment many candidate risk gene variants of neurodegenerative diseases remain non-validated by classic genetic models due to their costly construction, but the situation could possibly be changed by analyzing the effect of the risk variants in PSC-derived neurons. This approach even allows for testing various combinations of several risk gene variants which is unthinkable for the classic transgenic mouse approach. As elucidated in section 2.1, this is of highest relevancy for the analysis of neurodegenerative diseases due to their multifactorial etiology.

The analysis of neurodegenerative diseases based on familial models is limiting our understanding of the sporadic disease forms. This problem may possibly be overcome by generating iPSC from patients with manifestations of sporadic neurodegenerative diseases and differentiating these iPSC into neurons (Israel *et al.* 2012). As these neurons have exactly the same genetic predisposition as the donor, they provide the unique possibility to analyze live neurons in the context of the sporadic disease form. The hope is to generate a 'brain in the dish' that recapitulates analyzable pathological processes as they take place in the patient's brain where their analysis is very limited. Analysis and manipulation of pathological processes in a sporadic context as they take place and not decades after they started, might open the way to the identification of causative pathological events and related causative therapeutic interventions. In addition, this approach could be used for personal risk prediction to develop a NDD by using iPSC from symptom-free individuals for neuronal differentiation. The analysis of susceptibility to environmental factors (e.g. oxidative stress, high sugar diet) of those iPSC-derived neurons might further help to identify personalized critical environmental factors and preventive strategies. Further, this approach could allow for identification of novel biomarkers and so far unknown genetic influences. Understanding the complex influence of genetic risk factors might be facilitated by the correction or generation of risk gene variants in patient derived iPSC via site-directed mutagenesis.

Since the iPSC technology has been established only few years ago by Takahashis and Yamanakas seminal publication (Takahashi & Yamanaka 2006) and the efficient production of a homogeneous population of ESC-derived neurons has reached a satisfactory degree only in the last years (Bibel *et al.* 2004; Chambers *et al.* 2009; Gaspard *et al.* 2009), the potential of using these systems for the modeling of neurodegenerative diseases has not yet been fully explored. Although several studies

have made a proof of principle by showing that it is possible to study aspects of disease-specific phenotypes in PSC-derived neurons, many concerns and unresolved questions remain how representative these systems really are for the human diseases (Dolmetsch & Geschwind 2011). For example PD iPSC-derived neurons were more sensitive to oxidative stress (Nguyen *et al.* 2011) and AD iPSC-derived neurons showed an amyloid-beta production typical for AD (Israel *et al.* 2012) but no protein deposits typically associated with the diseases were reported.

To elucidate to what degree it is possible to recapitulate the late-onset phenotypes from neurodegenerative diseases in PSC-derived neurons and how relevant the gained insights are for understanding and treating the human diseases, many issues still need to be addressed (Ming *et al.* 2011). One major point is our ignorance concerning how much the PSC-derived neurons resemble the neurons in the brain that develop pathological symptoms, raising the following questions: Is the degree of maturation of a PSC-derived neuronal culture comparable to the one of an adult brain? In the brain, symptoms of neurodegenerative diseases typically become apparent after the sixth decade of life. As aging is the major risk factor for neurodegenerative diseases (Cohen & Dillin 2008), how does the aging status of PCS-derived neurons after 3 weeks in culture compare to neurons in a brain that has aged for decades? Which aging parameters should be analyzed to answer this question and is the aging status of a neuron crucial for the full development of pathology? Does the age of the donor individual for the generation of the iPSC have an impact on the aging status of the derived neurons? As in each neurodegenerative disease primarily one particular neuronal population is selectively affected, is it crucial to generate a homogeneous neuronal *in vitro* culture of the correspondent population? The etiology of many neurodegenerative diseases is considered to involve non-cell-autonomous effects, how can these effects be studied if only neurons and maybe only one neuronal subtype are generated? As epigenetic effects may contribute to neurodegeneration (Marques *et al.* 2011), does the reprogramming process create a discrepancy between the epigenetic profiles of iPSC-derived neurons and neurons in the brain? In addition to these biological considerations, there is a technical aspect which is relevant for disease modeling in PSC-derived neurons and, to my best knowledge, has not been analyzed in depth: which promoter systems are suited for the expression of transgenes in PSC-derived neurons? This is a crucial point e.g. for the analysis of risk gene variants in PSC-derived neurons.

The number and diversity of these uncertainties demonstrate how limited our knowledge about the validity and feasibility of neurological disease modeling with PSC-derived neurons currently is. In this work, I used transgenic iPSC- and ESC-derived

neurons for the establishment of a novel research model for gaining insights into the aspects mentioned above as described in detail in the following section.

2.4 Concept and Objective of This Thesis

The objective of this thesis was the analysis of Tau pathology in neurons derived from transgenic mouse ESC and iPSC (**Fig. 2.1**) to gain insights if a late-onset neurodegenerative symptom as Tau pathology can be modeled in PSC-derived neurons. To that end, ESC and iPSC were derived from existing familial Tau pathology mouse models that differed in the used transgenes and promoter systems: The 3xTg AD model (Oddo *et al.* 2003) expresses transgenic human Tau^{P301L} and APP^{swe} driven by Thy1.2 promoter and harbors a $PS1^{M146V}$ knock-in which enables for the analysis of Tau pathology in an Alzheimer's disease-like context. In the Tau^{P301S} model (Yoshiyama *et al.* 2007), prion-promoter drives expression of transgenic human Tau^{P301L} and in the hTau model (Andorfer *et al.* 2003), human MAPT promoter drives expression of all 6 human Tau isoforms while mouse Tau expression is completely ablated by knockout. All 3 mouse models develop robust Tau pathology in the brain after 6-9 month. Additionally, ESC lines were generated that provided CAG-driven expression of human Tau^{P301L} and APP^{swe}. These gene variants were used because they provide an AD-like context because Tau pathology, promoted here by the Tau^{P301L} mutation, can be aggravated by the APP^{swe} mutation as shown in transgenic mouse models (McGowan *et al.* 2006).

The generated transgenic iPSC and ESC (**Fig. 2.1**) lines were differentiated into neurons which were analyzed for their degree of maturation, neuronal subtype specification and expression of transgenic Tau. Suitable neuronal cultures were treated with oxidative stress or phosphatase inhibitor and then analyzed for Tau pathology. These analyses were driven by different motivations:

In total, the activities of 4 different promoter systems (Thy1.2-, prion-, hMAPT-, CAG-promoter) in PSC-derived neurons were compared. The activity pattern of these promoters is influenced by developmental stage and cell type and is well known from *in vivo* studies, but is not well characterized for PSC-derived neurons. By correlating maturation and regionalization with transgene expression level, I aimed for the identification of suitable promoter systems for *in vitro* generated neuronal cultures. This is an important prerequisite for using PSC-derived neurons as a tool that can be fast genetically modified and thus for example enables testing the effect of various combinations of NDD risk gene variants.

Two neuronal differentiation protocols were used that according to the publications (Bibel *et al.* 2007; Gaspard *et al.* 2009) generate populations of mainly fully mature

glutamatergic cortical neurons, hence the population which is most relevant in Tau pathology. In order to control the generated neuronal population, I analyzed their degree of maturation and their regional identity. This allowed for assessing how much the *in vitro* generated neurons resembled neurons in the adult mouse brain.

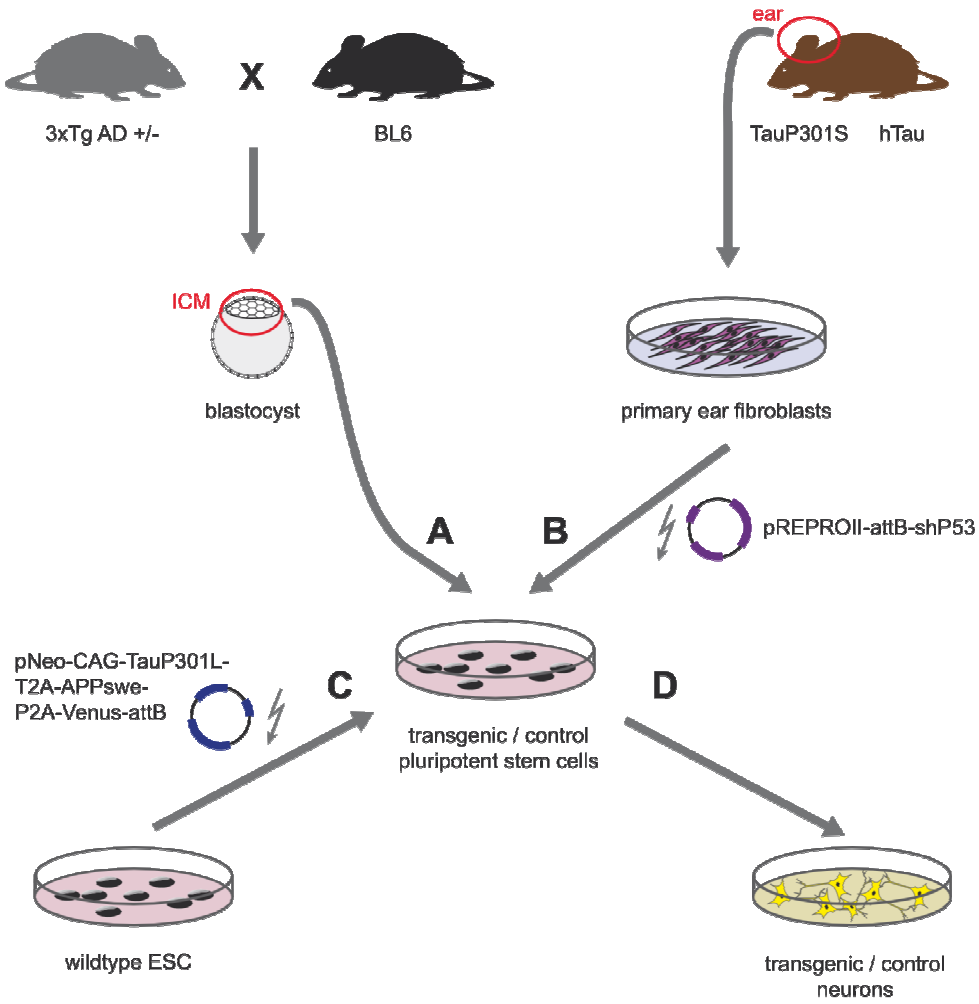

Fig. 2.1: Workflow for derivation of ESC and iPSC from transgenic Tau pathology mouse models and subsequent generation of neurons
(**A**) 3xTg AD heterozygous (+/-) mice were crossed with BL6 mice for the generation of blastocycsts. ESC lines were derived from the inner cell mass (ICM) of the blastocysts. (**B**) Adult ear fibroblast cultures were established from Tau^{P301L} and hTau mice and reprogrammed to iPSC lines by transfection with the vector pReproII-attB-shP53. (**C**) Wild type ESC were transfected with the vector pNeo-CAG-Tau^{P301L}-T2A-APP^{swe}-P2A-Venus-attB in order to generate ESC lines that expressed the Tau pathology-relevant transgenes Tau^{P301L} and APP^{swe}. (**D**) Transgenic ESC and iPSC harboring Tau pathology-relevant mutations and control lines were differentiated into neurons. The resulting transgenic neurons were analyzed for transgenic Tau expression and Tau pathology.

The transgenic PSC-derived neurons were analyzed for Tau pathology in order to elucidate, if it is possible to recapitulate a late-onset phenotype in young neurons which is currently not known and of highest relevancy for studies with iPSC from NDD patients. In the used mouse models, brain neurons exhibit Tau pathology after 6-9 month. By analyzing if standard *in vitro* conditions could elicit Tau pathology in the correspondent transgenic neurons, I aimed to gain insight into this question.

In order to examine if the transgenic PSC-derived neurons had an increased susceptibility to oxidative stress or decreased phosphatase activity I analyzed the influence of the correspondent treatments on Tau pathology. Oxidative stress is associated with aging and decreased phosphatase activity is known to influence Tau pathology. Hence, I aimed to analyze, if the treatments could recapitulate *in vitro* aspects of aging and neurodegeneration, if these treatments could elicit or aggravate Tau pathology, and if the mutant neurons were more vulnerable than the wild type neurons.

In summary, in this project I aimed for the establishment of a novel model system for the analysis of Tau pathology which allows for fast genetic manipulation and the convenient analysis of environmental factor effects as oxidative stress. The iPSC approach based on existing transgenic mouse models is unique in offering the possibility to compare iPSC-derived neurons with neurons in the correspondent mouse brain for every stage of Tau pathology. This is a unique feature of this approach and contrasts studies with iPSC of neurodegenerative disease patients in which the *in vitro* neurons can only compared to post-mortem tissue. This limitation obviously complicates the validation of results from human iPSC studies and can possibly be overcome by the presented approach. The overall objective of this work was to gain insights how late-onset diseases can be modeled in PSC-derived neurons and thus to contribute to the understanding of and the therapeutic development for neurodegenerative diseases which is urgently required by our aging society.

3 Results

3.1 Neuronal Differentiation of Heterozygous 3xTg AD ESC

3.1.1 Generation of Heterozygous 3xTg AD ESC Lines

For the differentiation of 3xTg AD ESC lines into neurons, these ESC lines had to be established *de novo*, as the 3xTg AD mice were generated by pronuclear injection (Oddo *et al.* 2003). Murine embryonic stem cell lines can be generated from the blastocyst stage of early embryonic development. As the inner cell mass (ICM) of a blastocyst consists of some hundred embryonic stem cells, these cells can be cultured by taking advantage of their unlimited proliferation potential under conditions that maintain their pluripotency starting from one single blastocyst. The matings for the production of 3xTg AD blastocysts, were set up between heterozygous 3xTg AD males and BL6 females (**Fig. 2.1**). Matings resulting in higher gene transmission frequencies were impossible as no 3xTg AD females or homozygous 3xTg AD were at the disposal at the moment of the matings. As in the 3xTg AD mouse the transgenes APP^{swe} and Tau^{P301L} are integrated at the same locus and are therefore co-inherited (Oddo *et al.* 2003), the expected frequency of the heterozygous 3xTg AD genotype ($PS1^{M146V}$/APP^{swe}/Tau^{P301L}) was 25% among the generated blastocysts and thus among the derived ESC lines. Because the neuronal differentiation potential varies between ESC lines (section 4.2), I decided to generate at least 5 ESC lines with the correct genotype which meant to generate at least 20 ESC lines in the context of the het-WT matings. In the matings for the production of 3xTg AD blastocysts, each heterozygous 3xTg AD male was mated to 2 superovulated BL6 females. In total, 3 such matings were set up. From the 6 females 68 blastocysts were obtained from which 33 ESC lines could be established. Genotyping by PCR (primers huAPP-1/2 and PS1-K13/K15) revealed that 7 from 33 lines or 21% had the intended heterozygous 3xTg AD genotype $PS1^{M146V}$/APP^{swe}/Tau^{P301L} (**Fig. 3.1**). These lines were further used for neuronal differentiation.

A

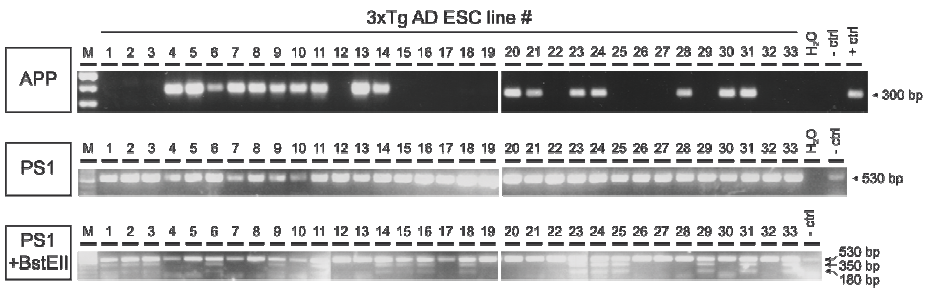

B

3xTg AD ESC clone	APP / Tau	PS1	3xTg AD ESC clone	APP / Tau	PS1	3xTg AD ESC clone	APP / Tau	PS1
1	-	+	12	-	-	23	+	+
2	-	+	13	+	-	24	+	+
3	-	+	14	+	+	25	-	+
4	+	-	15	-	+	26	-	-
5	+	-	16	-	+	27	-	-
6	+	+	17	-	-	28	+	-
7	+	-	18	-	+	29	-	+
8	+	-	19	-	-	30	+	-
9	+	+	20	+	-	31	+	+
10	+	-	21	+	-	32	-	-
11	+	+	22	-	-	33	-	+

Fig. 3.1: Genotyping of heterozygous 3xTg AD ES cell lines by PCR
(**A**) The generated ES cell lines were tested by PCR for the transgenes $hAPP^{swe}$ ('APP') and $hTau^{P301L}$. As these 2 transgenes are co-inherited, APP positive samples were considered to be positive for $hTau^{P301L}$ as well. The $PS1^{M146V}$ knock-in allele can be distinguished from the wild type allele by BstEII digestion of a 530 bp PCR product ('PS1'). The mutant amplicon is digested to fragments of 350 bp and 180 bp whereas the wild type amplicon does not contain a BstEII restriction site ('PS1+BstEII'). 7 of the 33 analyzed ES cell lines were tested positive for both $hAPP^{swe}$ and $PS1^{M146}$ and were therefore considered to be heterozygous for the 3xTg AD condition. (**B**) Summary of PCR results from (**A**)

3.1.2 Neuronal Differentiation of Heterozygous 3xTg AD ESC

3.1.2.1 *Selection of Neuronal Differentiation Protocols and Pluripotency of the ESC*

For the neuronal differentiation of heterozygous 3xTg AD ESC two of the many existing protocols were selected, taking the following considerations into account. In the 3xTg AD mouse model the Thy1.2 promoter drives expression of transgenic APP^{swe}/Tau^{P301L} mainly in adult cortex and hippocampus (Oddo *et al.* 2003). Additionally, these two are the most relevant regions for modeling Alzheimer's disease as these regions are the most affected in the pathology in the human brain. These facts demanded for the generation of neurons corresponding as much as possible to the regions of cortex and hippocampus. Ideally, the neurons would do so both in terms of regionalization as in terms of transmitter type, which is glutamatergic for most of the cortical and hippocampal neurons (Molyneaux *et al.* 2007). As mentioned earlier, this work focuses on Tau pathology whose comprehensive functional analysis requires a considerable amount of material, because it includes western blot based phosphorylation analysis and sample fractioning into soluble and insoluble Tau. Therefore an adequate neuronal

differentiation protocol should allow for the generation of a sufficient number of cells (10^6-10^7) with an acceptable investment of time and effort.

Finally, the capacity of ESC for neuronal differentiation can vary between different genetic backgrounds and even between clones while causative factors of this phenomenon remain elusive. Hence, I decided to confront this indeterminate variation by a variation in the method of neuronal differentiation. Mutually exclusive strategies for the generation of neuronal progenitors are monolayer protocols vs. embryoid body protocols and neuronal induction vs. neuronal selection. The selected protocols should therefore vary in these aspects as a possible inherent incapacity of an ESC line might be impairing in one strategy but circumvented by the other strategy.

Taken together, these considerations resulted in the selection of two different protocols, the ”Bibel & Barde protocol” (Bibel *et al.* 2004; Bibel *et al.* 2007) and the “Gaspard and Vanderhaeghen protocol” (Gaspard *et al.* 2009). According to the corresponding publications, both protocols yield high numbers of cortical glutamatergic neurons. The protocols vary in their strategies to generate neuronal progenitors as the Bibel & Barde protocol is based on embryoid bodies and neuronal induction while the Gaspard and Vanderhaeghen protocol is based on monolayer and neuronal selection. As these two protocols fulfilled the described criteria, 3xTg AD ESC lines were submitted to both protocols for neuronal differentiation.

Before neuronal differentiation, the 3xTg AD ESC lines were checked for some criteria which serve as indicators of pluripotency. For an ideal ESC (or iPSC) line, these criteria are: When cultured on feeders, the majority of colonies should be oval to spindle-shaped with straight edges, compact, and composed of small cells in various layers. When cultured on gelatin, a typical colony consists of only one cell layer. In this case, indicators of pluripotency are colonies composed of small cells with clear borders and a raised appearance. The major part of the cell is formed by the nucleus in which several nucleoli are observable. In contrast, indicators of differentiating cells are flat colonies of which the margins are unclear and frayed. Differentiating cells typically have filopodia and a soma that is bigger than the nucleus. The percentage of differentiated appearing cells should not exceed 10%. A crucial step in the differentiation protocol is the passaging from feeders to gelatin as in this step many cells can loose their pluripotency. Dense culturing of the cells, implying splitting every 2 days and almost confluent growth at day 2 after splitting, is supporting the maintenance of pluripotency on gelatin (Bibel *et al.* 2004). The 3xTg AD ESC lines that fulfilled best the described criteria were submitted to neuronal differentiation.

3.1.2.2 *Neuronal Differentiation of Heterozygous 3xTg AD ESC via Bibel & Barde Protocol*

1 Heterozygous 3xTg AD and 1 control ESC line were differentiated into neurons via the Bibel & Barde protocol (Bibel *et al.* 2004; Bibel *et al.* 2007) as outlined in section 6.4.3.2. According to the original publication, most of the cells are cortical progenitors at the day of embryoid body (EB) dissociation, in this work defined as d0. By dissociation of the EBs and single cell plating juxtacrine Notch signaling is interrupted and thus the transition from self-renewal to differentiation and maturation is achieved. At d10 after EB dissociation, the cultures were stained for the neuronal marker Tuj1 while the DNA labeling marker DAPI was used to stain the nuclei of all cell types. While the control lines showed between >60% Tuj1 positive cells ($Tuj1^+$ of $DAPI^+$ cells) and good survival, the 3xTg AD lines showed <20% Tuj1 positive cells and poor survival (**Fig. 3.2**). 3xTg AD cultures contained highly proliferative non-neuronal cells that were overgrowing the few neuronal cells after d14-21. This was not observed for the neuronal cultures derived from control lines. In several repeats of the neuronal differentiation, the outcome was always comparable to the mentioned results.

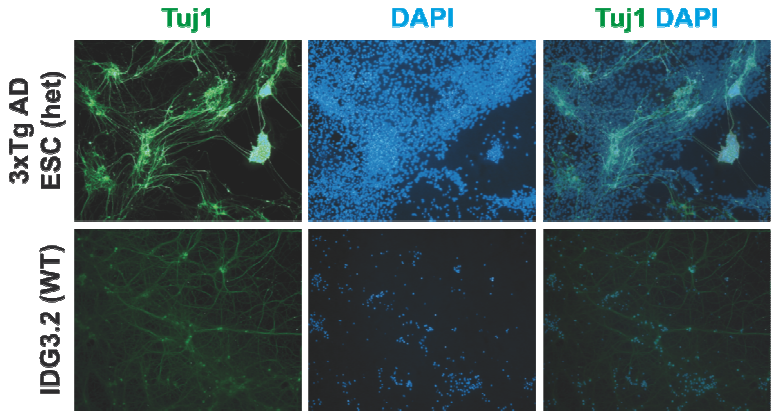

Fig. 3.2: Neuronal differentiation of heterozygous 3xTg AD ESC via the Bibel & Barde protocol
Immunostaining of 3xTg AD ESC-derived cultures for the neuronal marker Tuj1 and counterstaining of cells with DAPI. At day 10 after embryoid body dissociation the 3xTg AD cultures contained very few neuronal cells (<20%) and many proliferating non-neuronal cells. In contrast, the wild type control IDG3.2 ESC-derived cultures had high neuronal percentages (>60%) and no detectable proliferating non-neuronal cells. Due to clumping of cells, numbers had to be roughly estimated.

The described properties of the heterozygous 3xTg AD ESC derived neuronal cultures rendered them unusable for the analysis of Tau pathology. First, the analysis on the level of total protein extracts requires high neuronal percentages (>80%) as Tau pathology is a neuronal phenotype and would maybe not be detectable with low neuronal percentages. Second, as non-neuronal cells form the major part of the culture,

they could influence strongly the few neuronal cells and therefore interfere with any neuronal phenotype. Finally, the overgrowth of the proliferating, non-neuronal cells impedes analysis of long term cultures which might be important for the analysis of neurodegenerative symptoms that *in vivo* show a late onset phenotype. In summary, these results suggested that the heterozygous 3xTg AD ESC lines were not suited for neuronal differentiation with the Bibel & Barde protocol.

3.1.2.3 *Neuronal Differentiation of Heterozygous 3xTg AD ESC via Gaspard & Vanderhaeghen Protocol*

2 Heterozygous 3xTg AD and 2 control ESC lines were differentiated into neurons via the Gaspard & Vanderhaeghen protocol (Gaspard *et al.* 2009) as described in section 6.4.3.3. When the monolayer is dissociated and plated as single cells (d0), most of the cells are cortical progenitors as stated by Gaspard *et al*. (2009). As described for the case of EB dissociation (see previous section), this step represents the transition from self-renewal to differentiation and maturation due to interruption of juxtacrine Notch signaling. At d10 after monolayer dissociation, the cultures were estimated for the percentage of neuronal cells. Due to cell clumping exact quantification was impossible. Cultures derived from 3xTg AD ESC line 23 had >80% neurons ($Tuj1^+$ of $DAPI^+$ cells) whereas cultures derived from lines 11 (3xTg AD), 12 and 17 (both wild type) had neuronal percentages of <20% (**Fig. 3.3**).

Collectively, these results suggested that among the generated heterozygous 3xTg AD ESC lines, line-inherent variations in terms of neuronal differentiation capacity existed that were relevant for the Gaspard & Vanderhaeghen protocol. According to these results, line 23 seemed to be suited for the derivation of neuronal cultures that could be analyzed for parameters of Tau pathology. Therefore, line 23-derived neuronal cultures were selected for further characterization, starting with the analysis for expression of transgenic Tau.

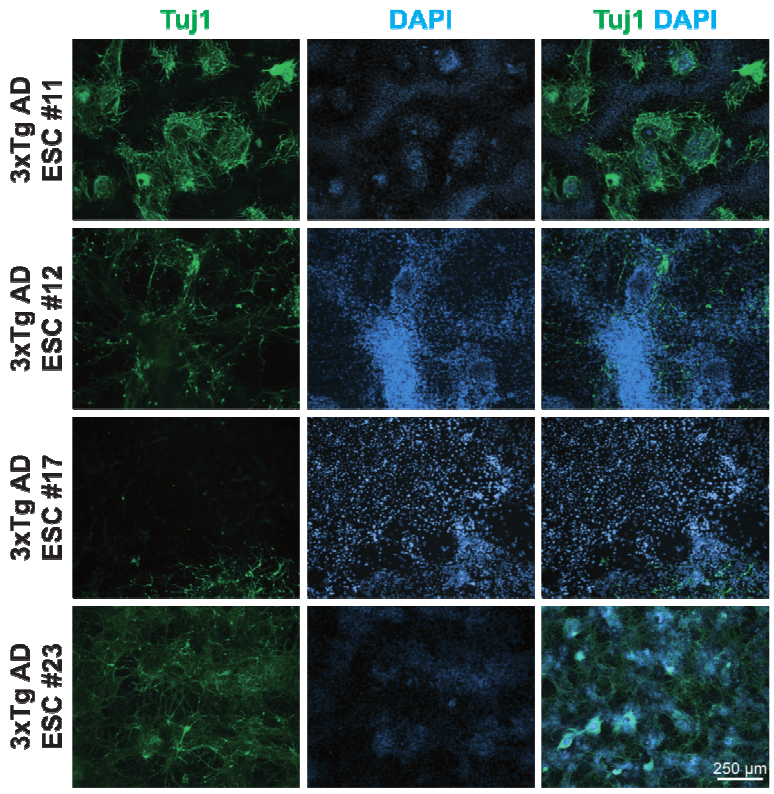

Fig. 3.3: Neuronal differentiation of heterozygous 3xTg AD ESC via the Gaspard & Vanderhaeghen protocol
Cultures derived by Gaspard & Vanderhaeghen protocol from two wildtype (#12 and #17) and from two heterozygous 3xTg AD ESC lines (#11 and #23) were analyzed at day 10 after monolayer dissociation for expression of the neuronal marker Tuj1 by immunostaining. Only line #23 yielded a sufficiently high enough neuronal percentage (>80%) and could thus be selected for further analysis. The other lines could not be used due to very low neuronal percentages (<20%) and overgrowing non-neuronal cells. Due to clumping of cells, numbers had to be roughly estimated. DAPI was used as nuclear marker.

3.1.2.4 *Analysis for Expression of Transgenic Tau in Heterozygous 3xTg AD ESC-Derived Neurons*

Neuronal cultures derived from heterozygous 3xTg AD ESC line 23 provided high neuronal percentages (see previous section) and were therefore analyzed for characteristics of a transgenic model for Tau pathology. In the homozygous 3xTg AD mouse, Thy1.2 promoter drives 6-8 fold overexpression of transgenic Tau in mature cortical and hippocampal neurons resulting in a pronounced Tau pathology in these regions. Consequently, the prerequisite for the *in vitro* reproduction of the 3xTg AD model and the first parameter to be analyzed in the neuronal cultures was the expression of transgenic Tau. ESC-derived neurons were analyzed at d18 by Western Blot using the human Tau specific antibody HT7 for the detection of transgenic human Tau. No expression of transgenic human Tau could be detected in the ESC-derived neurons (**Fig. 3.4**). Specificity of HT7 could be confirmed in a brain sample from an adult homozygous 3xTg AD mouse by detection of a strong ~51 kDa band. This size is

in accordance with the described apparent molecular weight of the human Tau isoform 0N4R (Goedert & Jakes 1990) which is used in the 3xTg AD mouse.

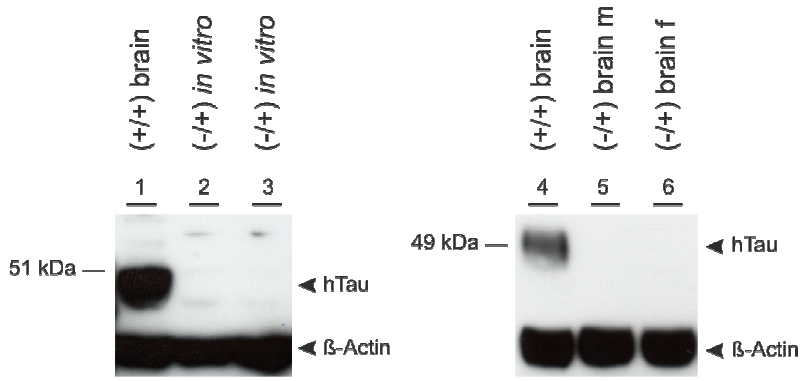

Fig. 3.4: Western Blot analysis for expression of transgenic human Tau in heterozygous 3xTg AD ESC-derived neurons and in heterozygous 3xTg AD brains
Expression of transgenic human Tau (hTau) could be detected neither in d18 heterozygous 3xTg AD neuronal cultures (lanes 2, 3) nor in heterozygous 3xTg AD brains (lanes 5, 6). Specificity of human Tau antibody HT7 was confirmed by detection of a ~50 kDa band in a homozygous 3xTg AD brain sample (lanes 1, 4). For the generation of the neuronal cultures via the Gaspard & Vanderhaeghen protocol heterozygous 3xTg AD ESC lines #23 (lane 2) and 24# (lane 3) were used which yielded neuronal percentages > 80%. m: male, f: female, ß-Actin: loading control.

As these results suggested that the first prerequisite of a transgenic model for Tau pathology, namely the transgene expression itself, was not fulfilled, the heterozygous 3xTg AD ESC-derived neurons were not analyzed for Tau pathology. Instead, I focused on the question, why Thy1.2 promoter failed to turn on transgenic Tau expression to a detectable level in the ESC-derived neurons.

The activity of Thy1.2 is known to be influenced by various factors (Caroni 1997), which are discussed later (section 4.4.1), but in this context the genetic background will be considered in more detail. It has become evident that 3xTg AD mice only show a pronounced phenotype when they are kept in the original background used in the publication of Oddo *et al*. (2003) (Jochen Herms and Thomas Floss, personal communications). This observation suggested, that Thy1.2 driven 6-8 fold transgene overexpression might be reduced in these animals, as overexpression is a crucial prerequisite for the development of hyperphosphorylated Tau and aggregates of Tau and Aß (section 2.2). As described in sections 3.1.1 and 6.4.1.2, the animals used for blastocyst and ESC line generation were not on the original genetic background of Oddo *et al*. (2003). This was due to 3-4 crosses on a BL6/129 background used in the mouse facility of the Helmholtz Zentrum München.

Taken together, these facts made the genetic background seem to be the most plausible causative factor for the absence of detectable levels of transgenic Tau in the ESC-derived neurons. Therefore, the heterozygous 3xTg AD animals that were used

for ESC line generation were analyzed for the expression of transgenic Tau using adult brain hemispheres. Total protein extracts were analyzed by Western Blot, using human Tau specific antibody HT7. When comparing brain extracts, it was revealed that detectable quantities of transgenic human Tau were only expressed in the homozygous 3xTg AD condition with the original background of Oddo *et al*. (2003) and not in the heterozygous 3xTg AD condition with a non-original background (**Fig. 3.4**, lanes 4-6).

This finding suggested that the genetic background in the heterozygous 3xTg AD condition impaired or at least strongly reduced the activation of Thy1.2 promoter and thus the expression of transgenic Tau. As a consequence, this finding provided a plausible explanation for the absence of detectable levels of transgenic Tau in the heterozygous 3xTg AD ESC-derived neurons as these have as well the non-original background. At the same time, by these results alone, the existence of other factors impeding transgene expression in the ESC-derived neuronal cultures could not be ruled out.

In summary, these results suggested that the expression level of transgenic Tau was strongly reduced in the heterozygous 3xTg AD brains and ESC-derived neurons by the influence of the genetic background that differed from the original genetic background used by Oddo *et al*. (2003). This insight suggested further, that for the creation of conditions allowing for expression of transgenic Tau in 3xTg AD neuronal cultures, the execution of the experiments in the original genetic background of Oddo *et al*. (2003) would be mandatory.

3.2 Neuronal Differentiation of homozygous 3xTg AD iPSC

3.2.1 Generation of 3xTg AD iPSC

In order to avoid the reduction of transgenic Tau expression by a possible interference of an unsuited genetic background, I decided to carry out the neuronal differentiation experiments in the original genetic background of Oddo *et al*. (2003). In combination with the usage of the homozygous condition, this approach would create optimal preconditions for a maximum expression level of transgenic Tau, according to my previous findings (section 3.1.2.3).

For the generation of homozygous 3xTg AD neurons by *in vitro* differentiation, two starting points were possible: the generation of ESC lines and the generation of iPSC using only homozygous 3xTg AD mice with the original genetic background of Oddo *et al*. (2003). As at the time point of experiment the stock of these mice in the mouse facility of the Helmholtz Zentrum München was so small that no females could be sacrificed for ESC line generation, the generation of iPSC lines was the only way as it

requires only a small piece of an ear. In addition to this rather practical reason, the following scientific reason argued for the iPSC approach: As it parallels similar approaches with patient-derived iPS cells, the iPSC approach adds an attractive layer of significance compared to the ESC-based concept of this work.

For the generation of homozygous 3xTg AD iPS cell lines, adult primary ear fibroblasts derived from a homozygous 3xTg AD mouse with the original genetic background of Oddo *et al*. (2003) were reprogrammed as outlined in section 6.4.2. For the reprogramming procedure, a stably integrating vector, expressing a cocktail of pluripotency factors was chosen as this approach promised a practical efficiency (section 4.1). In the used vector pReproII-attB-shp53 (**Fig. 3.5 A**), four elements are combined to yield an efficient, controllable reprogramming strategy. First, stable integration of the vector is mediated via C31 integrase by recombination of plasmid-located attB sites with genomic pseudo attP sites. This principle requires co-transfection with a constitutive C31 integrase expression vector and results in random and possible multiple integration, as pseudo attP sites are distributed randomly throughout the mouse genome (see also section 4.4). The advantages of this approach are the high integration efficiency by C31 integrase mediation and a spectrum of vector activity dependent on the genetic context of the integration (Thyagarajan *et al.* 2001). Second, the expression of reprogramming factors is induced by Doxycycline and repressed in its absence as depicted in **Fig. 3.5 B** and **C**. By omission of Dox it is therefore possible to check, if the supposedly reprogrammed cells express endogenous pluripotency factors or if they are dependent on the Dox-induced expression of exogenous pluripotency factors and can therefore not be considered as reprogrammed. Third, the core part of the vector is formed by the mouse cDNA sequences of the reprogramming factors Oct4, Sox2, cMyc, Klf4, together known as Yamanaka cocktail (Takahashi & Yamanaka 2006) which can induce reprogramming of differentiated cells to pluripotent stem cells (iPSC). Finally, in the presence of Dox, the vector expresses a shRNA directed against p53 which can increase the reprogramming efficiency by ~100 fold (Zhao *et al.* 2008).

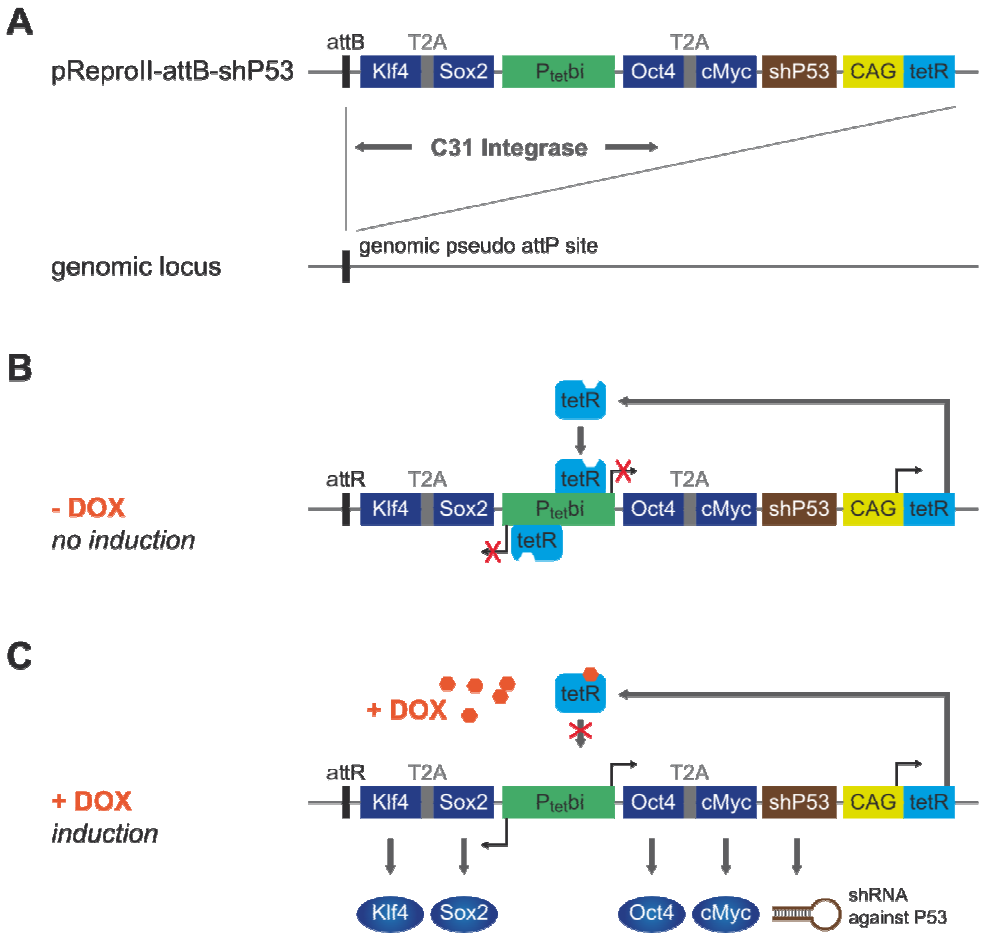

Fig. 3.5: Reprogramming vector pReproII-attB-shP53: design, integration and doxycycline-dependent induction
(**A**) In the vector used for reprogramming (pReproII-attB-shP53) a bidirectional tet-responsive promoter (P_{tet}bi) controls the expression of a cocktail of 4 reprogramming factors (Klf4, Sox2, Oct4, cMyc, pairwise linked by T2A sites) and of a shRNA (shP53) for the increase of reprogramming efficiency. Vector integration is achieved via C31 integrase mediated recombination of the attB site and a genomic pseudo attP site. (**B**) The CAG promoter drives constitutive expression of the tet repressor (tetR) which represses the expression of P_{tet}bi-promoter-driven elements by binding to it in the absence of doxycycline (DOX). (**C**) Upon addition of DOX, binding of tetR to P_{tet}bi is impaired by a conformational change and transcription of the 4 reprogramming factors and the shRNA against P53 takes place.

At day 4 after transfection of the homozygous 3xTg AD adult primary ear fibroblasts with the vectors pReproII-attB-shp53 and pCAG-C31-bpa, the cells were immunostained for the pluripotency marker Oct4 to check if transfection worked (**Fig. 3.6 A**). The negative staining of the majority of fibroblasts and the clear-cut localization of the staining to the nucleus (as expected for the transcription factor Oct4), indicated a highly specific staining and the successful transfection and induction of the reprogramming vector. As the cells passed this control, they were further cultivated until day 23 when in total 12 ESC-like colonies could be picked and expanded. As $8x10^5$ fibroblasts were used, this number corresponds to a reprogramming efficiency of 0.0004%. All 12 generated iPSC lines were genotyped by PCR (primers 5tauRev, APPinternal, Thy12.4 and PS1-K13/K15) and exhibited the expected 3xTg AD

genotype with exception of line 3 which was not used further (**Fig. 3.6 B**). The Verification of homozygosity was only possible for PS1, but the fibroblast donor mouse had been confirmed as homozygous by only producing entirely 3xTg AD positive litters (data not shown). Thus, the generated iPSC lines could be considered as homozygous for 3xTg AD and used for neuronal differentiation.

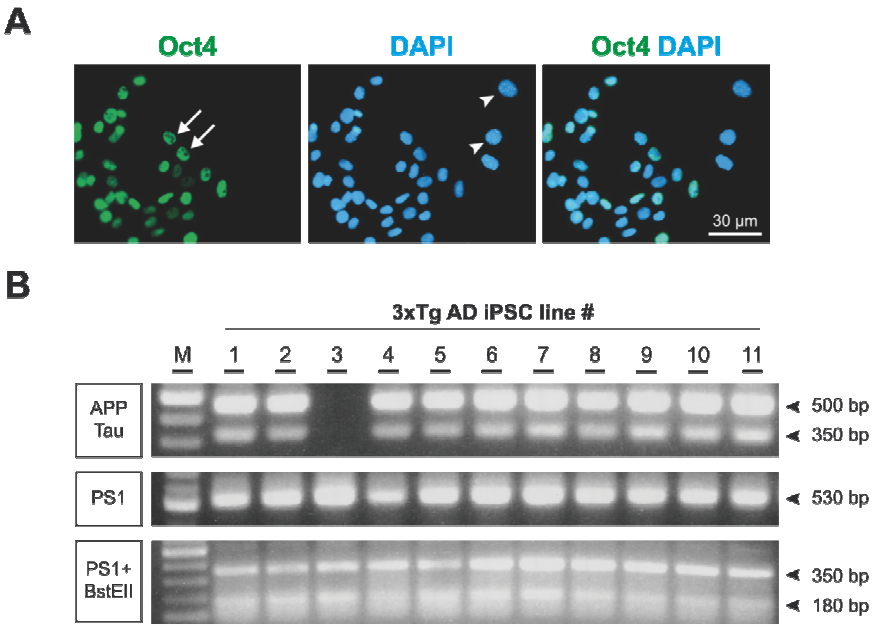

Fig. 3.6: Generation of homozygous 3xTg AD iPS cell lines
(**A**) Control for transfection and induction of the reprogramming vector by immunostaining for the pluripotency factor Oct4 at day 4 after the transfection of homozygous 3xTg AD ear fibroblasts. The staining indicated that vector transfection and induction was successful as Oct4 positive cells (arrows) were detected between Oct4 negative fibroblasts (arrowheads) which formed the major part. A magnification of a group of Oct4 positive cells is shown. (**B**) Genotyping of generated iPSC lines by PCR. A duplex PCR detected transgenic human APP^{swe} (500 bp) and human Tau^{P301L} (350 bp) in all samples except for iPSC line #3. All samples were homozygous for the $PS1^{M146}$ allele, as indicated by complete digestion of the 530 bp PCR fragment by BstEII to 2 fragments of 350 bp and 180 bp. DAPI: nuclear marker; M: 100 bp DNA marker.

3.2.2 Neuronal Differentiation of 3xTg AD iPSC via Gaspard & Vanderhaeghen Protocol

Before neuronal differentiation, several homozygous 3xTg AD iPSC lines were checked for criteria which serve as indicators of pluripotency as described in section 3.1.2.1. The tested lines showed line-inherent differences in the maintenance of pluripotency when cultured on gelatin. Some of the homozygous 3xTg AD iPSC lines that fulfilled best the described criteria were submitted to neuronal differentiation via the Gaspard & Vanderhaeghen protocol (Gaspard *et al.* 2009) as outlined in section 6.4.3.3. After plating of neuronal progenitors (d0), cells could differentiate and mature until samples for characterization by immunostaining and Western Blot were taken at day 18. The

neuronal percentages of the iPSC-derived cultures were estimated to be between 30-50% (quantified as Tuj1$^+$ of DAPI$^+$ cells, **Fig. 3.7 A**). As many cells grew in large clumps, exact quantification was not possible. Cells were stained for Nestin which is expressed in neural stem cells and disappears when cells enter the postmitotic stage of neuronal differentiation as designated by expression of the early neuronal marker Tuj1. At d18, Nestin$^+$ cells formed ~10-20% of DAPI$^+$ cells. Nestin$^+$ cells were observed all over the plated cells but predominately in the cell clumps (**Fig. 3.7 A**). In Western Blot analysis, d18 samples of 3 different homozygous 3xTg AD iPSC lines were analyzed for expression of Tau. As mentioned earlier, the expression of transgenic Tau is the crucial parameter in this state of the process for the establishment of the aspired Tau pathology model. No expression of transgenic human Tau could be detected using human Tau specific antibody HT7 (**Fig. 3.7 B**). Analysis for expression of total Tau was performed with antibody K9JA which detects all isoforms of both human and mouse Tau independent on their phosphorylation state. As confirmed by adult and embryonic (E15.5) mouse control brains, the antibody K9JA detected several bands above ~48 kDa in the adult brain and one band below ~48 kDa in the embryonic brain, representing adult and embryonic Tau isoforms (Buee *et al.* 2000). Thus, in the *in vivo* context, the transition from embryonic to adult Tau isoform expression mirrors the state of neuronal maturation. After 18 days of neuronal differentiation and maturation, only expression of the embryonic Tau isoform, but no expression of adult Tau isoforms could be detected in the homozygous 3xTg AD iPSC-derived neuronal cultures (**Fig. 3.7 B**). In other words, on the level of Tau expression, the neuronal cultures resembled neurons of an embryonic brain and not neurons of an adult brain.

In summary, the results from the analysis of homozygous 3xTg AD iPSC-derived neurons, generated via the Gaspard & Vanderhaeghen protocol, suggested the following: The established 3xTg AD iPSC lines generated neuronal cultures with 30-50% neurons and 10-20% Nestin-positive cells. As Nestin-positive cells were mostly associated with huge cell clusters, clumping of cells seemed to be associated with the impairment of transition from self-renewing progenitors (Nestin$^+$) to postmitotic neurons (Tuj1$^+$). This observation in the immunostainings suggested incomplete neuronal differentiation. It was corroborated by Western Blot data that suggested incomplete neuronal maturation because at d18 the neurons expressed only the embryonic but no adult Tau isoform.

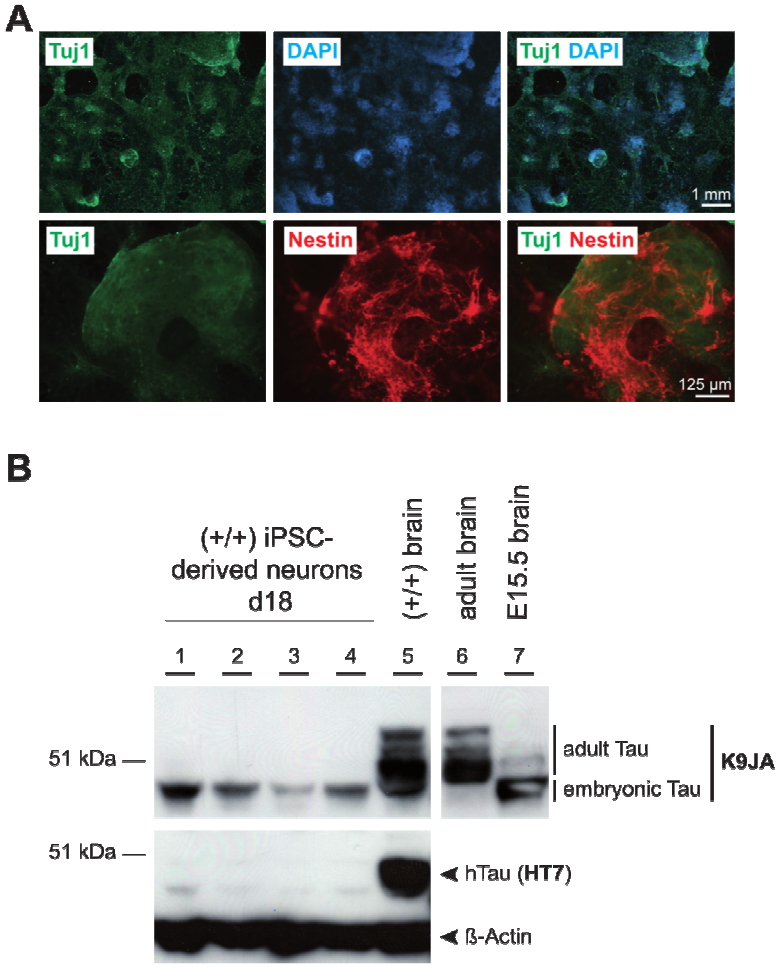

Fig. 3.7: Neuronal differentiation of homozygous 3xTg AD iPSC via the Gaspard & Vanderhaeghen protocol
(**A**) Immunostaining for the neuronal marker Tuj1 and counterstaining of cells with DAPI at day 18 after monolayer dissociation. The neuronal percentage of the 3xTg AD iPSC-derived cultures was estimated to be between 30-50% ($Tuj1^+/DAPI^+$). Due to clumping of cells, numbers had to be roughly estimated. Immunostaining for Nestin revealed that neuronal progenitors constituted 10-20% of the cells ($Nestin^+/DAPI^+$) and were present predominantly in the cell clumps. (**B**) Immunoblotting with total Tau antibody K9JA indicated incomplete maturation of day 18 neuronal cultures as they expressed only embryonic and no adult Tau isoforms. Absence of transgenic Tau expression rendered the cultures unusable for further analysis. Lanes 1-4: (+/+) 3xTg AD iPSC-derived neurons, lane 5: adult (+/+) 3xTg AD brain, lane 6: adult brain, lane 7: embryonic brain K9JA: total Tau, HT7: human Tau, ß-Actin: loading control.

Most important of the results in this section was the absence of transgenic Tau expression for which the most plausible explanation was as follows: The fact that the homozygous, original genetic background 3xTg AD iPSC-derived neurons were characterized as immature, in combination with the fact that Thy1.2 promoter is only active in mature neurons, starting between P6-12 (Caroni 1997), made it seem impossible that these neuronal cultures could express Thy1.2 promoter driven transgenic Tau. This important finding made the expression of transgenic Tau in the 3xTg AD iPSC-derived neurons become the first obstacle to be overcome and defined the next steps for tackling this issue. As neuronal immaturity seemed to impair

expression of transgenic Tau in neurons derived from iPSC via the Gaspard & Vanderhaeghen protocol, the follow-up experiments could be determined as: the identification of factors impairing maturation, the overcoming of these factors and the analysis if the latter would enable expression of transgenic Tau.

Because the described maturation experiments in the Gaspard & Vanderhaeghen would have meant a lot of time and effort, I decided to focus first on the analysis of the neuronal cultures derived from 3xTg AD iPSC by the Bibel & Barde protocol. As outlined in sections 2.3 and 3.1.2.1, the two neuronal differentiation protocols in this work use different strategies and therefore one can possibly circumvent problems of the other. In this case the question was, if the Bibel & Barde protocol would overcome the obstacle of lacking transgenic Tau expression. The characterization of 3xTg AD iPSC derived neurons generated via the Bibel & Barde protocol included the analysis of neuronal maturation and transgenic Tau expression and is described in the following sections.

3.2.3 Neuronal Differentiation of 3xTg AD iPSC via Bibel & Barde Protocol

Homozygous 3xTg AD iPSC lines with the original genetic background of Oddo *et al*. (2003) were submitted to neuronal differentiation via the Bibel & Barde protocol as described in section 6.4.3.2. Only 3xTg AD iPSC lines were used that had been selected for neuronal differentiation by criteria described in section 3.1.2.1. At the day of EB dissociation (d0), the plated cells were 17.5 % $Tuj1^+$ postmitotic neurons and 51.4 % $Pax6^+$ neuronal progenitors. After 10 days, 38.9 % of the cells were $Tuj1^+$ and only 4.1 % of $Pax6^+$ cells were left (quantified in relation to $DAPI^+$ cells, **Fig. 3.8 A, B**), indicating that most of the mitotic NSC ($Pax6^+$) cells became postmitotic neurons ($Tuj1^+$).

The neuronal cultures had a homogeneous appearance and were composed of mostly single cells and only few bigger cell clumps. The persisting $Pax6^+$ cells were distributed evenly all over the plated cells. The iPSC-derived neurons were cultured until day 21, but even 3 weeks after plating of the progenitors no expression of transgenic human Tau could be detected by Western Blot (**Fig. 3.9**). Not even single cells were positive for transgenic human Tau as tested by immunostaining with HT7 (**Fig. 3.8 C**, specificity of HT7 in immunostaining is exemplified e.g. in **Fig. 3.16 B**)

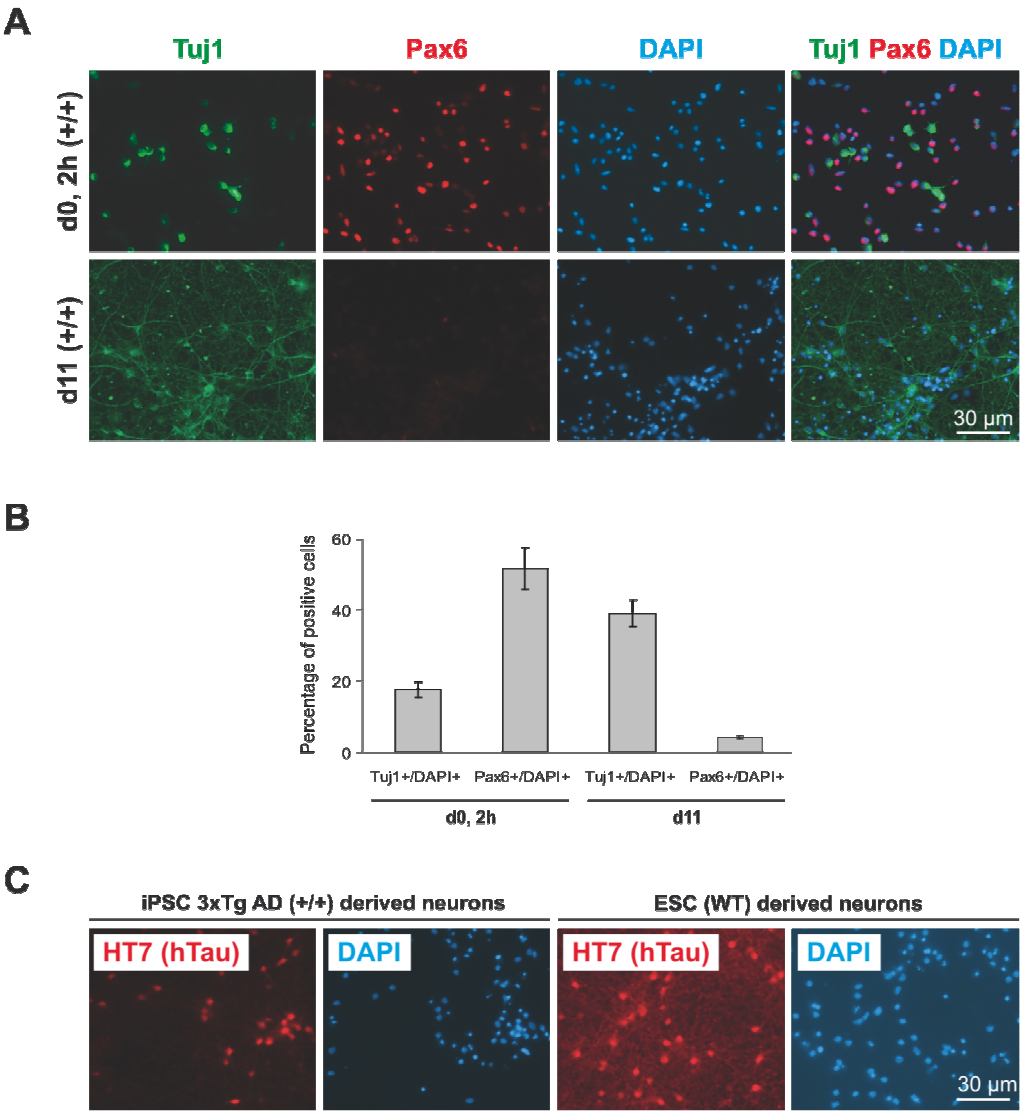

Fig. 3.8: Neuronal differentiation of homozygous 3xTg AD iPSC via the Bibel & Barde protocol
(**A**) Immunostainings for the neuronal marker Tuj1 and the neuronal progenitor marker Pax6. 2 hours after dissociation of the embryoid bodies (d0, 2h) more than 50% of the cells (**B**) were still in the progenitor state ($Pax6^+/DAPI^+$) and only few cells were postmitotic neurons ($Tuj1^+/DAPI^+$). At day 11 neuronal percentages were around 40% and only single $Pax6^+$ cells were detected. (**C**) Immunostaining of d11 neuronal cultures for transgenic human Tau with human Tau specific antibody HT7. No specific reactivity could be observed in the 3xTg AD iPSC-derived cultures, indicating absence of transgene expression. At long exposure time, a unspecific nuclear signal was observed in both mutant and wild type cultures and did not correspond to the axonally located Tau protein. DAPI: nuclear marker.

Analysis of neuronal maturation on the level of Tau isoform expression revealed, that in the course of 3 weeks the neuronal cultures increased the expression of adult isoforms and lowered the expression of the embryonic one (**Fig. 3.10 A**). The expression of embryonic Tau was not abolished and the extent of adult Tau isoform expression did not reach the situation in the adult brain which suggested incomplete maturation for each neuron or some neurons of the culture.

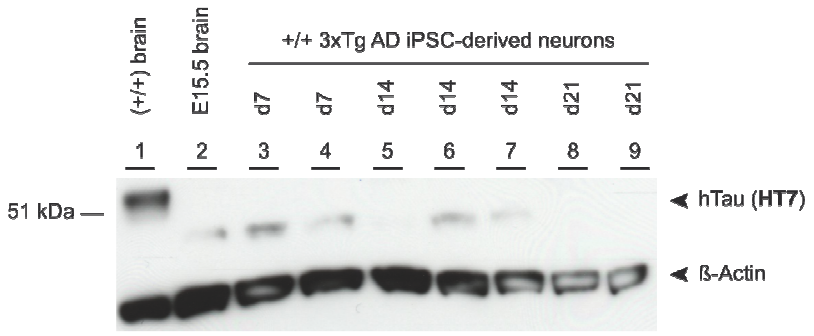

Fig. 3.9: Western Blot analysis for expression of transgenic human Tau in homozygous 3xTg AD iPSC-derived neurons
No expression of transgenic human Tau (hTau) could be detected in neuronal cultures derived from 3 different 3xTg AD iPSC lines (line #2: lanes 3, 5, 8; line #9: lanes 4, 7; line #8: lanes 6, 9) using immunoblotting with human Tau specific antibody HT7. Lane 1, positive control: homozygous adult 3xTg AD brain, lane 2, wild type embryonic brain, d7, d14, d21: days after embryoid body dissociation, ß-Actin, loading control.

In conclusion, the neuronal cultures shared the absence of transgenic Tau expression with the 3xTg AD iPSC-derived neurons generated via the Gaspard & Vanderhaeghen protocol. But in contrast to them, they showed properties which are mandatory for full neuronal differentiation and maturation as the almost complete disappearance of $Pax6^+$ proliferating cells and the expression of adult Tau isoforms. As they also had high neuronal percentages, the 3xTg AD iPSC-derived neuronal cultures generated via the Bibel & Barde protocol seemed suited for tackling the next major issue in this approach: the elucidation of the factors that impeded expression of transgenic human Tau. This intent was realized by a thorough characterization of the neuronal cultures regarding factors that are relevant for the activation of transgenic Tau driving Thy1.2 promoter and is presented in the following section.

3.2.4 Thorough Characterization of 3xTg AD iPSC-Derived Neurons

3.2.4.1 *Maturation Analysis 3xTg AD iPSC-Derived Neurons*

In order to identify factors that impaired the expression of transgenic Tau in 3xTg AD iPSC derived neurons, iPSC-derived neurons were analyzed in terms of their degree of maturation and their regional identity. As mentioned earlier, in the 3xTg AD mouse Thy1.2 promoter drives transgenic Tau expression almost exclusively in fully mature cortical and hippocampal neurons. As the 3xTg AD iPSC had the original genetic background of Oddo *et al*. (2003), no genetic background effects but e.g. immaturity or non-cortico-hippocampal regionalization of iPSC-derived neurons could explain for the absence of transgenic Tau expression. After the analysis of neuronal maturation in this section the analysis of neuronal regionalization is given in the following section.

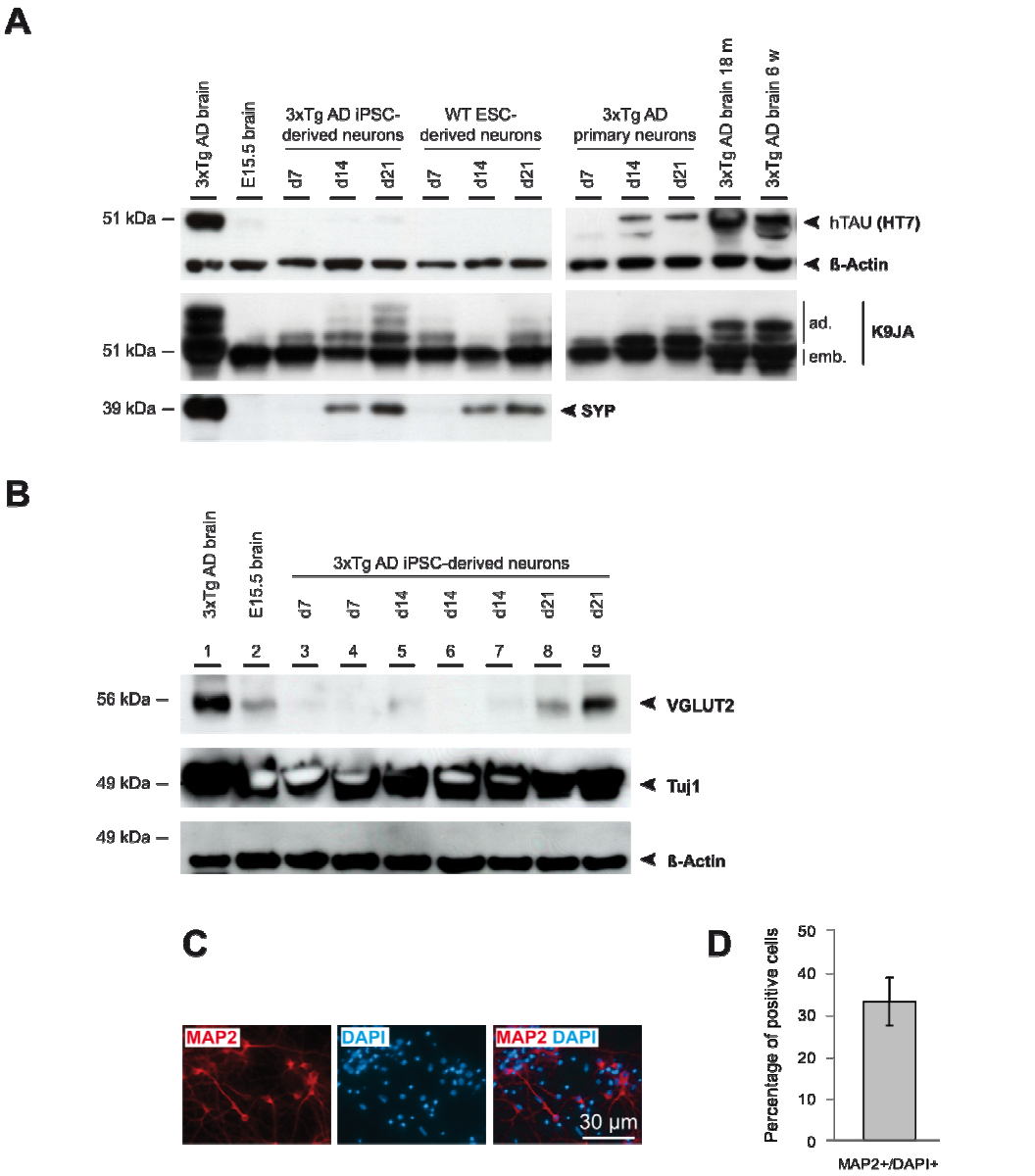

Fig. 3.10: Maturation analysis of 3xTg AD iPSC-derived neurons by Western Blot and immunostaining
(**A**) 3xTg AD (+/+) neuronal cultures that were generated *in vitro* via the Bibel and Barde protocol were compared by immunoblotting to 3xTg AD (+/+) primary neurons regarding expression of transgenic Tau (HT7) and endogenous Tau isoforms (K9JA). Expression of adult Tau isoforms after 2-3 weeks indicated maturation for all neuronal cultures. Only the 3xTg AD primary neurons exhibited some transgenic Tau expression but expression level was much lower than the level in the 3xTg AD (+/+) adult brains. Detection of markers for fully mature neurons (**A**: SYP, synaptohysin; **B**: VGLUT2, Vesicular Glutamate Transporter 2) confirmed the neuronal *in vitro* maturation, but their expression level was lower than in adult brain. Probing with the early neuronal marker Tuj1 (**B**) showed that all *in vitro* samples were comparable to the adult brain in terms of the neuronal percentages. (**C**, **D**) Immunostaining for MAP2 suggested that at d11 more than 30% of $DAPI^+$ cells were fully mature neurons. Lanes in (**B**): lane 1: homozygous adult 3xTg AD brain, lane 2, wild type embryonic brain; lanes 3, 5, 8: iPSC line #2; lanes 4, 7: iPSC line #9; lanes 6, 9: iPSC line #8. d7, d14, d21: days after embryoid body dissociation; ß-Actin: loading control; DAPI: nuclear marker.

The iPSC-derived neurons were analyzed for the markers MAP2, Synaptophysin and VGLUT2 which are only expressed in fully mature neurons. At d10 after plating of progenitors, 32.9 of $DAPI^+$ cells were expressing MAP2 (**Fig. 3.10 C, D**). The neuronal cultures started to express detectable amounts of Synaptophysin between day 7 and

14 and of VGLUT2 between d14 and 21. The expression levels of both proteins were much lower than the one in an adult brain, while neuronal percentages were comparable as revealed by probing with Tuj1 (**Fig. 3.10 B**). These results suggested, that the iPSC-derived neurons matured *in vitro*, but at day 21 individual neuronal maturation was not complete or only a part of the neurons in the culture was fully mature.

In order to assess which degree of maturation was really necessary for the activation of Thy1.2 promoter and if it could be activated at all *in vitro*, 3xTg AD embryonic primary neurons were analyzed for expression of total and transgenic Tau. The primary neurons started to express detectable amounts of transgenic human Tau between d7 and d14 after plating (**Fig. 3.10 A**). Assuming that the neurons prepared from E16.5 embryos matured as *in vivo*, this would correspond roughly to day P4-P11. At d21 (or P18), transgenic Tau expression level was still much lower than in the adult brain. Expression of adult Tau isoforms started before d7 but until d21 did not reach the extent of the adult brain while the embryonic isoform was still expressed.

In summary, these results suggested two things: First, the *in vitro* situation possibly constrained Thy1.2 activation and neuronal maturation directly, or impaired Thy1.2 activation indirectly by retarding neuronal maturation. Unfortunately, the closest available positive control was a 6 week adult brain and not the perfect positive control of a 3 week adult brain, which would correspond better to d21 *in vitro*. Second, iPSC-derived neuronal cultures were most probably mature enough at d21 to express transgenic Tau to at least some extent. This assumption is founded in the fact, that on the level of Tau isoform expression, the d21 iPSC-derived neurons appeared roughly as mature as the d14 primary cortical neurons. As the latter expressed transgenic Tau and the first did not, these findings suggested that other factors than the degree of neuronal maturation or the *in vitro* situation itself were impairing Thy1.2 activation in the iPSC-derived neuronal cultures. This notion was supported by the observation, that single neurons in the iPSC-derived neuronal cultures were $MAP2^+$, and thus supposedly mature enough for Thy1.2 activation, but negative for transgenic Tau as they were stained negative for HT7 (**Fig. 3.9 C**).

The overall conclusion of the maturation analysis was that most probably the degree of neuronal maturation was not responsible for the absence of transgenic Tau expression. Therefore I decided to focus on the regional identity of the iPSC-derived neuronal cultures as Thy1.2 promoter in the 3xTg AD model is almost exclusively active in cortical and hippocampal neurons (Oddo *et al.* 2003). The regionalization analysis is presented in the following section.

3.2.4.2 *Regionalization Analysis of ESC-Derived Neurons*

The ESC-derived neuronal cultures were analyzed for their regional identities by RT-PCR in order to check if the generated neurons really were of the expected glutamatergic cortico-hippocampal type. As mentioned earlier, Thy1.2 promoter is only active in cortico-hippocampal neurons which makes this regional identity a mandatory prerequisite for a model using 3xTg AD iPSC-derived neurons. In addition, this identity would show the successful reproduction of the results of Bibel *et al*. (2004, 2007) and represent neurons which are most relevant for studying Alzheimer's disease. The analysis of the regional identity of cultured neurons by RT-PCR (Reverse Transcription Polymerase Chain Reaction) is based on the principle which is explained briefly in the following.

The adult brain is patterned in regions and areas which can be further subdivided into smaller units. The smallest definable entity is the neuronal subtype. A neuronal subtype encompasses a group of neurons that have in common a unique combination of neuronal morphology, position, connectivity pattern and neurotransmitters. As knowledge is still growing, this categorization is subject to constant refinement. Because the developmental process of brain pattering is orchestrated by differential gene expression, it has been possible to correlate specific gene expression patterns to regions, areas and subgroups. This has enabled the identification of marker genes that are typical for a certain neuronal identity. A marker gene can for example label a whole brain region (e.g. *BF1*: forebrain), a confined area (e.g. *Cux2*: cortical layers II-IV), a transmitter type (e.g. *TH*: dopaminergic), an embryonic population (e.g. *Tbr2*: cortical layers II-IV progenitors) or an adult population (e.g. *Tbr1*: adult cortical layers II/III+VI). Thus, when expression of a marker gene is detected by RT-PCR, it can be concluded that neurons of the correspondent neuronal identity are present in the sample.

Total RNA samples of ESC-derived neuronal cultures were analyzed by RT-PCR for various marker genes covering all major brain regions and transmitter types. For reasons of availability at the time point of the experiment, wild type JM8 ESC-derived neurons generated via the Bibel & Barde protocol were used instead of 3xTg AD iPSC-derived neurons. The gene expression profile of the ESC-derived neuronal culture was compared to the ones of an embryonic and an adult brain because also in the *in vitro* differentiation, the cells should first pass through an embryonic state before reaching the adult one.

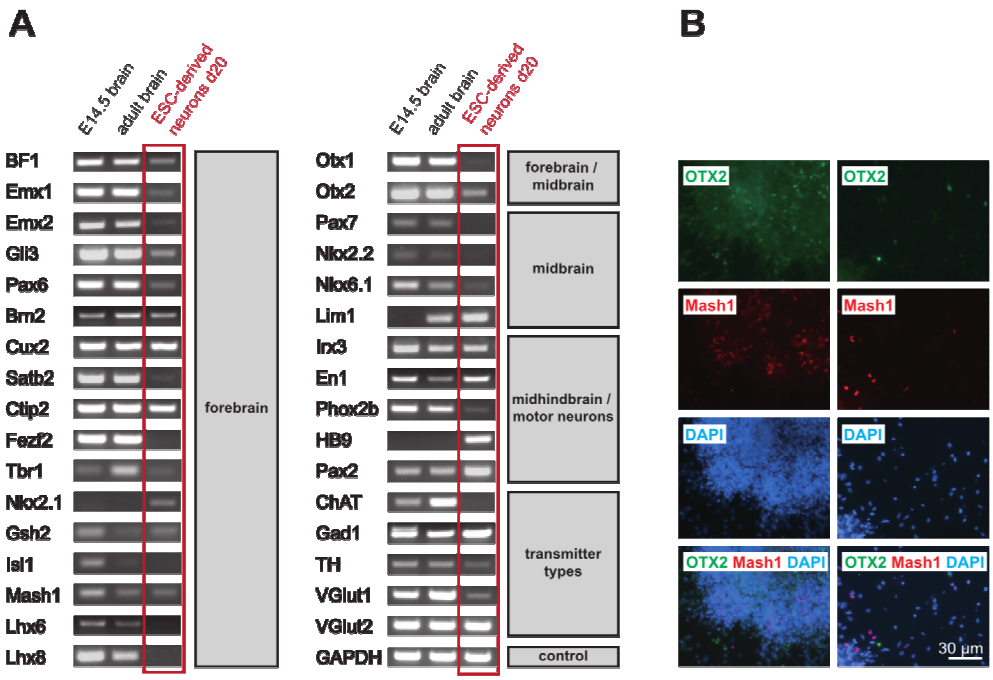

Fig. 3.11: Regionalization analysis of neuronal cultures generated via the Bibel & Barde protocol
(**A**) The expression of marker genes for neuronal identities was analyzed by RT-PCR in cDNA samples from a JM8 ESC-derived neuronal culture at d20. An embryonic and an adult wild type JM8 brain were used as positive control and for expression level reference. The detected expression pattern suggested mixed neuronal identities and not only the expected glutamatergic dorsal forebrain identities for the ESC-derived neurons. (**B**) Immunostainings of a JM8 ESC-derived neuronal culture at d20 for regional markers OTX2 and Mash1 detected positive cells as clusters (left panel) as well as single cells (right panel). This finding suggested a heterogeneous neuronal population. Expression patterns for each marker gene can be found in section 8.1.

In the analysis of ESC-derived neuronal cultures at day 20, gene expression markers of various neuronal identities were detected by RT-PCR (**Fig. 3.11 A**). Expression patterns for each marker gene used in this study were extracted from literature (Hartikka & Hefti 1988 ; Kawasaki *et al.* 2000; Schuurmans & Guillemot 2002; Echevarria *et al.* 2003; Hevner *et al.* 2003; Abe *et al.* 2003 ; Fremeau Jr *et al.* 2004; Okada *et al.* 2004; Wojcik *et al.* 2004; Watanabe *et al.* 2005; Hevner *et al.* 2006; Molyneaux *et al.* 2007; Eiraku *et al.* 2008; Gaspard *et al.* 2009; Kala *et al.* 2009; Koch *et al.* 2009; Nat & Dechant 2011) and can be found in section 8.1. Neurons with the expected cortico-hippocampal identity should express marker genes that are typical for dorsal forebrain and the glutamatergic transmitter type. For some cortical layer markers (*Brn2*, *Cux2*, *Ctip2*) the signal intensity of the *in vitro* cultures was comparable to the embryonic and adult samples (**Fig. 3.11 A**). The gene expression of other cortical layer markers (*Satb2*, *Fezf2*, *Tbr1*) and markers that are widely expressed in the whole (*BF1*) or in the dorsal forebrain (*Emx1/2*, *Gli3*, *Pax6*) was weak or not detectable. A strong signal for VGLUT2 and a weak signal for VGLUT1 indicated glutamatergic neurons with rather thalamic or brainstem than cortico-hippocampal identities. The detection of non-cortico-hippocampal marker expression indicated the presence of

several unwanted neuronal identities. As the signal intensity in some of these cases (e.g. *Mash1*, *Lim1*, *Gad1*) was comparable to the embryonic or the adult brain sample, the correspondent neuronal identity was considered to constitute a relevant part of the ESC-derived culture. According to the detected non-dorsal-forebrain markers, the *in vitro* generated neurons had additional identities of ventral forebrain, mid-hindbrain, motor neurons and GABAergic and dopaminergic neurons. To analyze the influence of genetic background effects, the marker gene expression profile of neuronal cultures derived from E14 ESC and JM8 ESC were compared (data not shown). The expression profile was almost identical. This suggested negligible influence of the genetic background and rendered the conclusions from the JM8 results suited to be extended to the 3xTg AD iPSC-derived neurons.

As the gene expression analysis by RT-PCR was performed with the cDNA of a whole ESC-derived neuronal culture, its outcome represents a summary of all genes expressed in the culture. It therefore allows for no conclusion, if the detected genes are expressed by all cells, according to the correspondent neuronal identity or in artificial combinations. To gain some insight into how gene expression was distributed in the *in vitro* culture, immunostainings were done for two of the marker genes tested in the RT-PCR. Otx2 and Mash1 immunostainings at day 10 revealed that only few cells expressed Otx2 and some cells expressed Mash1 which confirms the RT-PCR data for these genes (**Fig. 3.11 B**). The positive cells were observed as single cells as well as in clusters. Together with previous Pax6 immunostainings (section 3.2.3, **Fig. 3.8 A**) these results suggested that at least these 3 markers were only expressed in a part of the ESC-derived neurons indicating a heterogeneous neuronal population. Thereby it became clear, that the generated neuronal population was not homogeneous, which would imply expression of all markers in every cell. On the other hand, the expression of marker combinations that do not occur *in vivo* could not be excluded. Thus, the detection of a marker gene by RT-PCR in the ESC-derived neurons did not mean that the correspondent neuronal subtype really was present in the same form in the dish as it is in the brain.

In summary, the results of the regionalization analysis suggested that the ESC-derived neuronal cultures were heterogeneous and consisted of various neuronal identities. As genetic background influences seemed to be negligible, it was concluded that 3xTg AD iPSC-derived neuronal cultures also possessed mixed neuronal identities. Important dorsal forebrain markers (e.g. *Emx1*, *Gli3*) and some cortical layer markers were weakly or not expressed. This finding suggested, that the neuronal *in vitro* cultures only recapitulated a part of the neuronal identities found in cortex and hippocampus. As it is not clear, if Thy1.2 promoter drives transgenic Tau expression in

every cortical and hippocampal neuron, Thy1.2 activation may have been absent, because the neuronal cultures did not contain the right cortico-hippocampal identity. Additionally, identities of ventral forebrain, mid-hindbrain and spinal cord were detected. RT-PCR is only a semi-quantitative method, but as for some of these identities the signal intensity was as strong as for embryonic or adult brain, most probably a significant part of the *in vitro* generated neurons had non-dorsal forebrain identities. This finding offers an additional explanation for the absence of detectable amounts of transgenic Tau: As non-dorsal forebrain neurons do not activate the Thy1.2 promoter, their presence in the dish will dilute any possible transgenic Tau signal originating from cortico-hippocampal neurons. Incomplete covering of the cortico-hippocampal spectrum of neuronal identities on the one hand, with the presence of significant amounts of non-dorsal forebrain identities on the other, yielded together a plausible explanation for the failure of transgenic Tau detection in sections 3.2.3 and 3.2.4.1.

Taken together, neurons generated via the Bibel & Barde protocol seemed unsuited for the expression of Thy1.2 promoter driven transgene expression due to their neuronal composition. Or, from a different view point, Thy1.2 promoter was unsuited for driving transgene expression in iPSC-derived neurons because its very restricted activation pattern was disadvantageous for the heterogeneous neuronal *in vitro* population.

As the Bibel & Barde protocol proved to be robust and fast in generating cultures with high neuronal percentages it was reasonable to stick to it. Therefore I decided to design other approaches for the establishment of a model of Tau pathology using PSC-derived neurons. The new approaches were based on different promoters with broad and robust expression and are presented in the following sections.

3.3 Neuronal Differentiation of Tau^{P301S} iPSC and hTAU iPSC

3.3.1 Generation and Characterization of Tau^{P301S} iPSC Lines, hTau iPSC Lines and Correspondent Control iPSC Lines

3.3.1.1 *Concept of Experiments*

In the 3xTg AD approach the Thy1.2 promoter seemed to be the major obstacle for the achievement of transgene expression in PSC-derived neurons (see section 3.2.4.2). In order to establish a model for Tau pathology based on iPSC-derived neurons, I decided therefore to use different promoter systems for the expression of transgenic Tau. For this purpose, I continued to use published models of Tau pathology as they combine two advantages that were technically and strategically relevant: First, the genetic

framework of sufficient transgene expression level and genetic background influences has been verified to produce a phenotype. Second, results from the *in vitro* neuronal cultures can be compared to the published *in vivo* data in terms of Tau pathology.

Among the published Tau pathology mouse models only few are not based on the Thy1.2 promoter. Suited and available were only the Tau^{P301S} mouse (Yoshiyama *et al.* 2007) and the hTAU mouse (Andorfer *et al.* 2003) which use the Prion and the human MAPT (Microtubule-Associated Protein Tau) promoter, respectively. In order to generate the correspondent *in vitro* Tau pathology models, iPSC lines were derived from both mice, differentiated into neurons and analyzed for Tau expression and Tau pathology. Before presenting the experimental details and results in the following sections, important features of the 2 mouse models will be described briefly.

In the Tau^{P301S} mouse (Yoshiyama *et al.* 2007), Prion promoter drives 5 fold overexpression of transgenic human Tau (1N/4R) carrying the P301S mutation. The activity of Prion promoter in general in the mouse starts around E11.5 in neuronal cells that have ceased proliferating and drives transgene expression in the whole CNS (Tremblay *et al.* 2007). Hyperphosphorylated Tau and Tau tangles are observed in cortex and hippocampus at 5 month. Synaptic and neuronal loss occurs by 8 to 9 month while the median life span is about 9 month. In the hTAU mouse (Andorfer *et al.* 2003), the expression of all six isoforms of transgenic human wild type Tau is driven by human MAPT promoter resulting in Tau overexpression in neurons. Expression of human Tau starts as soon as the neuronal cells become post-mitotic (section 4.4.3). Insertion of EGFP cDNA into exon one of endogenous Tau results in a mouse Tau knockout and neuron-specific EGFP expression. Tau hyperphosphorylation appears at 6 month, aggregated Tau at 9 month. Thus, both mouse models exhibit CNS-wide early-onset transgenic Tau expression resulting in a robust Tau pathology and seemed suited for the planned experiments. Therefore they were used for the generation of iPSC lines as described in the following section.

3.3.1.2 *Reprogramming of adult primary ear fibroblasts*

In order to generate iPSC lines from the mouse lines Tau^{P301S} and hTau as well as from their wild type control lines BL6 C3 and BL6, the correspondent adult primary ear fibroblasts cultures were established as outlined in section 6.4.2.1. The reprogramming procedure was performed twice, the first time as described for the 3xTg AD line (section 3.2.1). Successful transfection and induction of the reprogramming vector was indicated by detection of Oct4 expression at day 4 after nucleofection for all 4 lines (**Fig. 3.12**). But at day 23, only colonies of the control line BL6 C3 could be picked, the other lines showed no colonies at all (**Table 3.1**).

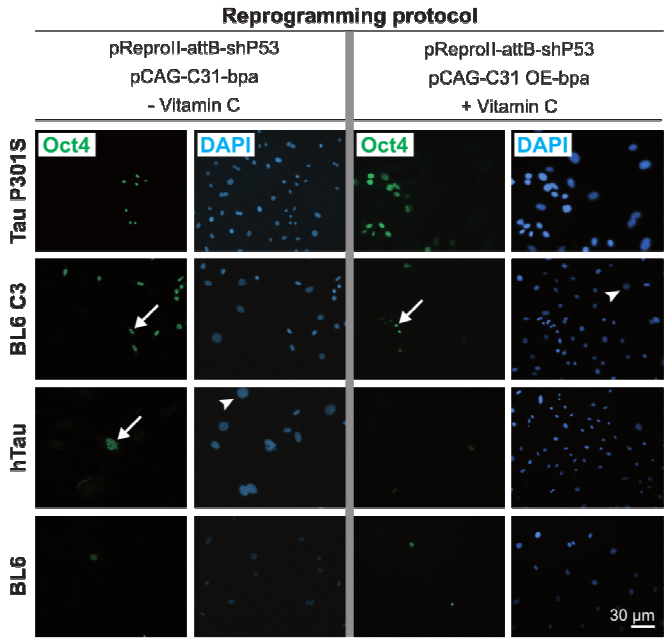

Fig. 3.12: Reprogramming of Tau^{P301S}, hTau, BL6 and C3 BL6 ear fibroblasts
Control for transfection and induction of the reprogramming vector by immunostaining for the pluripotency factor Oct4 at day 4 after the transfection of Tau^{P301S} and hTau ear fibroblasts and correspondent wild type control lines. The staining indicated successful vector transfection for both reprogramming protocols (left and right panel) and induction as Oct4 positive cells (arrows) were detected between Oct4 negative fibroblasts (arrowheads). DAPI: nuclear marker.

Table 3.1: Reprogramming efficiencies of Tau^{P301S}, hTau, BL6 and C3 BL6 ear fibroblasts with two different protocols

Reprogramming Vector	pReproII-attB-shp53				pReproII-attB-shp53			
C31 Integrase Vector	pCAG-C31-bpa				pCAG-C31OE-bpa			
Treatment	-VitC				+VitC			
Line	**Tau^{P301S}**	**hTau**	**BL6 C3**	**BL6**	**Tau^{P301S}**	**hTau**	**BL6 C3**	**BL6**
Surviving fibroblasts (d2)	8 x 10^5	8 x 10^5	16 x 10^5	3 x 10^5	13 x 10^5	19 x 10^5	13 x 10^5	12 x 10^5
Total colony number	0	0	12	0	7	50	12	0
Reprogramming efficiency	0	0	0.0008%	0	0.0005%	0.0030%	0.0009%	0

Therefore the reprogramming procedure was repeated with modifications for enhancement of efficiency. The second time, instead of C31 integrase expression vector pCAG-C31-bpa, vector pCAG-C31 OE-bpa was used. The latter contains a C31 sequence which is codon optimized for the expression in mammalian cells and therefore should result in a higher number of cells with the integrated reprogramming vector. Further, vitamin C was added to the culture medium, which has been reported to enhance reprogramming efficiency (section 4.1). At day 23, ESC-like colonies could be picked and expanded for the lines Tau^{P301S}, hTau and BL6 C3 but not for BL6. As detected by PCR-analysis (primers P301S F/R and Ctrl2 F/R for Tau^{P301S} genotype,

GFP F/R and Ctrl1 F/R for hTau genotype), the generated iPSC lines exhibited the expected genotypes (**Fig. 3.13**). The weak signal produced by the internal controlCtrl2 F/R primers Ctrl2 F/R in the Tau^{P301S} lines and two BL6 C3 lines was considered to be due to PCR conditions. The iPSC lines were tested for the maintenance of pluripotency criteria when cultured on gelatin as described in section 3.1.2.1. In addition, the iPSC lines were further characterized in terms of pluripotency markers and chromosome number.

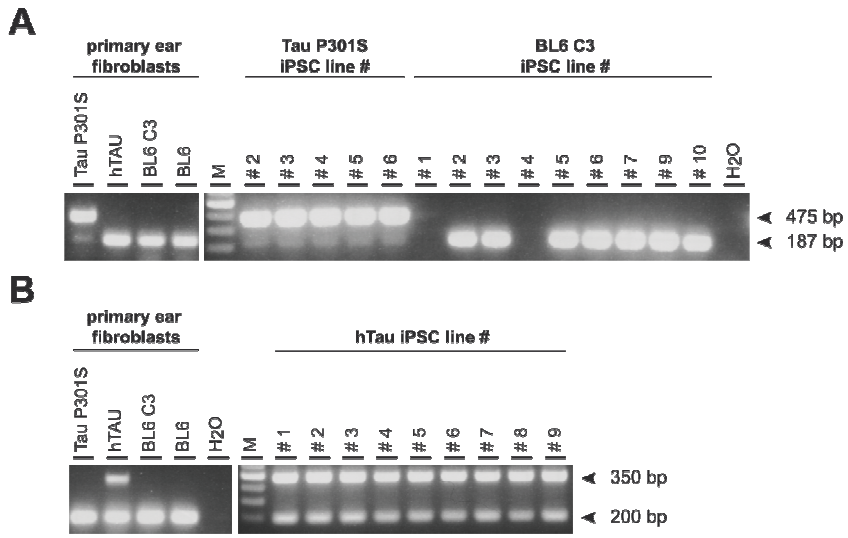

Fig. 3.13: Genotyping of Tau^{P301S}, hTau and BL6 C3 iPSC lines by PCR
(**A**) PCR results of a duplex PCR with primers for transgenic human Tau^{P301S} (475 bp) and internal control primers (187 bp). The Tau^{P301S} genotype could be confirmed for all Tau^{P301S} iPSC lines as well as the wild type condition for most of the BL6 C3 iPSC lines. (**B**) PCR results of a duplex PCR with primers for the hTau genotype (350 bp) and internal control primers (200 bp). The hTau genotype could be confirmed for all hTau iPSC lines, BL6 control iPSC lines could not be generated. Specificity of the PCR reactions was confirmed by using the correspondent ear fibroblast lines.

3.3.1.3 *Pluripotency Analysis of iPSC Lines*

In order to assess their pluripotency status, the generated iPSC-lines Tau^{P301S}, hTau and BL6 C3 were immunostained for the pluripotency markers Nanog, Oct4, Sox2, and Stella. In addition, they were tested for Alkaline Phosphatase (AP) expression which is also an indicator of pluripotency. For each line two clones of passage number 8-10 were tested. The cells had been kept in non-inducing Doxycycline-free conditions for at least 3 passages. As positive control, two wild type ESC-lines of different genetic backgrounds (BL6 and 129) were used. Negative staining of the co-cultured feeder cells indicated specificity of the stainings. The same exposure time was used for each marker to generate comparable pictures. All analyzed iPSC lines were tested positive for the used markers as shown in **Fig. 3.14**.

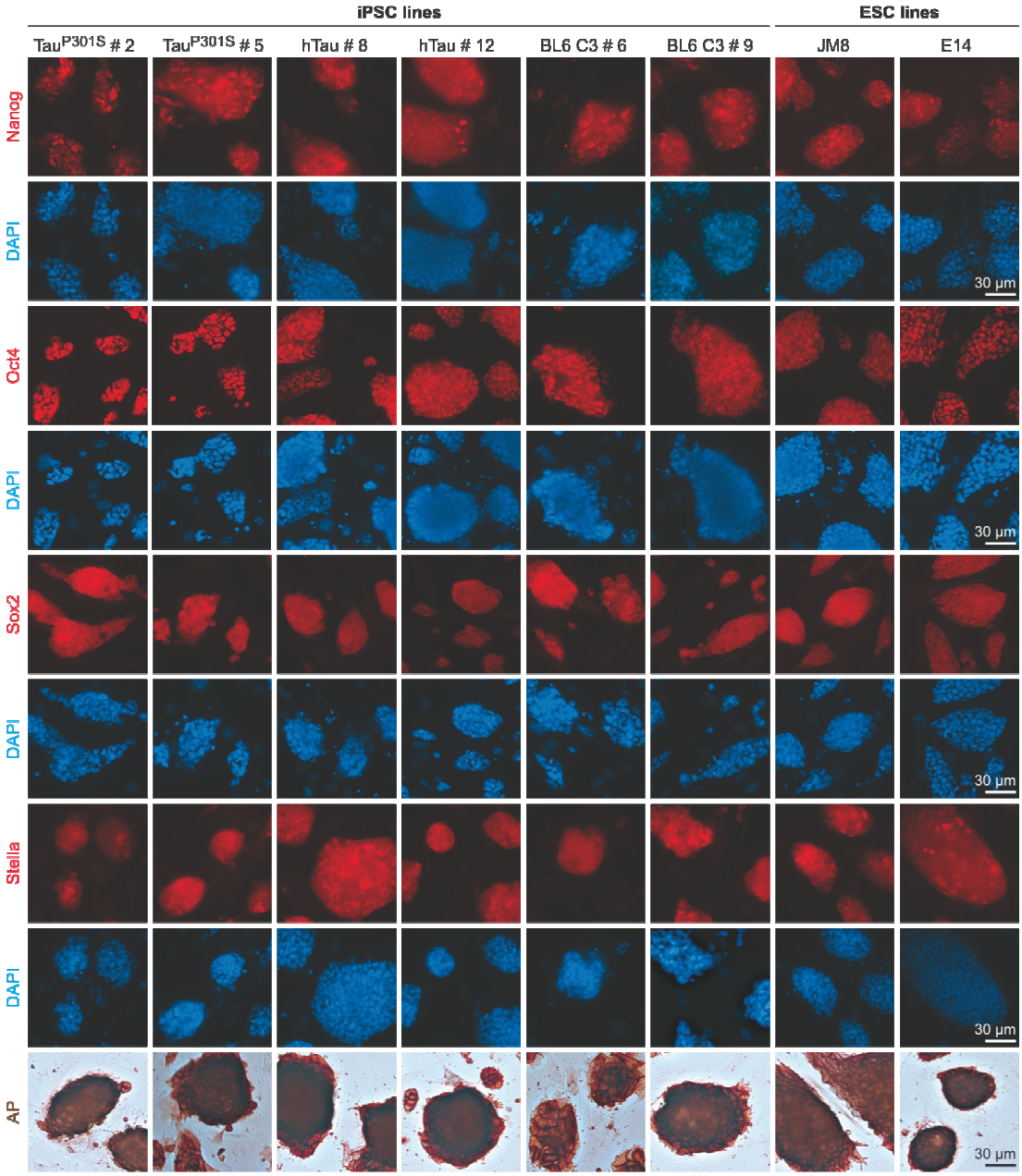

Fig. 3.14: Analysis of Tau^{P301S}, hTau and BL6 C3 iPSC lines for expression of pluripotency markers
2 iPSC lines of each genotype were analyzed by immunostaining for the expression of Nanog, Oct4, Sox2 and Stella. Expression of Alkaline Phosphatase (AP) was examined by AP staining. ESC lines of BL6 (JM8) and 129 (E14) backgrounds were used as positive controls. Within one marker the same exposure time was used. All iPSC lines were tested positive for the pluripotency markers and showed an expression level that was comparable to the ESC lines. This observation suggested a fully pluripotent status for the analyzed Tau^{P301S}, hTau and BL6 C3 iPSC lines. DAPI: nuclear marker.

The expression levels of the pluripotency markers in the iPSC were comparable to the expression levels in the ESC, indicating a comparable status of pluripotency. Collectively, these results indicated ESC-like expression of all analyzed pluripotency markers in all 6 tested iPSC lines which were therefore considered as fully pluripotent.

3.3.1.4 *Chromosome Countings of iPSC Lines*

For the detection of aberrations in chromosome number, chromosome countings were performed for the same 6 iPSC lines that were assessed for their pluripotency (previous section). The cells had been kept in non-inducing Doxycycline-free conditions for at least 3 passages and were of passage number 8-10. Chromosome counting was carried out as outlined in (section 6.4.2.3); for each line 30 metaphases were counted. The percentage of correct metaphases with 40 chromosomes was determined for each iPSC line as following: Tau^{P301S} #2: 83.3%, Tau^{P301S} #5: 83.3%, hTau #8: 66.7%, hTau #12: 50.0%, BL6 C3 #6: 63.3%, BL6 C3 #9: 43.3%. In general, a PSC line is considered to have the correct karyotype when more than 80% of the metaphases consist of 40 chromosomes. According to this threshold, only the two Tau^{P301S} iPSC clones could be considered to have the correct karyotype. The 6 lines were nevertheless used for the following experiments because they had performed best in pre-tests of neuronal differentiation and due to the lack of time for the characterization of more lines (see section 4.1 for further discussion).

3.3.2 Neuronal Differentiation of Tau^{P301S} iPSC and Analysis for Transgenic Tau Expression

Tau^{P301S} iPSC lines and corresponding BL6 C3 iPSC wild type control lines were differentiated into neurons via the Bibel & Barde protocol. The used iPSC lines were characterized in terms of pluripotency and chromosome number (sections 3.3.1.3 and 3.3.1.4) and tested for the maintenance of pluripotency criteria when cultured on gelatin as described in section 3.1.2.1. At day 10 after EB dissociation, the *in vitro* cultures were analyzed for neuronal percentages by the neuronal marker Tuj1. The iPSC-derived cultures contained 71.9% neuronal cells in case of the Tau^{P301S} culture and 64.8% in case of the BL C3 culture (Tuj1^{+} of DAPI^{+} cells, **Fig. 3.15 A, B**). Tau^{P301S} iPSC-derived neurons exhibited a strong signal in the HT7 staining in all neurons indicating neuron specific expression of transgenic human Tau. Specificity of HT7 was confirmed by a negative staining for the neuronal control cultures (**Fig. 3.15 A**). Expression of transgenic Tau in the Tau^{P301S} iPSC-derived neurons was confirmed by Western Blot (**Fig. 3.15 C**), with the onset of transgenic Tau expression between d7 and d14. The expression level of transgenic Tau was clearly lower than in the Tau^{P301S} brain of the fibroblast donor mouse when normalized to beta-Actin.

In summary, the Tau^{P301S} iPSC could be successfully differentiated into neuronal cultures with usable neuronal percentages (>60%). The detection of a medium

expression level of transgenic mutant human Tau rendered the *in vitro* generated neurons suitable for the analysis of Tau pathology (see section 3.3.4).

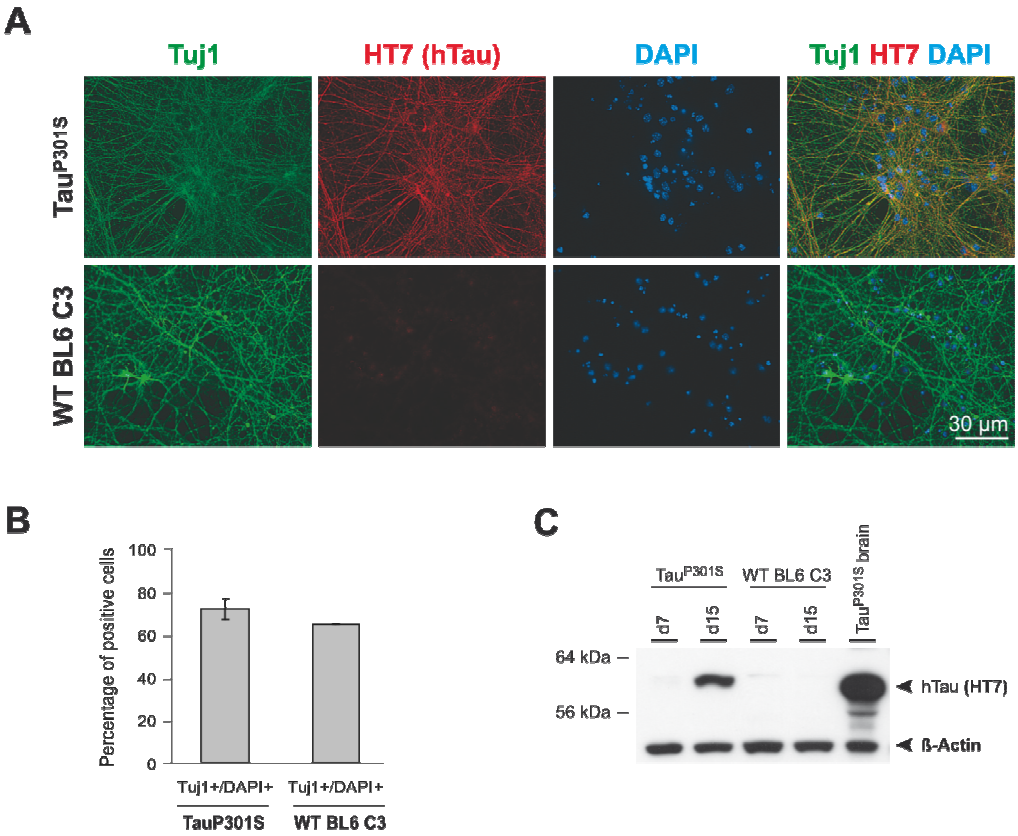

Fig. 3.15: Neuronal differentiation of Tau^{P301S} and BL6 C3 iPSC lines via the Bibel & Barde protocol
(**A**) Immunostainings for the neuronal marker Tuj1 at day 10 after dissociation of embryoid bodies. Both Tau^{P301S} and BL6 C3 iPSC-derived cultures showed neuronal percentages above 60% (**B**). According to immunostaining with HT7 only Tau^{P301S} neurons expressed transgenic human Tau (**A**). The expression level in the Tau^{P301S} culture was clearly below the level in an adult Tau^{P301S} brain as detected by immunoblotting with HT7 (**C**). The results suggested that onset of transgenic Tau expression was between d7 and d10. DAPI: nuclear marker; d7, d15: days after embryoid body dissociation; ß-Actin: loading control.

3.3.3 Neuronal Differentiation of hTau iPSC and Analysis for Transgenic Tau Expression

In order to generate neuronal *in vitro* cultures, hTau iPSC lines were submitted to the Bibel & Barde differentiation protocol. As no iPSC lines could be generated from the corresponding BL6 control fibroblasts (section 3.3.1.2), a BL6 JM8 ESC wild type line was used as control. The used iPSC lines were characterized in terms of pluripotency and chromosome number (sections 3.3.1.3 and 3.3.1.4) and tested for the maintenance of pluripotency criteria when cultured on gelatin as described in section 3.1.2.1. At day 8 after EB dissociation, the iPSC-derived cultures were composed of 85.2% neurons in the case of hTau cultures and of 90.2% neurons in the case of JM8

BL6 cultures (Tuj1$^+$ of DAPI$^+$ cells). Co-labeling of Tuj1 with GFP-fluorescence confirmed the neuronal expression of EGFP which is driven by neuron-specific endogenous MAPT promoter in the hTau mouse (**Fig. 3.16 A, C**).

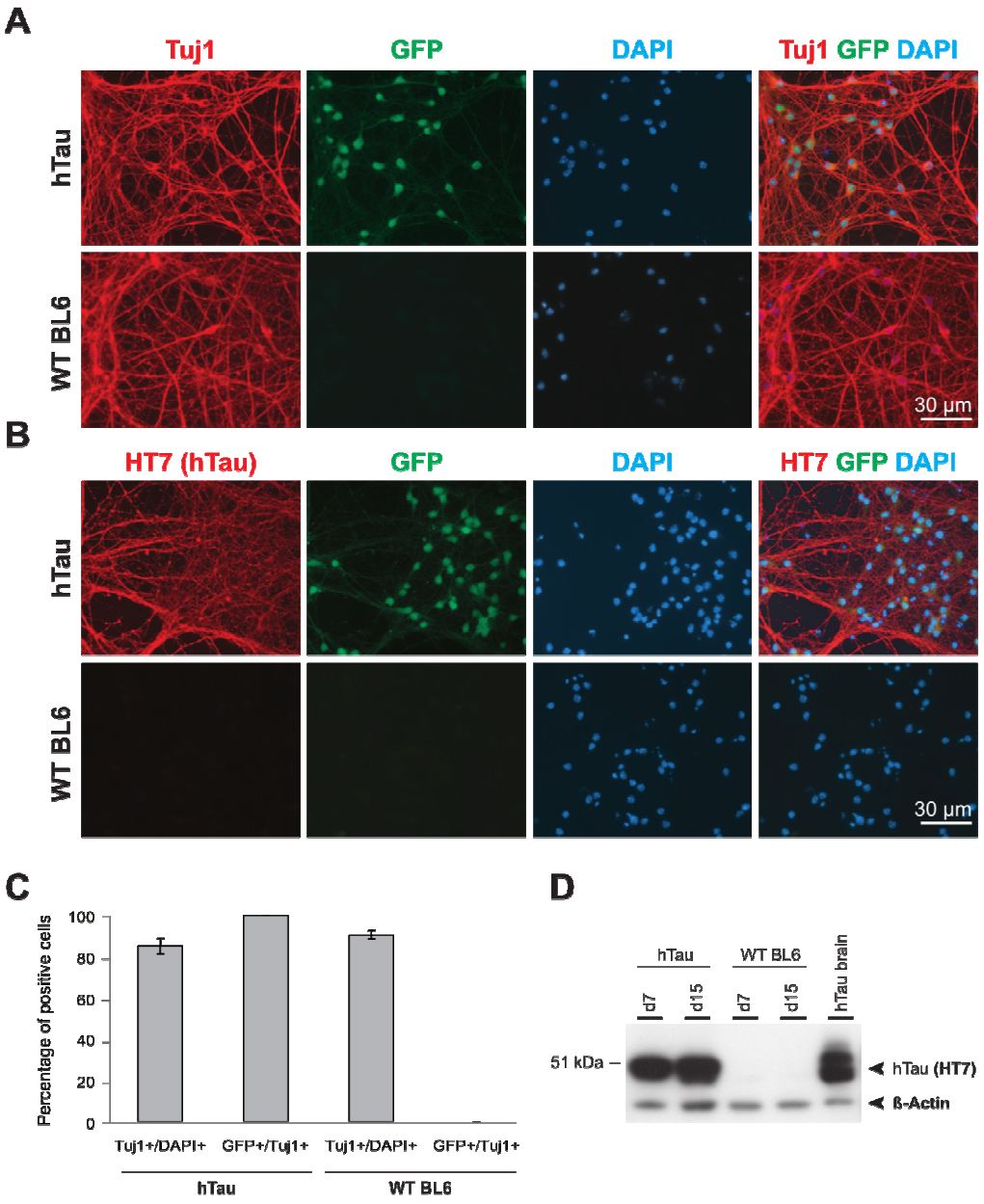

Fig. 3.16: Neuronal differentiation of hTau iPSC and BL6 ESC lines via the Bibel & Barde protocol
(**A**) Immunostainings for the neuronal marker Tuj1 at day 10 after dissociation of embryoid bodies. Both hTau and BL6 (JM8) PSC-derived cultures showed neuronal percentages above 80% (**C,** Tuj1$^+$/DAPI$^+$). Neuron specific expression of GFP in all hTau neurons confirmed the mouse Tau knockout (**A, C**). Immunostaining with HT7 showed that hTau neurons expressed transgenic human Tau and did so in a neuron specific manner as suggested by co-localization of the HT7-with the GFP-signal (**B**). Immunobloting with HT7 (**D**) suggested that expression of transgenic human Tau in the hTau cultures started before d7 and reached the expression level of transgenic human Tau in an adult hTau brain within 2 weeks. Specifity of the GFP signal and the HT7 immuno-detection was confirmed by the absence of signals in the negative control line JM8 BL6. WT: wild type; DAPI: nuclear marker; d7, d15: days after embryoid body dissociation; ß-Actin: loading control.

The hTau iPSC-derived neurons exhibited a strong signal in the HT7 staining in all neurons (labeled by neuron-specific EGFP-expression) indicating neuron-specific expression of transgenic human Tau. Neuronal control cultures were stained negative for HT7, thus confirming the specificity of the detection method (**Fig. 3.16 B**). By Western Blot, transgenic human Tau was detected at d8 and d15, indicating an onset of transgene expression before d8. Transgene expression level was as high as in the hTau brain of the fibroblast donor mouse when normalized to beta-Actin (**Fig. 3.16 D**).

The hTau mouse expresses all 6 Tau isoforms in its adult brain (Andorfer *et al.* 2003), which results from the combination of 0N/1N/2N and 3R/4R splice variants (Buee *et al.* 2000). As the Tau isoform expression pattern is correlated to the onset of Tau pathology (Buee *et al.* 2000), the generated hTau *in vitro* cultures were analyzed for the expression of Tau isoforms.

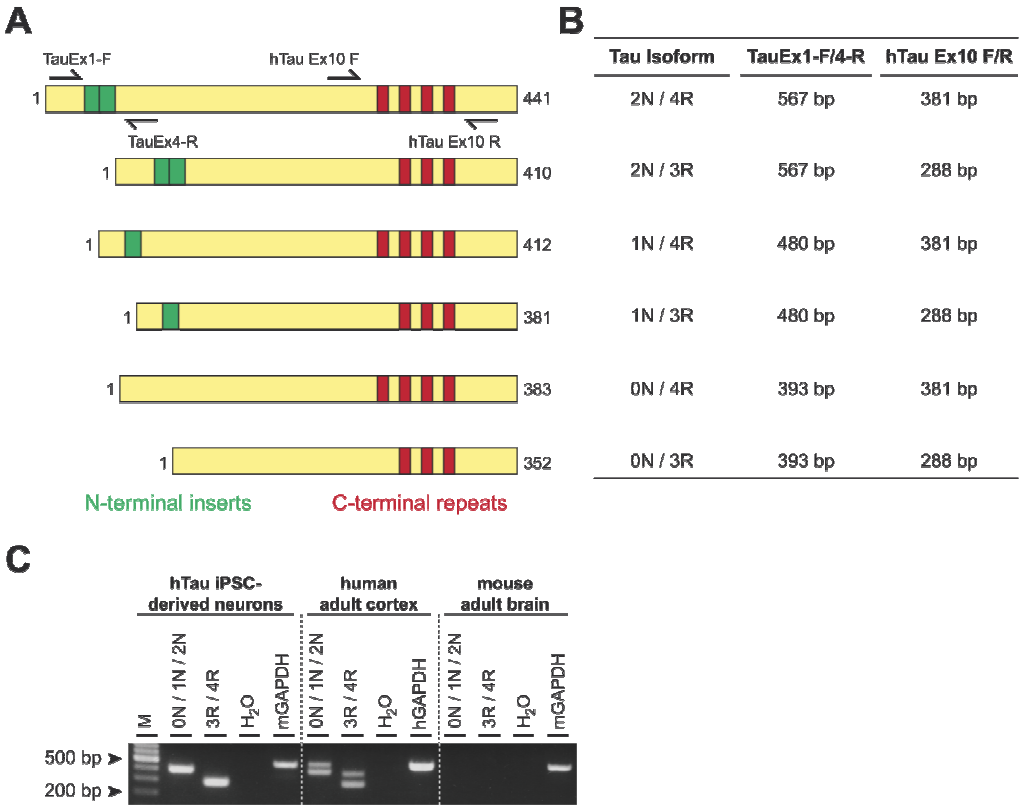

Fig. 3.17: Expression of human Tau isoforms in hTau iPSC-derived neurons
(**A**) The 6 Tau isoforms expressed in the adult hTau mouse brain and in the adult human brain vary in their composition of N-terminal inserts (N) and C-terminal repeats (R). The isoform sizes by number of amino acids and the positions of RT-PCR primers are indicated. (**B**) Tau isoform names and corresponding RT-PCR amplicon sizes. (**C**) RT-PCR analysis of human Tau isoform expression in hTau iPSC-derived neurons at d14. Human adult cortex and mouse adult brain were used as positive and negative control, respectively. The results suggested, that hTau iPSC-derived neurons expressed only the 0N/3R isoform as TauEx1-F/4-R primers produced a 393 bp fragment and hTAU Ex10 F/R primers produced a 288 bp fragment. The expression of the 2N isoforms could not be excluded because TauEx1-F/4-R primers failed to detect it in the human brain sample. Absence of signals in the mouse brain sample confirmed human specificity of the TauEx1-F/4-R and hTAU Ex10 F/R primers. M: 100 bp DNA marker; mGAPDH, hGAPDH: mouse and human specific loading control.

For this purpose, RT-PCR primers (**Fig. 3.17 A, B**) were used to analyze the total cDNA of a d7 hTau iPSC-derived neuronal culture. Because the cDNA sample for the hTau mouse adult brain was not available, a human adult cortex sample was used instead because it should also contain the cDNAs of all 6 Tau isoforms. The hTau Ex10 F/R primers detected both C-terminal repeat splice variants in the human brain sample (3R and 4R) but only the 3R variant in the hTau iPSC-derived neurons. The Tau Ex1-F/4-R primers detected expression of the 0N in the *in vitro* cultures and expression of the 0N and 1N splice variants in the human cortex sample but failed to detect the 2N splice variant. All primers showed specificity for human Tau as the mouse brain sample delivered no bands (**Fig. 3.17 C**). These results suggested that the hTau iPSC-derived neurons at d7 after EB dissociation expressed only the embryonic (0N/3R) Tau isoform. The expression of the 2N isoforms could not be excluded because Tau Ex1-F/4-R primers failed to detect it in the human brain sample.

Collectively, the hTau iPSC were successfully differentiated into neuronal cultures with usable neuronal percentages (>80%). Transgenic human Tau expression level was detected to be as high as in the adult hTau mouse brain. Even if not all 6 Tau isoform could be detected to be expressed in the *in vitro* generated neurons, the cultures were considered suitable for the analysis of Tau pathology (see section 3.3.4).

3.3.4 Analysis of Tau Phosphorylation in Tau^{P301S} iPSC- and hTau iPSC-Derived Neurons

In the brains of the Tau pathology mouse models Tau^{P301S} and hTau the hallmark of Tau hyperphosphorylation is observed after 5-6 months (Andorfer *et al.* 2003; Yoshiyama *et al.* 2007). In order to analyze if the Tau^{P301S} and hTau iPSC-derived neurons exhibit Tau pathology in the dish as the neurons do in the brain of the mouse model, the *in vitro* generated cultures were analyzed for Tau hyperphosphorylation. Tau pathology encompasses more criteria than phosphorylation status, e.g. Tau solubility, but the first logic focus for this study was Tau hyperphosphorylation. First, it is the earliest phenotype (see section 2.2) and should therefore be the most probable to be phenocopied within some weeks *in vitro*. Second, it is a well studied, important phenotype and its analysis by a range of phosphorylation dependent antibodies is well established.

The question if the Tau^{P301S} and hTau iPSC-derived neurons would exhibit Tau hyperphosphorylation after some weeks *in vitro* gets to the very heart of the matter of this work. *In vivo*, the phenotype is only observed in neurons of an age of several months, but how the aging status of a 2 week old iPSC-derived neuron compares to this, is completely unclear. As the iPSC-derived neurons could not be cultured for more

than 3-4 weeks due to cell survival, I intended to recapitulate conditions that are found in the context of an aged cell and in the context of Alzheimer's disease. Both conditions are known to favor the hyperphosphorylation of Tau. Regarding the first condition, an important aspect of aging is the increase of oxidative stress effects (Mattson & Magnus 2006). For the generation of oxidative stress, the iPSC-derived neurons where treated with the glutathione synthetase inhibitor BSO (buthionine sulfoximine) which causes oxidative stress by glutathione (GSH) depletion. Regarding the second condition, decreased phosphatase activity in AD brains is discussed to be favoring Tau hyperphosphorylation (Iqbal *et al.* 2009) which can be induced by an inhibition of phosphatases (Jin *et al.* 2011). For the inhibition of phosphatases, the iPSC-derived neurons where treated with okadaic acid (OA) which is a strong inhibitor of protein serine / threonine phosphatases 1, 2A, and 2B (PP1, PP2A, PP2B). The BSO and okadaic treatments were chosen because they both recapitulate aspects that favor Tau hyperphosphorylation and therefore allowed to assess if the mutant iPSC-derived neurons are more susceptible to develop this phenotype.

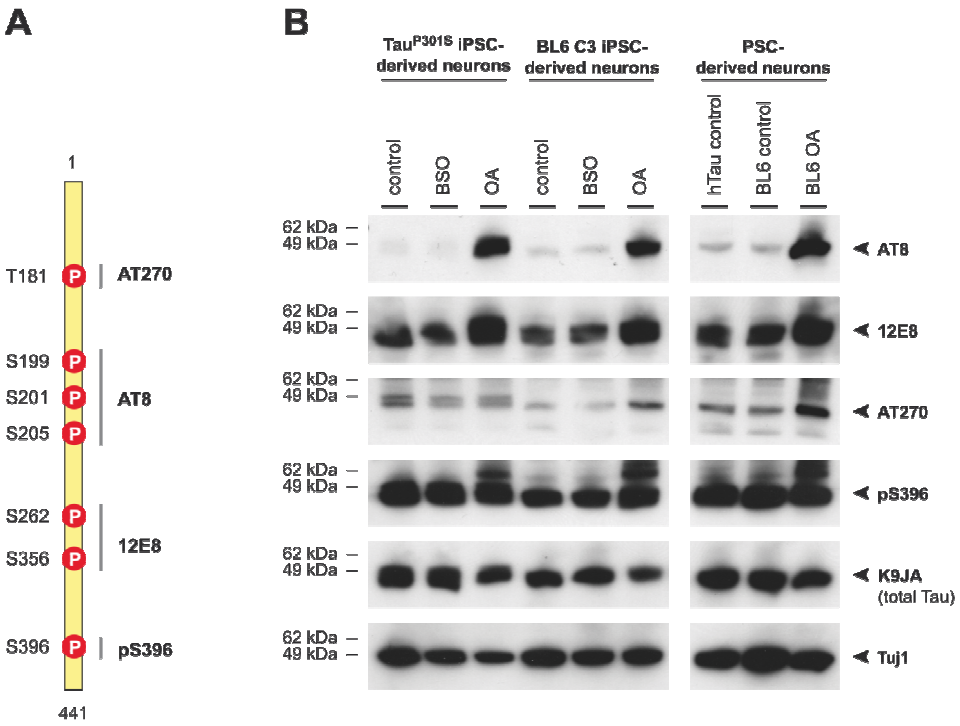

Fig. 3.18: Phosphorylation of Tau in Tau^{P301S} and hTau iPSC-derived neurons
(**A**) Antibodies (right) used in this work for detection of pathologic phospho-epitopes (left) of Tau protein (**B**) Western Blot analysis of iPSC-derived neurons with phospho-specific Tau antibodies (AT8, 12E8, AT270 and pS396) indicated that treatment with the phosphatase inhibitor okadaic acid (OA) induced hyperphosphorylation of Tau at the AT8 and 12E8 epitopes but not at the AT270 and the pS396 epitopes. Under all conditions (including oxitdative stress by BSO treatment) the Tau phosphorylation state of the mutant neurons (Tau^{P301S} and hTau) was similar to the wild type neurons (BL6 C3 and BL6). This finding contradicted an increased hyperphosphorylation susceptibility of the mutant neurons compared to the wild type neurons. Probing with K9JA and Tuj1 suggested similar total Tau levels and neuronal percentages for all samples. T: Threonine, S: Serine, BSO: buthionine sulfoximine for 24 h at 100 µM; OA: okadaic acid for 3 h at 1 µM.

In order to analyze the phosphorylation status of Tau protein, neuronal cultures derived from Tau^{P301S} and hTau iPSC were cultured until d14 after EB dissociation. BL6 C3 iPSC and BL6 JM8 ESC were used as controls for Tau^{P301S} and hTau, respectively. Tau^{P301S} and BL6 C3 cultures were treated with BSO and okadaic acid, for hTau and BL6 JM8 cultures only standard conditions were used. The antibodies that were used in this work for the study of Tau phosphorylation are shown together with the detected phosphoepitopes in **Fig. 3.18 A**. Immunoblotting revealed that okadaic treatment induced a strong increase in signal intensity for the antibody AT8 and a medium increase for the antibody 12E8 (**Fig. 3.18 B**) compared to control conditions. In each case the Tau^{P301S} signal intensity was comparable to the one of the BL6 C3 wild type sample (OA). In immunoblotting with antibody AT270, a weak increase in signal intensity for the OA-treated BL6 C3 sample was observed. For antibody pS396, in no sample such an increase was detected. Under control and oxidative stress conditions (BSO) signal intensities of Tau^{P301S}, BL6 C3, hTau and BL6 samples were comparable for all 4 tested phospho-specific antibodies. Probing with K9JA and Tuj1 suggested that total Tau levels and neuronal percentages of all samples were similar, which allowed for a direct comparison of signal intensities.

Taken together, these results suggested that treatment with the phosphatase inhibitor okadaic acid induced clear hyperphosphorylation of Tau in the iPSC-derived neurons at the AT8 and 12E8 epitopes but not at the AT270 and the pS396 epitopes. The most important observation was that under all conditions the Tau phosphorylation state of the mutant neurons (Tau^{P301S} and hTau) was similar to the wild type neurons (BL6 C3 and BL6). This finding contradicted an increased hyperphosphorylation susceptibility of the mutant neurons compared to the wild type neurons. Additionally this observation implied that standard *in vitro* conditions after 2 weeks did not fulfill the requirements that are necessary for the induction of Tau hyperphosphorylation in Tau^{P301S} and hTau neurons.

3.4 Neuronal Differentiation of pNeo-CAG-Tau^{P301L}/APP^{swe}/Venus-ESC and pHygro-CAG-$CreER^{T2}$-ESC

3.4.1 Concept and Vector Production

The results of the Thy1.2 promoter based 3xTg AD approach indicated, that the identification of a suited promoter system was the crucial issue for the expression of transgenic Tau in PSC-derived neurons (section 3.2.4.2). In addition to the Prion and human MAPT promoter based iPSC approaches (Tau^{P301S} and hTau models, section 3.3) I decided to follow a third approach based on another non-Thy1.2 promoter: The

establishment of a CAG promoter based ESC system for the expression of transgenic Tau in *in vitro* generated neurons. The reasoning was as follows: First, the CAG promoter is one of the most widely used systems for strong constitutive expression in mammalian cells (see section 4.4.4) and was therefore expected to drive overexpression of transgenes in neurons of all maturation stages and of all neuronal identities. As the extent of the activity of Prion and MAPT promoter in PSC-derived neurons was not known before the experiments, the CAG promoter provided an alternative route with a high probability for transgene overexpression. Second, ESC lines that have successfully been used for germline transmission should be fully pluripotent and therefore provide optimal conditions for neuronal differentiation. As such ESC lines were available, their confirmed pluripotency status represented an advantage compared to newly generated iPSC lines. Finally, the genetic background has been reported to influence the neuronal differentiation capacity of a PSC line. Because ESC lines of different genetic backgrounds were used, the ESC approach increased the probability for the generation of *in vitro* cultures with high neuronal percentages. Thus, the CAG promoter-based ESC approach fulfilled important criteria that generated excellent preconditions for the expression of transgenic Tau in ESC-derived neurons.

The engineered vector construct pNeo-CAG-Tau^{P301L}/APP^{swe}/Venus-attB (pTAV, **Fig. 3.19 A**) contained the cDNA of human 2N4R Tau with the P301L mutation (Tau^{P301L}). Overexpression of this mutation has been successfully used for the generation of Tau pathology in cell culture and in the mouse brain, for example in the 3xTg AD mouse (Oddo *et al.* 2003). Further, the cDNA of human APP carrying the Swedish mutation (APP^{swe}, K670N/M671L) was included in the construct, because it can trigger or aggravate Tau pathology (Oddo *et al.* 2003) and thus increased the probability for the detection of Tau pathology. Additionally, the inclusion of APP^{swe} generated an Alzheimer's Disease-like context as for example in the 3xTg AD model which is based on the overexpression of the same APP and Tau mutations. As third genetic element, the cDNA of the fluorescent protein Venus was included for convenient monitoring of vector integration and transgene expression. Sequences of Tau^{P301L}, APP^{swe} and Venus were linked with a T2A and a P2A sequence, respectively (**Fig. 3.19 A**). The T2A and P2A sequences mediate cotranslational cleavage which results in the release of the three individual protein products (Osborn *et al.* 2005). This strategy allowed for the simultaneous expression of Tau^{P301L}, APP^{swe} and Venus under the same CAG promoter and simplified the vector cloning procedure. The usage of a PGK promoter-driven neomycin resistance gene enabled the selection of vector-containing cells with the neomycin analog G418 (Geneticin). As strategy for vector

integration into the genome of the ESC, the C31 integrase-mediated recombination of a vector-located attB site with a genomic pseudo attP site was used (see section 3.2.1 for details). As pseudo attP sites are distributed randomly throughout the mouse genome, this approach results in random integration.

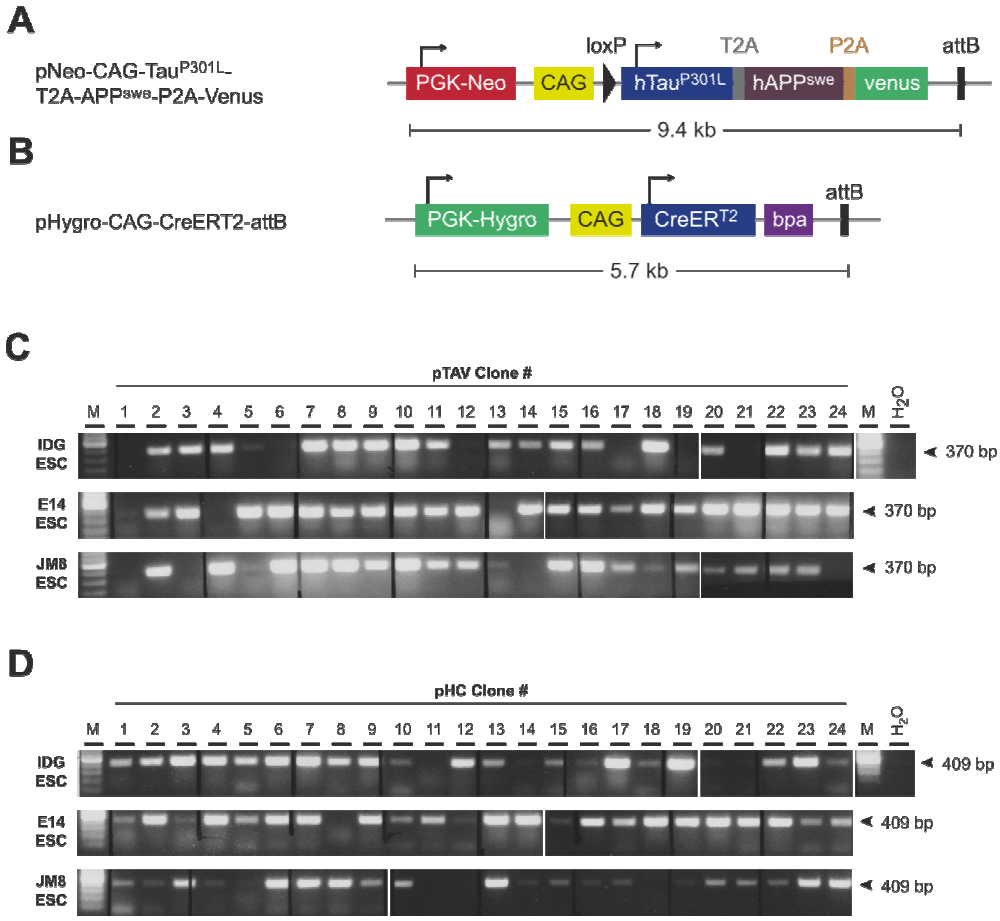

Fig. 3.19: Generation of pNeo-CAG-Tau^{P301L}/APP^{swe}/Venus and pHygro-CAG-CreER^{T2} ESC lines
(**A**) In the engineered vector for expression of Tau^{P301L}, APP^{swe} and Venus, T2A and PTA sites enabled for simultaneous expression of the 3 transgenes under the same constitutive CAG promoter. Vector integration was achieved via C31 integrase mediated recombination of the attB site and a genomic pseudo attP site while a PGK promoter driven neomycin resistance served as selection marker. (**B**) In the vector for constitutive, CAG-controlled expression of CreER^{T2}, C31 integrase mediated integration was used as described for (**A**). PGK promoter driven hygromycin resistance served as selection marker. Construction of both vectors is detailed in sections 6.2.2.2 and 6.2.2.3. (**C**) Genotyping of ESC clones of 3 different backgrounds (IDG, E14, JM8) after the transfection with vector pCAG-Tau^{P301L}/APP^{swe}/Venus (pTAV). The detection of a 370 bp fragment indicated that most of the clones were suitable for further experiments. (**D**) Genotyping of ESC clones of 3 different backgrounds (IDG, E14, JM8) after the transfection with vector pHygro-CAGER^{T2} (pHC). The detection of a 409 bp fragment indicated that most of the clones were suitable for further experiments. M: 100 bp DNA marker; IDG: IDG3.2 with BL6*129 background; E14: 129 background; JM8: BL6 background.

The decision for this strategy was owed to the uncertainty, which transgene expression level would produce optimal conditions for the generation of Tau pathology and which integration site would provide optimal activity of the CAG promoter. Therefore the C31-pseudo attP site approach seemed ideal, as it produces clones with a spectrum of vector integration sites and thus a spectrum of site-dependent vector activity. The

vector pNeo-CAG-Tau^{P301L}/APP^{swe}/Venus-attB (pTAV) was produced as outlined in section 6.2.2.2 and transfected into ESC as described in section 3.4.2.

For a side-project, the vector pHygro-CAG-CreER^{T2}-attB (pHC, **Fig. 3.19 B**) was engineered. This side-project was not fully realized, but as an intermediate result of it delivered pivotal data for the pTAV ESC approach, the relevant information about the pHC project is included in this work. The pHygro-CAG-CreER^{T2}-attB vector enabled for constitutive CreER^{T2} expression controlled by CAG promoter and selection of vector containing cells by a PGK-driven Hygromycin resistance. The integration strategy consisted of C31 integrase mediated recombination of an attB site with a genomic pseudo attP site as described for the pTAV approach earlier in this section. The vector pHygro-CAG-CreER^{T2}-attB (pHC) was produced as outlined in section 6.2.2.3 and transfected into ESC as described in section 3.4.2.

3.4.2 Transfection and Genotyping

For the generation of ESC lines with stably integrated vector pNeo-CAG-Tau^{P301L}/APP^{swe}/Venus-attB or pHygro-CAG-CreER^{T2}-attB, the plasmids were transfected separately into ESC. For catalyzing the integration process, a plasmid for transient expression of C31 integrase was cotransfected (see section 3.4.1). In order to vary the genetic background, 3 different ESC lines were used: JM8 (BL6 background), E14 (129 background) and IDG3.2 (BL6*129 background). From the resulting 6 transfections 24 clones per construct and background were amplified after selection. Genotyping by PCR (primers pTAV 1F/R for pTAV genotype, SeqCAG and CreERT2 Rev for pHC genotype) revealed that most of the clones were positive for the correspondent construct (**Fig. 3.19 C, D**) and could therefore be used for neuronal differentiation as described in the following sections.

3.4.3 Neuronal Differentiation of pNeo-CAG-Tau^{P301L}/APP^{swe}/Venus-ESC and Analysis for transgenic Tau Expression

In order to differentiate the pNeo-CAG-Tau^{P301L}/APP^{swe}/Venus ESC lines (ESC pTAV) into neurons via the Bibel & Barde protocol, for each genetic background 3 clones that had been tested positive by PCR for the pTAV construct (previous section) were cultured on gelatin. For each of the three genetic backgrounds, the 2 clones that fulfilled best the criteria which serve as indicators of pluripotency (section 3.1.2.1) were used for neuronal differentiation. The chosen clones were: Clones #4 and #6 of the JM8 background (ESC pTAV JM8 #4 and JM8 #6), clones #5 and #24 of the E14

background (ESC pTAV E14 #5 and #24) and clones #15 and #18 of the IDG3.2 background (ESC pTAV IDG #15 and #18).

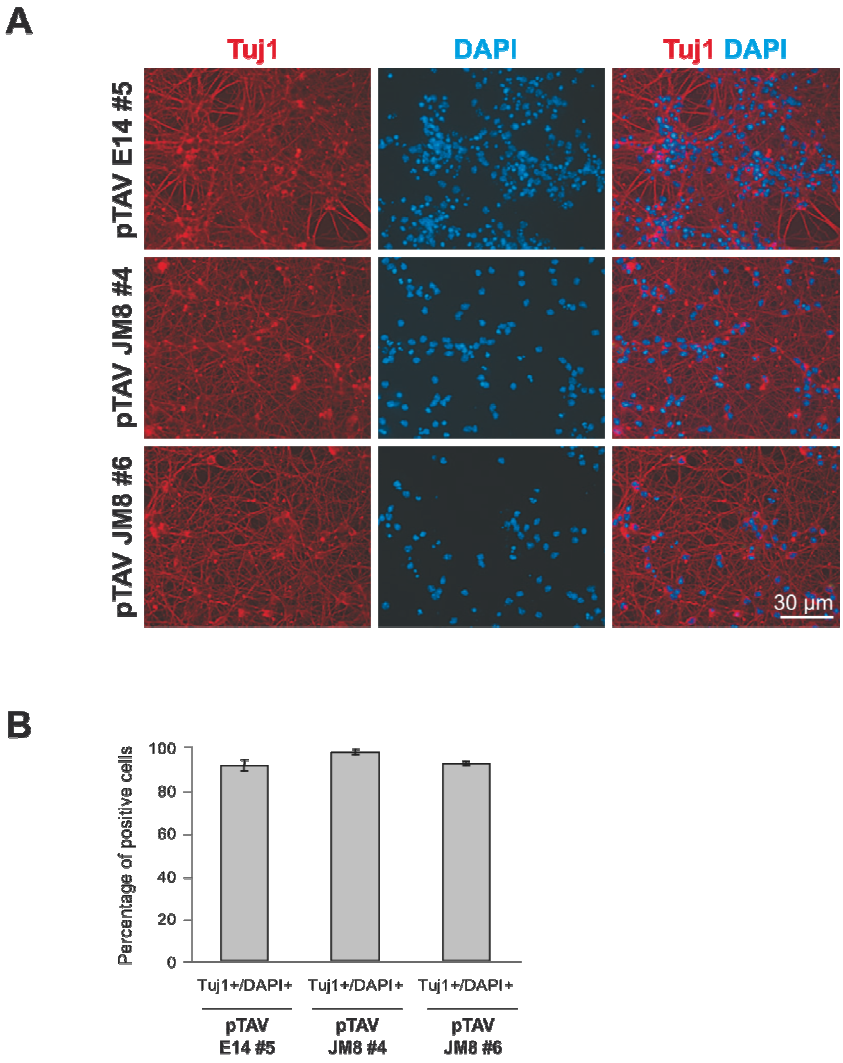

Fig. 3.20: Neuronal differentiation of pNeo-CAG-Tau^{P301L}/APP^{swe}/Venus ESC lines via the Bibel & Barde protocol
(**A**) Immunostainings of pTAV ESC-derived cultures for the neuronal marker Tuj1 at day 8 after dissociation of embryoid bodies. Lines of both backgrounds (E14: 129, JM8: BL6) showed neuronal percentages above 90% (**B**). pTAV: pNeo-CAG-Tau^{P301L}/APP^{swe}/Venus; DAPI: nuclear marker.

All 6 clones were submitted to neuronal differentiation via the Bibel & Barde protocol and the resulting cultures were analyzed in terms of neuronal percentages. At day 8 after EB dissociation, the pTAV JM8 and E14 neuronal cultures showed high neuronal percentages: JM8 #4: 97.4% Tuj1$^+$/DAPI$^+$, JM8 #6: 92.1% Tuj1$^+$/DAPI$^+$, E14 #5: 91.3% Tuj1$^+$/DAPI$^+$, E14 #24: not quantified (**Fig. 3.20 A, B**). As the two used pTAV clones of the IDG3.2 background failed to produce analyzable neuronal cultures, they had to be excluded from further analysis.

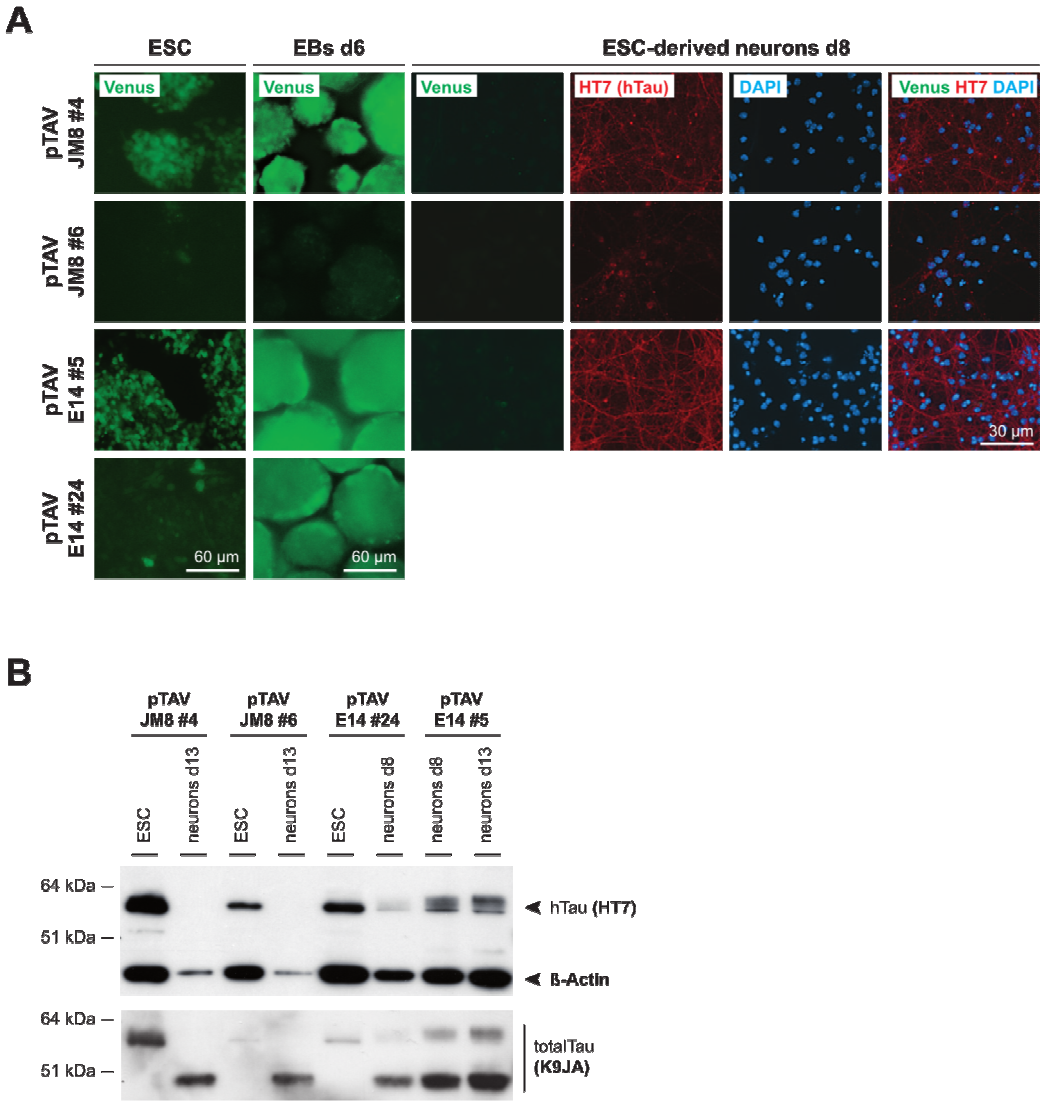

Fig. 3.21: Expression of transgenic Tau and Venus during neuronal differentiation of pCAG-Tau^{P301L}/APP^{swe}/Venus (pTAV) ESC lines
(**A**) Fluorescence images for monitoring of Venus expression and immunostaining for transgenic human Tau with HT7 antibody. Strong Venus expression was observed in 2 of the clones (JM8 #6 and E14 #5) in both ESC and neuronal progenitors (EBs d6). Correspondent postmitotic neuronal cultures of clones pTAV JM8 #6 and E14 #5 (d8 after EB dissociation) showed almost no Venus expression but positive immunostaining with HT7 suggested at least some expression of transgenic human Tau. (**B**) Immunoblotting with HT7 detected transgenic Tau expression levels in the ESC state that were largely consistent with the Venus fluorescence signal (**A**) in the same state. In the postmitotic neuronal state only clone pTAV E14 #5 showed clearly detectable amounts of transgenic human Tau but reprobing with antibody K9JA suggested that the level of transgenic human Tau expression was far below the expression level of endogenous mouse Tau. The observations of (**A**) and (**B**) suggested a strong reduction of CAG promoter driven transgene expression in postmitotic neurons. pTAV: pCAG-Tau^{P301L}/APP^{swe}/Venus; EBs: embryoid bodies; DAPI: nuclear marker; K9JA: total Tau; ß-Actin: loading control. Immunosamples of E14 #24 and the ESC Western Blot sample of E14 #5 were lost.

In order to assess the level of transgene expression at different stages of the neuronal differentiation, expression of Venus and Tau transgenes was analyzed in the ESC state, in the neuronal progenitor state (d6 after EB formation), and in the postmitotic neuronal

state (d8 and d13 after EB dissociation). Clone pTAV JM8 #6 showed consistent results, as in no differentiation stage expression of transgenes could be detected (**Fig. 3.21 A, B**). Clone pTAV E14 #24 showed only few Venus-expressing ESC, but exhibited medium expression levels of transgenic Tau in the ESC state and of Venus in the EB state (**Fig. 3.21 A, B**). In the postmitotic neuronal state, only very low expression of transgenic Tau was detectable by immunoblotting with HT7 for this clone. Clones pTAV JM8 #4 and E14 #5 exhibited strong expression of Venus in both the ESC and EB stage (**Fig. 3.21 A, B**). This was consistent with detection of strong transgenic Tau expression in the ESC state by HT7 immunoblotting for clone pTAV JM8 #4. Postmitotic neuronal cultures from clones pTAV JM8 #4 and E14 #5 were immunostained positive for transgenic Tau, but showed at maximum sparse Venus expression (**Fig. 3.21 A, B**). Analysis of the correspondent Western Blot samples revealed that the expression level of transgenic Tau was very low in case of clone pTAV JM8 #4 and low to medium in case of clone pTAV E14 #5 (**Fig. 3.21 B**). For a comparison of transgenic (human) and total (mouse and human) Tau expression levels, the blot was reprobed with K9JA antibody which recognizes Tau protein of both species with the same affinity. Transgenic human 2N/4R Tau can be conveniently distinguished from the endogenous Tau, as all expressed mouse Tau isoforms have a significantly smaller apparent molecular weight. According to the K9JA signal, transgenic Tau expression level was far below the expression level of endogenous Tau (**Fig. 3.21 B**). This indicated that at d8 and d13 after EB dissociation neurons derived from clone pTAV E14 #5 did not overexpress the transgenic human Tau.

In summary, pTAV ESC clones with the JM8 (BL6) and E14 (129) background could be differentiated successfully into *in vitro* cultures with high neuronal percentages (>90%) that were suited for analysis of transgene expression. In contrast, both pTAV ESC clones with the IDG3.2 background (BL6*129) failed to produce analyzable neuronal cultures. The results obtained from the neuronal differentiation of the pTAV JM8 and E14 clones suggested that between the clones the expected variation in the activity of the CAG promoter existed, as it was indicated by different transgene expression levels in the ESC state. The pattern of CAG activity variation ranged from very low to high and was mostly consistent for both Venus and transgenic Tau expression in the analyzed proliferation stages (ESC and EB state). In the postmitotic neuronal stage however, the picture changed drastically as only very low to medium transgene expression levels could be detected, even in clones that had exhibited high expression levels in the ESC state. The transgenic Tau was far from being overexpressed in the neuronal cultures when compared to the endogenous Tau expression level. As the overexpression of mutant Tau is considered to be a mandatory

prerequisite for the induction of Tau pathology (see section 2.2), the latter finding rendered it unlikely that the generated pTAV neuronal cultures could serve as a model for Tau pathology.

Most importantly, the transition from the proliferative to the postmitotic neuronal state seemed to reduce significantly the transgene expression level. From the obtained results it could not be concluded, if the decrease of detectable amounts of transgene products in the neuronal cultures was due to detrimental effects of the transgene expression itself or if the CAG promoter activity varied with the cellular context of the different developmental stages. As the extent of the reduction seemed to vary from clone to clone, the next logic step would have been a screening for pTAV clones with a high transgene expression level in the postmitotic neuronal state. However, results obtained in the meantime in the technically comparable pHygro-CAG-CreER^{T2} approach gave an important clue that influenced the further treatment of the pTAV approach. Therefore, first the data from the CreER^{T2} approach will be presented in the next section and then the conclusions from both approaches will be described comprehensively at the end of the next section.

3.4.4 Neuronal Differentiation of pHygro-CAG-CreER^{T2}-ESC and Analysis for CreER^{T2} Expression

For the derivation of neurons from the pHygro-CAG-CreER^{T2} ESC lines (ESC pHC), clones from all three genetic backgrounds that had been tested positive by PCR for the pHC construct (section 3.4.2) were cultured on gelatin and selected for indicators of pluripotency as described in section 3.1.2. Before neuronal differentiation, strong expression of CreER^{T2} was detected by antibody ERα (HC-20) as a band of an apparent molecular weight around 62 kDa (**Fig. 3.22 A**). Specificity of the antibody was verified by the absence of the band in wild type controls and the detection of CreER^{T2} in a brain sample of a GLAST-CreER^{T2} mouse, which expresses CreER^{T2} astrocyte-specific (Mori *et al.* 2006). The expression level of CreER^{T2} in all pHC ESC clones in the ESC state was very high compared to the GLAST-CreER^{T2} brain, because the latter signal was only clearly detectable after a 2 min exposure time (**Fig. 3.22 A**). Thus, all of the analyzed pHC ESC clones could be used for neuronal differentiation, but only one E14 pHC clone and one JM8 pHC clone were used as IDG3.2 pTAV clones had not produced analyzable neuronal cultures.

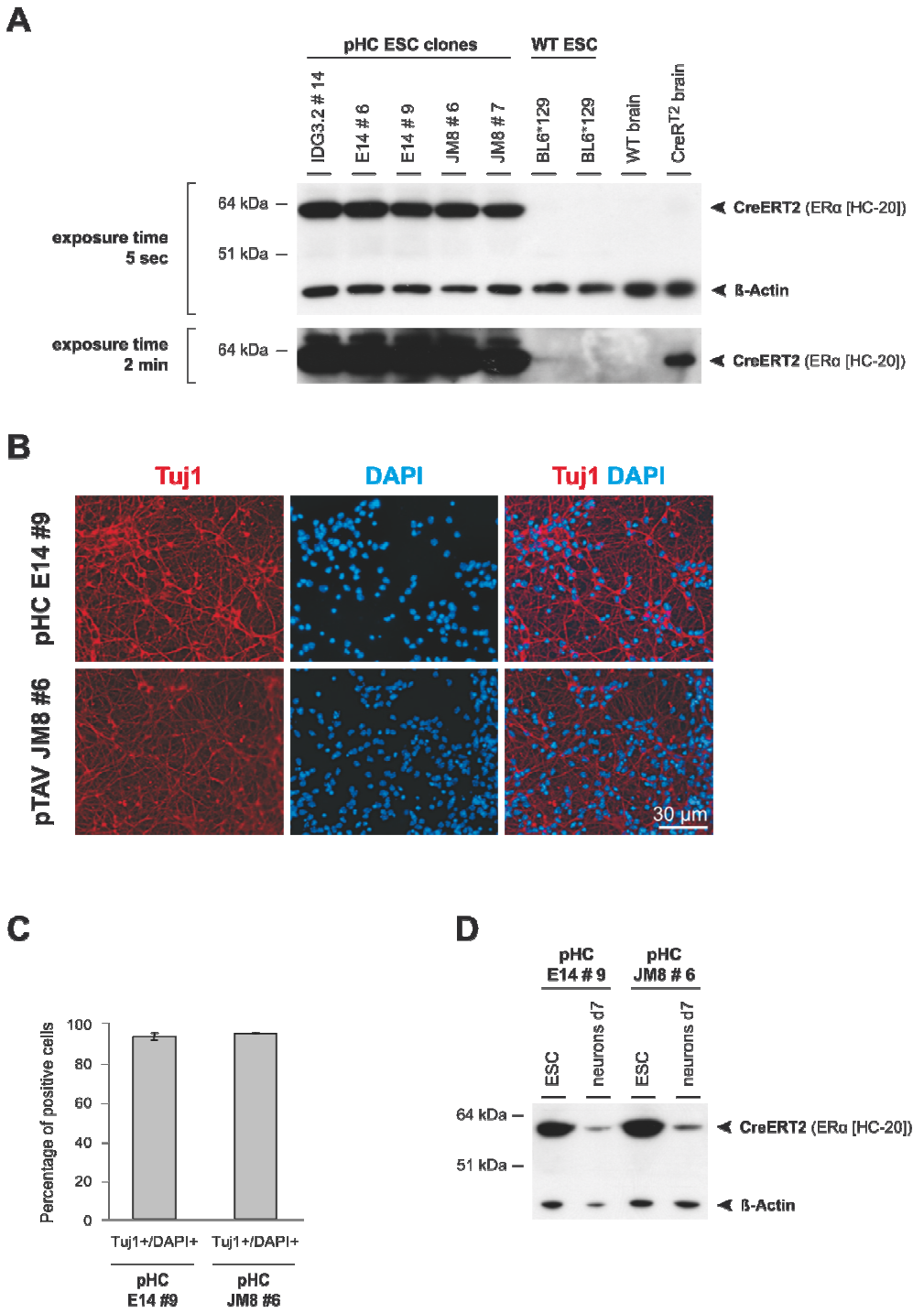

Fig. 3.22: Expression of CreER^{T2} during neuronal differentiation of pHygro-CAG-ER^{T2} (pHC) ESC lines via the Bibel & Barde protocol
(**A**) Immunoblotting with ERα [HC-20] detected strong CreER^{T2} expression in pHC ESC samples of all 3 backgrounds (IDG, E14, JM8) as a band of ~62 kDa. Specificity of antibody ERα [HC-20] was confirmed by detection of a ~62 kDa band in a GLAST-CreER^{T2} brain after longer exposure. (**B**) Immunostainings of pHC ESC-derived cultures for the neuronal marker Tuj1 at day 8 after dissociation of embryoid bodies. Lines of both backgrounds (E14: 129, JM8: BL6) showed neuronal percentages above 90% (**C**). (**D**) Analysis for expression of CreER^{T2} in the pHC ESC-derived neuronal cultures by immunoblotting with ERα [HC-20] suggested that CreER^{T2} expression was strongly reduced compared to the ESC state. DAPI: nuclear marker; ß-Actin: loading control.

Clones pHC E14 #9 and JM8 #6 were submitted to neuronal differentiation via the Bibel & Barde protocol and the resulting cultures were analyzed in terms of neuronal percentages and expression of CreER^{T2}. At day 7 after EB dissociation the cultures consisted of 93.2% (E14 #9) and 94.9% (JM8 #6) neurons, quantified as Tuj1^{+}/DAPI^{+} (**Fig. 3.22 B, C**). The expression level of CreER^{T2} at day 7 in the pHC ESC-derived neuronal cultures and in the ESC state was compared for each clone by immunoblotting with antibody ERα (HC-20). In both the E14 and the JM8 samples the CAG promoter-driven CreER^{T2} expression was drastically decreased in the postmitotic neuronal state (**Fig. 3.22 D**).

In summary, these results suggested that at some point in the transition from the ESC state to the postmitotic neuronal state the activity of the CAG promoter was strongly reduced by a developmental stage-dependent alteration in the cellular context. Detrimental effects of CreER^{T2} seemed very unlikely, because its expression in postmitotic neurons to my knowledge has not been reported to be harmful to the cell. This finding represented a crucial clue for the unclear situation of the strong decrease of transgene expression levels in post-mitotic neurons in the pTAV approach. The pHC and the pTAV approach were comparable in the way that they both used the same CAG promoter for transgene expression and the same vector integration principle of C31 integrase mediated recombination of a vector attB site with a genomic pseudo attP site. Because of this comparability, the observed CreER^{T2} reduction suggested that most probably also in the pTAV approach the activity of the CAG promoter was reduced due to alterations in the cellular context.

Taken together, the results from the pTAV and the pHC approach suggested, that the vector design in combination with the used integration principle was disadvantageous for the expression of transgenes in postmitotic neurons which were generated via the Bibel & Barde protocol. Because in the pTAV approach the neuronal transgene expression levels exhibited clone-dependent variation, the identification of a clone with the aspired strong postmitotic transgene expression seemed to be possible. However, as the screening procedure would have been very laborious and the success was very unlikely, it was not considered reasonable to pursue the pTAV approach any further.

4 Discussion

4.1 Generation and Characterization of iPSC lines

In this work, iPSC were generated from fibroblasts with efficiencies that varied between 0.0004% and 0.003%. Reprogramming efficiency is strongly dependent on the vector delivery system and was reported to be for example 0.0001% for a non-integrative system, 0.1% for a retroviral integrative system and 2% for a RNA delivery system (Gonzalez *et al.* 2011). Efficiencies are typically calculated by the number of iPSC colonies generated from donor cells that received the reprogramming vector which implies inaccuracy since transfection efficiency usually is estimated indirectly. The comparability of different reprogramming approaches is further complicated as their efficiency also depends on donor cell type, reprogramming factors and their stoichiometry, promoter system, amount of transfected DNA and efficiency enhancing treatments (Gonzalez *et al.* 2011). The treatments used in this work have been reported to increase reprogramming efficiency by ~100-fold in the case of valproic acid (Huangfu *et al.* 2008), by 5- to 10-fold in the case of vitamin C (Esteban *et al.* 2010) and by ~100-fold in the case of p53 ablation (Zhao *et al.* 2008). Due to these many variables, a direct comparison with other studies is difficult. Ye *et al*. (2010) used the same reprogramming cocktail (Sox2, Klf4, Oct4, cMyc) and the same vector integration principle (C31-integrase/attP-site) as in this work and obtained a reprogramming efficiency of 0.003% as in the most efficient case in this work. Because I used additionally combinations of the mentioned reprogramming efficiency enhancing treatments, the efficiency of my reprogramming approach must be regarded to be considerably lower. The origin of this discrepancy is difficult to trace and most probably lies in variations between both protocols as fibroblast quality, promoter system or other factors mentioned above.

In contrast, regarding the efficiency variations in this work that existed between different reprogramming protocols and fibroblasts of different genetic backgrounds (see section 3.3.1.2), several conclusions can be made. Concerning the reprogramming protocols, the protocol with vitamin C and codon-optimized C31 integrase (VitC+/C31 OE) clearly increased the reprogramming efficiency compared to the protocol without VitC and with the standard sequence C31 integrase (VitC-/C31). As for each line 2 electroporations were performed and pooled later, it seems unlikely that the increase is due to coincidental variations in the electroporations. In addition, Oct4 staining confirmed the presence of successfully transfected cells for both protocols. Because VitC and C31 OE were applied together, the increasing effect can not be clearly assigned. The mechanism how VitC increases reprogramming efficiency is considered

to be reduction of p53, acceleration of transcriptome changes during reprogramming and facilitation of conversion from pre-iPSC to iPSC (Esteban *et al.* 2010). As the reprogramming strategy included ablation of p53 by expression of a correspondent shRNA, a VitC-induced efficiency increase via p53 reduction seems unlikely. Besides the non-p53-mediated effects of VitC, the observed efficiency increase could also be due to the improved recombination capacities that have been observed for mouse codon-optimized C31 integrase (Raymond & Soriano 2007). This should result in a higher number of fibroblasts with integrated reprogramming vector and thus increase the number of obtained iPSC colonies.

Concerning the differences of reprogramming efficiencies that existed between fibroblast lines of different genetic backgrounds, two basic principles could account for this observation. First, the genetic background could influence the reprogramming process or the maintenance of the pluripotent state. For the derivation of mouse ESC from blastocysts which also requires pluripotency maintenance, strong genetic background influence has been reported (Batlle-Morera *et al.* 2008). This parallel continues, as the BL6 background is known to be recalcitrant to ESC-derivation (Batlle-Morera *et al.* 2008) and with no reprogramming protocol used in this work could iPSC be generated from BL6 fibroblasts. ESC-derivation on a BL6 background has been achieved by MEK pathway inhibition (Batlle-Morera *et al.* 2008) and simultaneous inhibition of MEK and GSK3 pathway inhibition has been shown to promote pluripotency maintenance in both ESC and iPSC (Ying *et al.* 2008; Feng *et al.* 2009). Thus, genetic background influences that possibly impaired iPSC generation from BL6 fibroblasts in this work might be overcome by adding small molecule inhibitors of MEK and GSK3 pathway to the culture medium. Second, the quality of the primary ear fibroblast culture could also influence the reprogramming process. Cultured fibroblasts accumulate DNA damages and cease to divide after a certain number of cell divisions, the latter is known as Hayflick limit or cellular senescence (Campisi & d'Adda di Fagagna 2007). Both aspects are most probably unfavorable for reprogramming and their impact increases with the number of fibroblast divisions. The primary ear fibroblast cultures used for iPSC generation in this work might have varied significantly in their number of executed cell divisions, depending on the amount of ear starting material and surviving cells. Thus, the percentage of cells which were unsuited for reprogramming due to senescence or DNA damage might have varied accordingly between the fibroblast cultures. This possible variation might be counteracted by preparing several primary ear fibroblast cultures for each line and keeping passage number at transfection as low as possible. Conclusively, both genetic background and

quality of primary ear fibroblasts might have accounted for varying reprogramming efficiencies.

Chromosome countings of the generated iPSC lines revealed, that only Tau^{P301S} lines had a percentage of correct metaphases above the critical threshold of 80% whereas the ones of hTau and BL6 C3 iPSC lines were significantly below 80% (see section 3.3.1.4). The overall genomic integrity might have been influenced by ablation of p53 during reprogramming. The protein p53, known as 'guardian of the genome' shuts down cell division when the DNA damage passes a critical threshold. Therefore it has been suggested, that gene silencing of *p53* increases reprogramming efficiency by preventing cells from exiting the cell cycle with the downside of possibly generating iPSC lines with an inferior DNA integrity (Marion *et al.* 2009). As this effect would have affected all lines equally, other mechanisms have to account for the observed differences in chromosome numbers. On the one hand, genetic stability variations between ESC lines have been reported to be influenced by the genetic background (Hughes *et al.* 2007). This influence could explain the differences in correct chromosome number that were observed between the generated iPSC lines although Tau^{P301S} and BL6 C3 should have the same background as BL6 C3 is the control strain for Tau^{P301S}. On the other hand, in ESC the percentage of cells with incorrect chromosome number increases with the passage number (Liu *et al.* 1997). As all counted iPSC lines were of passage number 8-10 it is unlikely, that different passage numbers accounted for the huge variations in correct chromosome number. Nevertheless, it would have been advantageous to evaluate chromosome numbers at earlier passages. At passage number 10, it can not be decided, if chromosomal aberrations already were inherent in the donor fibroblasts or if they accumulated during iPSC culture.

4.2 Variable Efficiency of Neuronal Differentiation of ESC and iPSC

Neuronal differentiation of ESC and iPSC in this work showed a wide range of efficiencies from yielding almost no neurons to almost 100% neurons and was found for all used genetic backgrounds and both neuronal differentiation protocols. This observation is in accordance with published studies, as distinct differentiation propensities for pluripotent stem cell lines have been reported for mouse ESC (Martinez *et al.* 2012), mouse iPSC (Kim *et al.* 2010), human ESC (Osafune *et al.* 2008) and human iPSC (Kim *et al.* 2010a). This might be due to the same differentiation potential of a homogenous PSC population or due to mixed differentiation potentials of a heterogeneous PSC population. Mouse ESC have been shown to be heterogeneous as they consist of individual cell types with distinct

differentiation potentials which is maintained in derived clones (Martinez *et al.* 2012). Clonal diversity regarding neuronal differentiation potential is also known for iPSC lines derived from the same donor cells (Hu *et al.* 2010; Devine *et al.* 2011).

This variation of differentiation propensity in ESC and iPSC is only partly understood and sometimes only vaguely explained by genetic background and epigenetic effects (Osafune *et al.* 2008), but some of the underlying mechanisms could be identified. Pluripotent ESC-populations have been characterized to be heterogeneous because undifferentiated, self-renewing ESC continuously oscillate between a 'naïve', ICM-like state (Stella$^+$) and a 'primed', epiblast-like state (Stella$^-$) (Hayashi *et al.* 2008). The authors found epigenetic mechanisms to be separating both pluripotency states. Marked differences in gene expression patterns in pluripotent mouse ESC clones were suggested to cause the distinct inherent differentiation propensities observed in ESC clones (Martinez *et al.* 2012). Obviously, oscillation between pluripotency states and cell inherent differentiation propensities are very likely to occur as well in iPSC. Generation of iPSC by reprogramming of somatic cells includes extensive epigenetic remodeling as e.g. DNA-demethylation of key pluripotency genes as Oct4 and Nanog (Hanna *et al.* 2010). The resulting iPSC clones can be epigenetically unique despite being derived from the same donor cells (Hu *et al.* 2010). The epigenetic differences are not considered to be inherent in the donor cells but to be introduced by reprogramming and the consequence of different reprogramming levels (Liu *et al.* 2010). Hence, distinct epigenetic regulation of gene expression is considered to influence the pluripotency status and the neuronal differentiation potential of iPSC clones. In fact, epigenetic silencing in the *Dlk1-Dio3* cluster has been shown to correlate with the pluripotency status of iPSC (Stadtfeld *et al.* 2010).

The distinct neuronal differentiation efficiencies observed in this work for ESC and iPSC were most likely caused by their pluripotency status or by distinct differentiation propensities which were caused by the mechanisms detailed above. Only some of the PSC lines subjected to neuronal differentiation were analyzed for the expression of pluripotency markers (section 3.3.1.3). Therefore it can not be excluded that the PSC lines with low neuronal differentiation efficiencies were not fully pluripotent. The most representative analysis for correlating the PSC pluripotency status with their neuronal differentiation capacity would have been a staining for pluripotency markers of the PSC after at least two feeder-free passages, because cells of this state were used for all neuronal differentiation protocols. The identification of PSC lines with a good neuronal differentiation capacity was performed in this work by submitting several PSC lines to

neuronal differentiation and selecting the best performing. As this is very laborious and time consuming, a more straightforward method would be desirable.

Three basic approaches can be imagined to improve the efficiency of neuronal differentiation of PSC. First, a marker indicating the neuronal differentiation potential of a PSC line would be of great help. PSC lines can vary markedly in their differentiation potential despite similar expression levels of classic pluripotency markers as Oct4 and Nanog (Osafune *et al.* 2008). The differential methylation of the *Dlk1-Dio3* region and the expression of the correlated miRNA cluster might prove useful as a marker for the pluripotency status of PSC (Liu *et al.* 2010). As activation of the *Dlk1-Dio3* region correlates with the capacity of iPSC to generate mice by tetraploid complementation (Stadtfeld *et al.* 2010), the gold standard for true pluripotency (Zhao *et al.* 2009), it should also correlate with good neuronal differentiation capacity. Second, the above mentioned heterogeneity of a PSC population should be counteracted, especially when cells are cultured on gelatin which is known to promote undirected differentiation of PSC. Differentiated cells are not amenable for the neuronal differentiation but can persist and generate an overgrowth of non-neuronal cells in the generated cultures. It seems to be possible to 'homogenize' and stabilize a PSC population in the 'naive', ICM-like state by treatment with GSK3b and ERK1/2 inhibitors which reverts PSC from epiblast-like to ICM-like state (Hanna *et al.* 2010). Third, robustness of neuronal differentiation protocols can be improved by suppressing non-neuronal differentiation. Simultaneous inhibition of Activin/Nodal and BMP pathways with small molecules has been shown to enhance neural differentiation of human PSC despite distinct line-inherent neural differentiation propensities (Kim *et al.* 2010a).

Taken together, the different neuronal differentiation capacities of ESC and iPSC observed in this work seemingly mirrored the well-studied variability of PSC lines. The identification of PSC lines suited for neuronal differentiation was retarding the overall progress of this work due to imperfect methods for assessing PSC differentiation propensity and due to the low robustness of available neuronal differentiation protocols. This unsatisfying situation could be improved by the development of a bona fide marker for PSC differentiation propensity, stabilizing the PSC population in a 'naive', ICM-like state and by using Activin/Nodal and BMP pathway inhibitors to increase the robustness of neuronal differentiation protocols.

4.3 Incomplete Maturation and Mixed Neuronal Identities of PSC-Derived Neurons

4.3.1 Incomplete Maturation and Differentiation in Neuronal Cultures Generated via the Gaspard & Vanderhaeghen Protocol

The cultures generated in this work via the Gaspard & Vanderhaeghen protocol that showed the highest neuronal yield consisted largely of immature neurons and a considerable part of neural stem cells (NSC, Nestin$^+$) at d18 after monolayer dissociation (see section 3.2.2). This finding was unexpected, because in the first description, the cultures are composed of less than 10% are NSC and more than 50% fully mature neurons at d7 after monolayer dissociation (Gaspard *et al.* 2008; Gaspard *et al.* 2009). As I followed exactly the instructions of the Gaspard & Vanderhaeghen protocol and a full neuronal maturation status was imperative for this part of the work, the crucial question is how this discrepancy in the maturation status could come about.

An obvious difference of the results from this work to the work of Gaspard *et al*. (2008), was the existence of large cell clumps with NSC in the cultures after dissociation of the monolayer (section 3.2.2, **Fig. 3.7 A**). At the day of monolayer dissociation, most cells are NSC and the plating of single cells is critical for achieving optimal neuronal differentiation (Gaspard *et al.* 2009). The underlying mechanism is the disruption of Notch signaling, which is a juxtacrine signal system requiring direct cell-cell contact. In NSC, notch signaling maintains the cell in its progenitor state and possibly even stimulates its proliferation. Thus, Notch signaling inhibits neuronal differentiation of neighboring NSC. *In vivo*, a correct differentiation cue causes the NSC to become a postmitotic neuron (Louvi & Artavanis-Tsakonas 2006). *In vitro*, the inhibition of neuronal differentiation by Notch signaling is interrupted by dissociation of the NSC as Notch signaling requires directly neighboring cells. As complete separation of NSC in the monolayer dissociation step was not successful in this work, continuing Notch signaling most probably was responsible for the persistence of NSC (Nestin$^+$) in the cell clumps.

The incomplete maturation observed for the PSC-derived neurons (section 3.2.2, **Fig. 3.7 B**) might be a consequence of relatively high numbers of neural progenitors that conditioned the culture medium. Neural progenitors do secrete growth factors into the medium (Zhang *et al.* 2006) and growth factors as FGF2 have been shown to impair neuronal maturation (Chen *et al.* 2007). Thus, the high number of persisting neural progenitors could have caused a conditioned medium that was unfavorable for complete neuronal maturation.

I envisaged two possibilities that to overcome the problem of persisting NSC and the supposedly incomplete maturation: First, improved dissociation of NSC and second, inhibition of Notch signaling. Better dissociation of the monolayer is not trivial as NSC are very sensitive and easily die by too harsh pipetting. Inhibition of Notch signaling has been shown to accelerate neuronal differentiation *in vitro* (Crawford & Roelink 2007; Borghese *et al.* 2010). As the implementation of both approaches would have meant considerable effort and the parallel approach based on the Bibel & Barde protocol seemed more promising, I decided to focus first on the better working approach which is discussed in the next section.

4.3.2 Partial Maturation of Neuronal Cultures Generated via the Bibel & Barde Protocol

The neurons generated in this work by the Bibel & Barde protocol began to show characteristics of fully mature neurons 10-14 days after EB dissociation. These results suggested that after 3 weeks only a part of the neurons was fully mature or that the individual degree of maturation was incomplete. In contrast to the Gaspard & Vanderhaeghen protocol (see previous section), neuronal progenitors could be plated as single cells so that clumping of cells could not impair maturation. In the initial publications of the Bibel & Barde protocol (Bibel *et al.* 2004; Bibel *et al.* 2007), markers of fully mature neurons as Glutamate Receptor 1 and Synaptophysin were detected already 5 days after EB dissociation, but this could be due to a more sensitive detection method or a higher neuronal percentage. In this work I considered the maturation to be incomplete at day 21 since the levels of maturation markers (VGLUT2, Synaptophysin and adult Tau isoforms) did not reach a plateau as their level was higher at day 21 compared to day 14. It is conceivable that growth of neuronal processes of mature neurons could account for this increase, but I would expect a weaker effect considering that the neurons already had 2 weeks to form connections. However, MAP2 staining suggested that already at day 10 almost all neurons were fully mature, thus supporting the idea of assigning the maturation marker increase to neuronal outgrowth. As some MAP2 proteins are already expressed in immature neurons, the MAP2 staining could possibly be unspecific and also detect immature neurons. The expression of the two maturation markers associated with synapses (VGLUT2 and Synaptophysin) was considerably lower in the PSC-derived cultures compared to an adult brain. This could be due to a decreased synaptogenesis because the *in vitro* neurons have one dimension (2D versus 3D) and many neuronal inputs less than *in vivo* neurons. Thus, the neurons could be as mature as in the brain but only form less synapses. Contradicting a fully mature PSC-derived neuronal population is

the observation that at d21 the PSC-derived neurons expressed higher levels of the embryonic Tau isoform than of the adult Tau isoforms.

Considering these contradicting observations, the most logic interpretation is that only a part of the PSC-derived neurons achieved full maturation whereas the other part was still immature at day 21. This heterogeneity in maturation has been described by others and is considered to be detrimental, especially for the analysis of late-onset phenotypes (Dolmetsch & Geschwind 2011). More analyses, including immunostainings for other maturation markers and electrophysiological characterization, would be necessary for obtaining a clearer picture of the maturation of PSC-derived neurons. Inhibiting Notch signaling in the late NSC phase of the Bibel & Barde protocol might synchronize and accelerate neuronal maturation (Crawford & Roelink 2007; Borghese *et al.* 2010).

4.3.3 Heterogeneous Neuronal Identities in Cultures Generated via the Bibel & Barde Protocol

The ESC-derived neuronal cultures generated in this work via the Bibel & Barde protocol were quite heterogeneous and contained different neuronal identities such as of forebrain, mid-hindbrain, motor neurons and glutamatergic and GABAergic neurons. As the neuronal identity required for this part of the work was cortical glutamatergic and the neuronal cultures generated in the original publications were characterized to consist to 90% of exactly this cell type (Bibel *et al.* 2004; Bibel *et al.* 2007), the crucial question was, what could have been the reason for this discrepancy.

Bibel *et al.* (2004, 2007) state, that the usage of ESC with a high proliferation rate and a homogenous morphology is the most crucial prerequisite for obtaining a homogenous culture of 90% glutamatergic dorsal forebrain neurons. Accordingly, only ESC with the described characteristics will respond to the retinoic acid induction with becoming $Pax6^+$ radial glial cells which then differentiate into cortical glutamatergic neurons as they do *in vivo* (Malatesta *et al.* 2003). In this work, the criteria described for the ESC by Bibel *et al.* (2004, 2007) were recapitulated as close as possible. However, as some of these criteria are quite subjective it was difficult to evaluate, how closely the state of the ESC used in this work resembled the state of the ESC used by Bibel *et al.* (2004, 2007). The indication of more objective parameters, as for example the expression of pluripotency markers, would be helpful to overcome this inaccuracy. Therefore it is possible, that the observed heterogeneity in neuronal identities was exclusively due to an imperfect recapitulation of the homogeneous, highly proliferative ESC population as used by Bibel *et al.* (2004, 2007).

From another viewpoint, Bibel *et al.* (2004, 2007) characterized the generated neurons only superficially. The statement that the generated neurons have a cortical glutamatergic identity is mainly based on the observation that more than 80% of the progenitors are Pax6 positive and that 93% of the neurons are VGLUT1 positive (Bibel *et al.* 2004). As Pax6 is widely expressed during early development and VGLUT1 also occurs in non-cortical neurons, the ESC-derived neurons could also be of another than the proposed cell type (Glaser & Brüstle 2005). A more detailed study suggested that the neurons generated via the Bibel & Barde protocol are not bona fide cortical glutamatergic neurons due to the lack of typical characteristics (Ideguchi *et al.* 2010). Kim *et al.* (2009) followed the Bibel & Barde protocol and although the majority of the neurons were glutamatergic, many cells expressed the non-cortical marker Hoxb4.

The heterogeneity observed in the neuronal cultures generated in this work might have also been promoted by retinoic acid (RA). *In vivo*, RA is involved in anteroposterior patterning of the neural tube where it suppresses expression of anterior genes (Maden 2007). *In vitro*, high concentration of RA has been reported to be a strong neural inducer whereas the anteroposterior patterning effect of RA has been reported to be concentration dependent (Okada *et al.* 2004; Kim *et al.* 2009). In an EB-based protocol (RA: 2d-/4d+), RA concentrations higher than 10 nM almost completely abolished expression of forebrain and midbrain markers and promoted expression of hindbrain and spinal cord markers in neural progenitors, which provides evidence for the caudalizing role of RA (Okada *et al.* 2004). As comparison, the Bibel & Barde protocol uses 5 µM RA in a 4d-/4d+ protocol and yields supposedly glutamatergic forebrain neurons (Bibel *et al.* 2007). As a solution for reconciling this obviously contradicting observations, it has been hypothesized, that under certain circumstances, RA inhibits caudalizing Wnt signaling and thereby promotes induction of anterior $Pax6^+$ radial glia (Glaser & Brüstle 2005). Accordingly, Bibel *et al.* (2004) were successful in generating these conditions, but as these were defined quite subjectively, others (Kim *et al.* 2009; Ideguchi *et al.* 2010) and this work, were not successful in recapitulating them. The observed resulting heterogeneity of the ESC-derived neurons might not only be due to the ESC state (see above), but also to a combinatory effect of embryoid body (EB) morphology and the dependency of the RA regionalization effect on concentration. As diffusive transport of RA is influenced by EB morphology (Sachlos & Auguste 2008), the cells in an EB will be exposed to different RA concentrations. This heterogeneity could be increased further by the variability of the EBs, which typically vary in their size by at least factor two and additionally in their form. Considering the concentration-dependent effect of RA on the induction of different regional neuronal identities (Okada

et al. 2004), this heterogeneity caused by EB morphology could well explain for the heterogeneity in neuronal identities observed in this work.

In summary, the protocol published by Bibel *et al.* (2004, 2007) yields a homogeneous population of cortical glutamatergic neurons only under certain conditions. The obtained neurons seem to correspond only partly to *in vivo* cortical glutamatergic neurons. As it is, the Bibel & Barde protocol seems well suited for the fast and efficient generation of heterogeneous neuronal cultures from PSC. From a pragmatic viewpoint, it thus constitutes an attractive tool for model systems based on PSC-derived neurons, but conclusions regarding their *in vivo* counterpart should be drawn with precaution. The heterogeneity of the ESC-derived neurons in this work was probably due to a non-homogeneous ESC population and to a variable RA effect because of the influence of EB morphology.

4.4 Different Promoter Suitabilities for Driving Transgene Expression in PSC-Derived Neurons

The four promoter systems used in this work yielded different levels of transgene expression in PSC-derived neurons. An onset of promoter activity latest within the first week after plating of progenitors and overexpression of the transgene were considered as mandatory prerequisites for being able to study Tau pathology. The promoter activities seemed to be influenced by maturation and cell type in different ways.

4.4.1 Thy1.2 Promoter

Thy1.2 promoter was used in this work because it controls expression of transgenic Tau and APP in the 3xTg AD mouse model (Oddo *et al.* 2003) which was used for the derivation of 3xTg AD ESC and iPSC lines (see section 3.1 and 3.2). The 3xTg AD model contains the Thy1.2 expression cassette which drives strong constitutive transgene expression in CNS neurons of transgenic mice. Transgene expression is reported to begin at P6-10 and to establish the final expression level before P14 (Caroni 1997). However, for the 3xTg AD model, threefold overexpression of transgenes has been reported for E15 3xTg AD cortices (Smith *et al.* 2005) and for E15-18 3xTg AD primary cortical cultures at day 11 *in vitro* (Vale *et al.* 2010). In the adult brain, transgenes are 6-8 fold overexpressed (Oddo *et al.* 2003). Thus, full onset of transgene expression by Thy1.2 promoter seemingly requires fully mature neurons. The expression pattern in the CNS seems to be strongly dependent on the integration-site of the construct, as different transgenic lines using Thy1.2 promoter exhibited transgene expression in different highly restricted neuronal populations (Caroni 1997).

Strong overexpression of transgenes and a clearly confined activity pattern make the Thy1.2 promoter attractive for a transgenic AD model. Overexpression facilitates aggregation of Tau and APP and expression in mainly AD-relevant regions avoids a motor phenotype appearing when Tau is overexpressed in spinal cord, which would preclude behavioral studies (Eckermann *et al.* 2007). In the 3xTg AD model, transgenic Tau and APP are mainly expressed in the AD-relevant regions of cortex and hippocampus (Oddo *et al.* 2003). Additionally, at least in the 3xTg AD model, Thy1.2 promoter activity seems also to be strongly influenced by the genetic background (Jochen Herms and Thomas Floss, personal communications; results from this work, see section 3.1.2.4)

In this work, Thy1.2 promoter driven expression of transgenic Tau was analyzed in three types of 3xTg AD PSC-derived neuronal cultures which had been generated by 3 different approaches: (1) heterozygous 3xTg AD ESC-derived neurons, generated via Gaspard & Vanderhaeghen protocol (section 3.1.2.4), homozygous 3xTg AD iPSC-derived neurons generated via (2) Gaspard & Vanderhaeghen protocol (section 3.2.2.) and via (3) Bibel & Barde protocol (section 3.2.3.). In none of them could expression of transgenic Tau be detected. Considering the activity properties of Thy1.2 promoter detailed above and the findings from this work, the inactivity of Thy1.2 promoter was probably due to different reasons in each of the three approaches. For approach (1), the genetic background was identified to primarily impair activation in heterozygous 3xTg AD ESC-derived neurons because it did so in the correspondent heterozygous 3xTg AD brains (section 3.1.2.4, **Fig. 3.4**). The genetic background of a mouse model can have a strong influence on the phenotype due to differential gene expression (Doetschman 2009). The Thy1.2 promoter seems to be very sensitive to cues that vary with the cellular context as demonstrated by its confined activity pattern which distinguishes between specific neuronal populations (Caroni 1997). Hence, the Thy1.2 promoter might also be very sensitive to cues that vary with the genetic background due to differential gene expression. This might therefore be responsible for the inactivity of Thy1.2 promoter on the genetic background used in this work as it was not the same as used by Oddo *et al.* (2003). In approach (2), the genetic background was identical to the one of Oddo *et al.* (2003) but the degree of maturation of the PSC-derived neurons resembled embryonic neurons (section 3.2.2 **Fig. 3.7 B**). As full neuronal maturation is mandatory for full activation of the Thy1.2 promoter (Caroni 1997), the immaturity of the cultures explains for its observed inactivity. In approach (3), the cultures seemed to be mature enough to activate Thy1.2 promoter, but neuronal identities which exhibit Thy1.2 promoter activity *in vivo*, constituted only a part of the PSC-derived neuronal population. This observation yielded a plausible explanation for

the absence of transgene expression (section 3.2.4.2). Taken together, the Thy1.2 promoter turned out to be very unsuitable for transgene expression in PSC-derived neurons due to its strictly confined expression pattern in the 3xTg AD model.

4.4.2 Prion Promoter

The Prion promoter MoPrP (Borchelt *et al.* 1996) was used in this work in the context of iPSC derived from the Tau^{P301S} mouse model (Yoshiyama *et al.* 2007). In the Tau^{P301S} mouse 5 fold overexpression of transgenic Tau is controlled by the Prion promoter. *In vivo*, the activity of Prion promoter is observed throughout the CNS and starts around E11.5 when cells become postmitotic (Tremblay *et al.* 2007). In the neuronal *in vitro* differentiation, the transition to the postmitotic state correlates with the onset of Tuj1 expression. According to the Bibel & Barde protocol, the cells become postmitotic few days after plating of the progenitors (Bibel *et al.* 2004) and the ESC-derived cultures in this work expressed similar levels of Tuj1 at d7 and d21 (section 3.2.4.1, **Fig. 3.10 B**) indicating that most of the cells were postmitotic at day 7. Additionally, 2 days after plating of progenitor cells, the antimitotic AraC (cytosine arabinoside) was added to the culture medium to select for postmitotic cells. Thus, the absence of Prion promoter-driven Tau expression at day 7 (section 3.3.2, **Fig. 3.15 C**) is in contrast to the fact, that at this day of culture most of the cells were considered to be postmitotic. As expression of transgenic Tau in Tau^{P301S} iPSC-derived neurons was detected earliest at d10 and expression did not reach the level observed in Tau^{P301S} adult brain (section 3.3.2, **Fig. 3.15 C**), important prerequisites for the full activation of the Prion promoter seemed to be lacking. Obviously, the Prion promoter required *in vitro* a higher degree of neuronal maturation than only the postmitotic status. This might be an artifact of *in vitro* culture conditions or an uncharacterized feature of the Tau^{P301S} model. As neuronal *in vitro* maturation was not completed at d14 (section 3.2.4.1, **Fig. 3.10 B**), Prion promoter activation might have been still increasing. On the other hand, the Bibel & Barde protocol might produce neurons that do not fully correspond to *in vivo* neurons (Ideguchi *et al.* 2010), thus these neurons might fail to recapitulate crucial aspects of CNS neurons that are necessary for full activation of the Prion promoter. In conclusion, the Prion promoter was shown to be suited for medium transgene expression levels in PSC-derived neurons. For studies in which early onset and high levels of transgene expression are required, the Prion promoter did not seem well suited.

4.4.3 Human MAPT Promoter

In this work, the human MAPT promoter was used in the context of iPSC derived from the hTau mouse model where it drives overexpression of human Tau (Andorfer *et al.* 2003). In humans and rodents MAPT promoters drive strong and neuron specific expression of Tau protein (Buee *et al.* 2000). Tau expression starts before gestational week 20 in humans and around E15 in mice (Kampers *et al.* 1999; Takuma *et al.* 2003). Neuronal *in vitro* differentiation of a mouse ESC line with an EGFP knockin in the endogenous *mapt* locus revealed, that Tau expression starts within the first week after plating of progenitors and correlated with Tuj1 expression (Wernig *et al.* 2002; Bibel *et al.* 2004). Thus, Tau protein in humans and mice seems to be expressed shortly after neuronal cells become postmitotic. The activity of human MAPT promoter in the mouse has not been completely analyzed, but robust expression of human MAPT promoter-driven Tau before P6 has been reported (McMillan *et al.* 2008). In the hTau iPSC-derived neurons, expression of transgenic Tau reached almost final adult levels as early as d7, indicating an earlier onset of human MAPT promoter (section 3.3.3, **Fig. 3.16 C**). This observation is in line with the reported expression pattern of mouse Tau and suggests that the transgenic human MAPT promoter in the hTau model is activated at a comparable neuronal developmental stage as it is the case for the mouse MAPT promoter.

The switch from the expression of embryonic to adult Tau isoforms occurs in wild type mice around P6. In contrast, when the entire human MAPT gene is expressed in mouse Tau knockout mice (thus genetically similar to the hTau mouse model) the switch from embryonic to adult Tau occurs around P24 (McMillan *et al.* 2008). This indicates that the human and mouse MAPT promoters react differently to developmental cues in the maturing neuron. In 6 month old hTau mice all human Tau isoforms are expressed (Andorfer *et al.* 2003). This suggests, that the hTau iPSC-derived neurons in this work expressed only the embryonic Tau isoform (0N/3R) because the human MAPT promoter delayed the switch to the adult isoform, or because the neurons were not fully mature at day 14 after plating of progenitors (section 3.3.3, **Fig. 3.17 C**). As the expression of all 6 isoforms seems to be a prerequisite for Tau pathology (Andorfer *et al.* 2003), a more detailed analysis of Tau isoform expression in wildtype and hTau iPSC-derived neurons, e.g. at d14 and d21, is necessary to thoroughly evaluate the usability of this model for the analysis of Tau pathology. In conclusion, the human MAPT promoter seems to be excellently suitable for strong expression of transgenes in PSC-derived neurons.

4.4.4 CAG Promoter

In this work, the CAG promoter was used to drive transgene expression in the pTAV and pHC constructs in ESC-derived neurons; the expression vectors were integrated via C31 integrase (section 3.4). The widely used CAG promoter consists of a cytomegalovirus (CMV) enhancer and a chicken beta-actin promoter and has been shown to produce high transgene expression levels in all cell types at all developmental stages (Hitoshi *et al.* 1991; Okabe *et al.* 1997; Pratt *et al.* 2000). The C31 integrase has been derived from a *Streptomyces* phage and catalyzes the recombination of short recognition sites *attP* (39 bp, phage attachment site) and *attB* (34 bp, bacterial attachment site). Mammalian genomes contain attP and attB sequence homologues, termed 'pseudo attP' and 'pseudo attB' sites that are recognized by C31 integrase. The mouse genome exhibits at least 57 pseudo attP sites. These are targeted with different frequencies when the C31 integrase approach is used for transgene integration (Thyagarajan *et al.* 2001). Usually, only a single copy per cell is integrated and integration events mostly occur in intergenic regions (Ye *et al.* 2010).

The observation that transgene expression levels in pTAV ESC in the ESC state varied significantly between clones (section 3.4.3, **Fig. 3.21**) could result from vector integration at different pseudo attP sites with site-specific vector activation characteristics. In apparent contradiction to this hypothesis were the little variability in transgene expression levels in the ESC state in the pHC ESC clones which were all comparably high (section 3.4.4, **Fig 3.22**). This discrepancy can be reconciled when considering that the pTAV and the pHC vectors differed in their size (9.4 kb and 5.7 kb) and in their sequence. Both could account for a preferential integration of the pHC vector at pseudo attP sites in genomic regions that are highly activated in ESC. An imaginable mechanism could be a sequence homology between the pHC vector and a flanking region of a 'high activity' pseudo attP site. Such a sequence homology could possibly greatly increase the affinity of a vector to a certain pseudo attP site. The strong reduction of CAG promoter-driven expression of transgenic Tau and $CreER^{T2}$ in neurons derived from pTAV and pHC ESC clones (section 3.4, **Fig. 3.21, 3.22**), suggested that a common and transgene-independent mechanism was causative for this observation. As the CAG promoter can be highly active throughout the brain (Novak *et al.* 2000) and in ESC-derived neurons (Haupt *et al.* 2007), the approach of this work must contain factors, that are detrimental to full CAG promoter activity in neurons. Conceivable factors are: First, pTAV and pHC vectors could have been integrated preferentially at pseudo attP sites which are located in regions that become silenced in neurons. In this scenario it is imaginable, that also clones with other

integration sites and accordingly no or little silencing were generated, but that these clones were not detected in the screening. The influence of the integration site on the allover activation or tissue-specific silencing of transgene expression is a well known problem in the generation of transgenic models and termed 'positional effect' (Wallace *et al.* 2000). Second, transgene expression could have been repressed by the artificiality of neuronal *in vitro* differentiation. Retinoic acid at high concentration could have unknown epigenetic effects or the generated neurons do not fully recapitulate the factors, that permit the reported full CAG promoter activation in *in vivo* neurons (Novak *et al.* 2000). Third, a crucial factor for enabling full CAG promoter activation might have been present in the ESC and EB culture conditions, but not in the neuronal culture conditions. For example, ESC and EB medium contained fetal calf serum which is composed of many biologically active factors, but ESC-derived neurons were cultured serum-free.

In conclusion, the variability of CAG promoter driven transgene expression in the ESC state seemed to be due to positional effects. For the strong reduction of CAG promoter activation in neurons as well positional effects or *in vitro* artifacts might have accounted. As a result, CAG promoter driven transgene expression in combination with integration via C31 integrase and genomic pseudo attB sites seemed to be very unsuited for the envisaged purpose. As the supposed effects might be inherent in the C31 integrase – pseudo attP site approach, the general usability of the CAG promoter for strong expression of transgenes in PSC-derived neurons can not be reliably evaluated. A possibility to overcome uncontrolled silencing of transgenes has been reported to be targeting of the *ROSA26* locus which is not affected by chromatin configurations that could lead to transcriptional repression of inserted transgenes (Chen *et al.* 2011).

4.5 Tau Hyperphosphorylation in iPSC-Derived Neurons Occurs Only Upon Phosphatase Inhibition

No Tau hyperphosphorylation was observed in Tau^{P301S} and hTau iPSC-derived neurons under standard conditions (section 3.3.4) but in the correspondent mouse brains, Tau gets hyperphosphorylated (Andorfer *et al.* 2003; Yoshiyama *et al.* 2007). This indicated that the *in vitro* neurons differed from their *in vivo* counterparts in aspects that are important for Tau pathology. As mentioned earlier (section 2.2), overexpression of transgenic Tau and the ratio of Tau isoforms are considered to influence the onset of Tau pathology. Low transgenic Tau levels in Tau^{P301S} iPSC-derived neurons and the absence of adult Tau isoforms in hTau iPSC-derived neurons could therefore explain the absence of Tau hyperphosphorylation. The fact, that the

iPSC-derived neurons did not fulfill the technical requirements of a typical Tau pathology model provides a sufficient explanation for the absence of Tau hyperphosphorylation.

In addition, after 2 weeks of culture the iPSC-derived neurons probably did not resemble 5-6 month old neurons of an adult brain by means of aging. In the used models, 5-6 months of aging are required before Tau pathology is observed (Andorfer *et al.* 2003; Yoshiyama *et al.* 2007). Aging is associated with several processes that can trigger Tau hyperphosphorylation, e.g. increased levels of ROS (reactive oxygen species) or a dysregulation of ion homeostasis. Additionally, age-related changes as an increased ROS-induced DNA and protein damage and a decreased function of the protein shaping and clearance machineries favor the aggregation of proteins (Mattson & Magnus 2006). This can explain that aged neurons are more vulnerable for aggregation of Tau and it has been hypothesized, that damaged, malfunctional Tau protein gets hyperphosphorylated to reduce the negative consequences of its erroneous interaction with other proteins (Morris *et al.* 2011). All these age-related triggers of Tau pathology might have been absent in the 2 week old iPSC-derived neurons, which could have contributed to the absence of Tau pathology. Another aspect is that Tau pathology could be promoted by non-cell autonomous effects in the Tau^{P301S} and hTau mouse brains, e.g. by influences of glia cells. These influences would probably be lacking in the iPSC-derived neuronal cultures. On the other hand, overexpression of mutated Tau in cell culture models can produce Tau hyperphosphorylation and aggregation within weeks, suggesting the cell culture condition to increase significantly the vulnerability of the cells (Brandt *et al.* 2005; Hall & Yao 2005; Wang *et al.* 2007). However, the few studies that used PSC-derived neurons for the expression of mutated Tau (Iovino *et al.* 2010) or that used AD patient iPSC-derived neurons (Israel *et al.* 2012) only report maximum 1-2 hyperphosphorylated sites and no aggregation of Tau protein, suggesting at best a mild Tau pathology. The best way to gain insight into the mechanisms that are causative for this discrepancy would be the overexpression of the same Tau mutation in a mouse, primary neurons, other cellular systems (N2a, SH-SY5Y) and in PSC-derived neurons. A thorough comparison of these systems regarding Tau pathology and parameters indicative of aging should contribute to our understanding which parameters are crucial for Tau pathology and are therefore imperative to be recapitulated in a model based on PSC-derived neurons.

Moreover, the onset of Tau pathology in the iPSC-derived neurons might have been hampered by their heterogeneous neuronal identities. In the Tau^{P301S} and hTau models the most affected brain regions are cortex and hippocampus (Andorfer *et al.*

2003; Yoshiyama *et al.* 2007). The presence of neurons of other regional identities in considerable quantities in the iPSC-derived cultures (section 3.2.4.2) might have contributed to the absence of Tau hyperphosphorylation in the Tau^{P301S} and hTau neurons *in vitro*.

Oxidative stress through BSO treatment similar to this work has been shown to induce Tau hyperphosphorylation in neuroblastoma cells (Su *et al.* 2010). In this work, only normally phosphorylated Tau could be observed after BSO treatment in both mutant and wild type iPSC-derived neurons which indicated that the Tau^{P301S} and hTau neurons were not more susceptible to oxidative stress (section 3.3.4). However, as no ROS or GSH levels were determined, an ineffectiveness of the BSO treatment could not be excluded.

Okadaic acid (OA) treatment of primary neuronal cultures with conditions similar to this work increased the phosphorylation level of Tau at several sites. A strong phosphorylation increase was detected at the AT8 and 12E8 epitopes whereas only a weak increase was detected at the AT270 and PHF-1 (pS396/pS404) epitopes (Jin *et al.* 2011). In this work, the effect of OA treatment was quite similar, as it caused a strong increase in signal intensity in case of the AT8 and 12E8 antibodies, but not in case of the AT270 and pS396 antibodies. The absence of an increase for AT270 and pS396 most probably was due to a detection artifact because of low specificity of the antibodies to the correspondent phospho-epitope. As the successful phosphatase inhibition by OA was confirmed by AT8 and 12E8, and the inhibited phosphatases are also active at the AT270 and pS396 epitopes (Iqbal *et al.* 2009), partial inhibition of phosphatases can be excluded as causative factor. Because more than 10 kinases with overlapping phosphorylation sites can phosphorylate Tau (Buee *et al.* 2000), a lack of Tau hyperphosphorylation at the AT270 and pS396 epitopes due to differential kinase activity seems also unlikely. However, the OA treatment proved to be a valuable method to verify the functionality of the detection method. Thus, the absence of hyperphosphorylation was really a significant finding and not due to a loss of the phospho-epitope during sample processing.

Taken together, the iPSC-derived neurons did not exhibit Tau hyperphosphorylation or an increased sensitivity to oxidative stress and phosphatase inhibition. This indicated that crucial parameters such as transgenic Tau expression level or its isoform expression ratio did not enable the development of Tau pathology. Beyond these technical prerequisites, the iPSC-derived neurons were probably lacking aging-dependent and non-cell autonomous triggers that might promote Tau pathology in the mouse model. Thus, every Tau pathology model based on PSC-derived neurons

should be characterized for transgenic Tau expression level, the Tau isoform ratio, neuronal identity(Yoshiyama *et al.* 2007) and for parameters that are relevant for aging.

4.6 Conclusions and Outlook

In this work I successfully generated iPSC lines from the Tau pathology mouse models 3xTg AD, Tau^{P301S} and hTau (Andorfer *et al.* 2003; Oddo *et al.* 2003; Yoshiyama *et al.* 2007) and derived a transgenic Tau^{P301S}/APP^{Swe}/Venus ESC line. All four PSC lines were used for the generation of neurons according to the Bibel & Barde protocol (Bibel *et al.* 2007). Although the protocol reportedly produces a homogeneous population of fully mature cortical glutamatergic neurons, a detailed analysis revealed that the PSC-derived neurons in this work were immature and very heterogeneous in respect to their neuronal identitiy. The four promoter systems proved to be differently well suitable for driving transgene overexpression in the PSC-derived neurons. The results showed that the suitability of the promoters was strongly influenced by the immaturity and the heterogeneity of the neuronal population. In the neurons derived from Tau^{P301S} and hTau iPSC no hyperphosphorylation was detectable under standard and oxidative stress conditions and they did not show an increased sensitivity to phosphatase inhibition. Thus, the *in vitro* neurons did not recapitulate the Tau pathology that is observed in their *in vivo* counterparts in the brains of the Tau^{P301S} and hTau mouse models. Reasons for this discrepancy were supposedly a significantly lower transgenic Tau expression level and a different Tau isoform ratio in the PSC-derive neurons. Additionally, age-related changes that might promote Tau pathology were supposedly less present in the 2 week old PSC-derived neurons than they are in the mouse brain after 6 month when Tau pathology is observed. From the findings in this study, several conclusions can be drawn that are important for the modeling of neurodegenerative diseases with mouse and human iPSC- and ESC-derived neurons.

First, due to the immaturity and heterogeneity of the neuronal population, a promoter with a restricted and late-onset expression pattern as the Thy1.2 promoter was shown to be very unsuited for the expression of transgenes. In this study, the human MAPT promoter has been identified as best suited, although the CAG promoter might as well be of use when the expression vector is integrated in a genomic region that is never silenced as e.g. the *ROSA26* locus. Thus, this study delivered important insights for the choice of the best promoter system for the construction of further research models based on PSC-derived neurons.

Second, the immaturity and heterogeneity of the PSC-derived neurons in this work suggested, that this might be a common phenomenon when PSC are differentiated into neurons. As in neurodegenerative diseases mostly a defined subset of neurons in the

adult brain is affected, the generation of fully mature neurons of only the relevant neuronal identity is commonly desired. Therefore, all PSC-derived neurons that are used to model neurodegenerative diseases should be thoroughly analyzed regarding their maturation and neuronal identity. Otherwise the relevancy of the findings for the studied disease must be treated with great precaution.

Third, the 3xTg AD, Tau^{P301S} and hTau iPSC-derived neurons revealed technical limitations of the approach, as they did not recapitulate the transgene expression which is observed in the correspondent mouse brain and considered to be crucial for the development of Tau pathology. This might be due the immaturity of the neurons but might also be an artifact of the *in vitro* differentiation. The culture conditions could lack a mandatory component for full vector activation or the control of gene expression might have been affected by extensive epigenetic remodeling during the reprogramming process. As this might be true for all genes in neurons derived from iPSC, including iPSC from neurodegenerative disease patients, it seems to be worthwhile to compare the gene expression patterns of iPSC-derived neurons and *in vivo* brain neurons.

Fourth, the results in this work suggested, that because of their immaturity the iPSC-derived neurons after 2 weeks did not recapitulate the aging status of 6 months old neurons in the mouse brain. As this aging status seems to be required for the onset of Tau pathology, two conclusions were drawn from this observation: The model system should be characterized in terms of aging status and aspects of aging should be recapitulated *in vitro*. One problem concerning the first aspect is the vague molecular definition of the aging process and the associated scarceness of bona fide markers of aging. Age-related epigenetic changes were characterized (Fraga & Esteller 2007) and might be exploited for the development of useful markers for assessing the aging status of an *in vitro* population. The best starting point to understand how aging affects the development of a late-onset phenotype are iPSC from mouse models of neurodegenerative diseases. Comparing brain neurons and iPSC-derived neurons at any age and developmental stage regarding aging and phenotype, will help to understand which age-related changes are important for the etiology and should therefore be recapitulated *in vitro*. It has been questioned if late-onset phenotypes can be modeled with young, iPSC-derived neurons (Ming *et al.* 2011) and in some cases patient iPSC-derived neurons did not show the typical late-stage manifestations of protein aggregates (Dolmetsch & Geschwind 2011; Han *et al.* 2011). It remains an open question if the aging process can be modeled or accelerated *in vitro*. It was proposed to use oxidative stress to accelerate aging in the dish (Saha & Jaenisch 2009). Additionally, long-lived mutants and associated pathways have been identified

(Kenyon 2010). It seems intriguing to manipulate these pathways in the opposite direction with the possible consequence of accelerated aging. Further, it might be possible to recapitulate aspects of the epigenetic drift associated with aging (Fraga & Esteller 2007) by targeted epigenetic manipulations as e.g. specific HDAC inhibitors. The ideal model system for controlling the effect of the age-related modifications would be a transgenic mouse model and the correspondent iPSC-derived neurons as it allows for a constant comparison. By this approach conditions might be identified that allow for the development of the correspondent late-onset phenotype. The identified conditions could be of great value for the modeling of neurodegenerative diseases with iPSC from patients with the sporadic form of the disease.

In summary, this work provides valuable insights about the modeling of neurodegenerative diseases in PSC-derived neurons and the hurdles that have to be overcome in future. We still need to understand much better the nature of *in vitro* generated neurons and how we can accelerate their aging before we can use them reliably. In this context, this work represents a stepping stone for improving the analysis of neurodegenerative diseases in neurons derived from patients' iPSC. Thereby it contributes to the understanding of neurodegenerative diseases and the development of causal therapies.

5 Materials

5.1 Instruments

autoclave	*Aigner, type 667-1ST*
balances	*Sartorius, LC6201S, LC220-S*
centrifuges	*Sorvall, Evolution RC; Eppendorf, 5415D, 5417R; Heraeus, Varifuge 3.0R, Multifuge 3L-R*
chambers for electrophoresis (DNA)	*MWG Biotech; Peqlab*
developing machine	*Agfa, Curix 60*
digital camera	*Zeiss, AxioCam MRc*
electroporation system	*BioRad, Gene Pulser XCell*
freezer (−20°C)	*Liebherr*
freezer (−80°C)	*Heraeus HFU 686 Basic*
fridges (4°C)	*Liebherr*
gel documentation system	*Herolab, E.A.S.Y.*
gel-/blottingsystem “Xcell SureLock™ Mini-Cell”	*Invitrogen*
glass homogenizer (tissue grinder, 2 ml)	*KIMBLE / KONTES*
glass pipettes	*Hirschmann*
glassware	*Schott*
ice machine	*Scotsman, AF 30*
incubators (for bacteria)	*New Brunswick Scientific, innova 4230*
incubators (for cell culture)	*Heraeus*
laminar flow	*Nunc Microflow 2*
light source for microscopy	*Leica KL 1500*
magnetic stirrer / heater	*Heidolph, MR3001*
microscope	*Zeiss Axioplan 2*
microwave oven	*Sharp R-937 IN*
Neubauer counting chamber	*Brand*
Nucleofector	*Amaxa*
PCR machine	*Eppendorf, MasterCycler Gradient*
pH-meter	*InoLab, pH Level 1*
photometer	*Eppendorf, Biophotometer 6131; PeqLab, NanoDrop ND-1000*
pipette filler, electronic	*Eppendorf, Easypet; Hirschmann, Pipettus akku*
pipettes	*Gilson, Pipetman P10, P20, P200, P1000*
power supplies for electrophoresis	*Consort, E443; Pharmacia Biotech, EPS200; Thermo, EC250-90, EC3000-90*
radiation monitor	*Berthold, LB122*
shaker	*Heidolph, Promax 2020*
stereomicroscope	*Zeiss, Stemi SV6*
thermomixer	*Eppendorf, comfort*
UV-lamp	*Benda, N-36*
vortex	*Scientific Industries, Vortex Genie 2*
water bath	*Lauda, ecoline RE 112; Leica, HI1210; Memmert, WB7*
water conditioning system	*Millipore, Milli-Q biocel*

5.2 Chemicals

acetic acid	Merck
agarose (for gel electrophoresis)	Biozym
ammonium acetate	Merck
ampicillin	Sigma
Ampuwa	Fresenius
Aqua-Polymount	Polysciences
AraC (Cytosine b-D-arabinofuranoside)	Sigma
B27-supplement	Gibco
B27-supplement (minus vitamin A)	Gibco
bacto agar	Difco
bacto peptone	BD Biosciences
bis-tris	Sigma
boric acid	Merck
bovine serum albumin (BSA, 20 mg/mL)	NEB, Sigma
bromphenol blue	Sigma
BSA (albumin fraction V)	Roth
BSO (buthionine sulfoximine)	Sigma
chloroform	Sigma
Colcemid	Gibco
Complete® Mini (protease inhibitors)	Roche
Cyclopamin	Sigma
DAPI (4',6-Diamidino-2-phenylindole)	Sigma
dithiotreitol (DTT)	Roche
DMEM	Gibco
DMEM/F-12, GlutaMAX™	Gibco
DMSO (Dimethyl Sulfoxide)	Sigma
dNTP (100 mM dATP, dTTP, dCTP, dGTP)	Fermentas
Doxycycline hyclate	Sigma
EDTA	Sigma
ethanol absolute	Merck
ethidiumbromide	Fluka
fetal calf serum (FCS)	PAN
Ficoll 400	Sigma
G418	Invitrogen
gelatin	Sigma
glycerol	Sigma
HBSS	Gibco
HCG (Human chorionic gonadotropin)	Intervet
Hepes	Gibco
hydrochloric acid (HCl)	Merck
hygromycin	Merck
isopropanol	Merck
Knock Out DMEM	Invitrogen
Laminin	Roche
L-Glutamine 200 mM (100x)	Gibco
LIF (ESGRO® LIF)	Millipore
Light mineral oil (Fluka)	Sigma

M2-Medium (blastocyst manipulation)	Sigma
MEK-Inhibitor	Cell Signaling
MEM Non essential amino acid solution 10 mM (100x)	Gibco
methanol	Merck
$MgSO_4$ (magnesium sulfate)	Sigma
mineral oil	Sigma
N2-supplement (100x)	Gibco
Neurobasal	Gibco
NuPAGE® MES SDS Running Buffer (20x)	Invitrogen
NuPAGE® MOPS SDS Running Buffer	Invitrogen
NuPAGE® Transfer Buffer (20x)	Invitrogen
okadaic acid	Sigma
PAA FCS (for feeder culture)	PAN
PAN FCS (for PSC culture)	PAN
paraformaldehyde (PFA)	Sigma
PBS	Gibco
Penicillin - Streptomycin 100x Solution	Gibco
PhosSTOP Phosphatase Inhibitor Cocktail Tablets	Roche
PMSG (pregnant mare's serum gonadotropin)	Intervet
poly-D Lysin	Millipore
Poly-DL-ornithine hydrobromide (PORN)	Sigma
potassium chloride (KCl)	Merck
Retinoic acid	Sigma
RNaseZAP®	Sigma
S.O.C. medium	Invitrogen
skim milk powder	BD Biosciences
sodium acetate (NaOAc)	Merck, Sigma
sodium chloride (NaCl)	Merck
sodium dodecylsulfate (SDS)	Merck
sodium hydroxide (NaOH)	Roth
Sodium pyruvate	Gibco
TriReagent	Sigma
Tris (Trizma-Base)	Sigma
Triton-X 100	Biorad
TrypLE™ Express (1X)	Gibco
trypsin-EDTA (0.05%)	Gibco
tryptone	BD Biosciences
Tween 20	Sigma
Valproic Acid	Sigma
Vitamin C	Sigma
X-Gal	Fermentas
yeast extract	Difco
β-mercaptoethanol	Sigma, Gibco

5.3 Consumables and Others

100 bp DNA ladder	Fermentas
1kb+ DNA Ladder	Invitrogen
bacterial dishes (embryoid body formation)	Greiner Bio-One
cell culture dishes (Ø 60 mm, 100 mm, 150 mm)	Nunc
cell strainer (40 µm)	BD Biosciences
centrifuge tubes (15 ml, 50 ml)	Corning
Coverslip (round, 14 mm)	Hecht Assistent
Cryovials	Nalgene
cuvettes for electroporation (0.2 cm, 0.4 cm)	Biorad
filter paper	Whatman 3MM
Hyperfilm (chemiluminescence detection)	Amersham
HyperLadder I	Bioline
ibidi slides	ibdi
multiwell plates (6, 12, 24, 96 wells)	Nunc
NuPAGE® Novex Bis-Tris gels (10 %, 4-12%)	Invitrogen
Pasteur pipettes	Brand
PCR reaction tubes (0.2 ml)	Biozym
PCR sealing film (78 x 120 mm)	Kisker
pipette tips 10 µl, 20 µl, 200 µl, 1000 µl	Art, Gilson, Starlab
plastic pipettes (1, 5, 10, 25 ml)	Greiner
PVDF membrane	Millipore
reaction tubes (0.5, 1.5, 2.0 ml)	Eppendorf
SeeBlue® Plus2 pre-stained protein standard	Invitrogen
SmartLadder DNA marker	Eurogentec
Superfrost Plus slides	Menzel Gläser

5.4 Kits

AP Staining Kit	System Biosciences
ECL Detection Kit	Amersham
High-Capacity cDNA Reverse Transcription Kit	Applied Biosystems
MEF Nucleofector Kit 1	Amaxa
Pierce® BCA Protein Assay Kit	Thermo Scientific
QIAGEN Plasmid Maxi Kit	QIAGEN
QIAprep Spin Miniprep Kit	QIAGEN
QIAquick Gel Extraction Kit	QIAGEN
QIAquick PCR Purification Kit	QIAGEN
RNeasy Mini Kit	QIAGEN
Wizard Genomic DNA Purification Kit	Promega

5.5 Enzymes

Alkaline Phosphatase, Calf Intestinal (CIP)	NEB
Collagenase/Dispase	Roche
Cre recombinase	NEB
DNA Polymerase (Phusion)	NEB
DNase I (for cell culture)	Roche
Herculase II Fusion DNA Polymerase	Stratagene
Klenow fragment of DNA Polymerase I	NEB
PCR-Mastermix 5x	5 PRIME
Proteinase K	Roche
Restriction enzymes	NEB, Fermentas, Roche
T4 DNA ligase	NEB

5.6 Antibodies

5.6.1 Primary Antibodies

Name	Specificity	Host	Use[1)]	Dilution	Provider	Catalog Nr.
12E8	Tau pS262, pS356	mouse	WB	1:1000	Neotope	kind gift of P. Seubert
AT270	Tau pT181	mouse	WB	1:1000	Pierce	MN1050
AT8	Tau pS199, pS202, pT205	mouse	WB	1:1000	Pierce	MN1020
beta-Actin	beta-Actin	mouse	WB	1:100 000	GeneTex	GTX26276
ERα [HC-20]	human estrogen receptor	rabbit	WB	1:1000	Santa Cruz	sc-543
HT7	human Tau	mouse	WB	1:1000	Autogen Bioclear	90222
			ICC	1:500		
K9JA	human + mouse Tau	rabbit	ICC	1:1000	Dako	A 0024
			WB	1:100 000		
MAP2	MAP2	mouse	ICC	1:1000	Sigma	M 1406
Mash1	Mash1	mouse	ICC	1:500	BD Biosciences	556604
Nanog	Nanog	rabbit	ICC	1:200	abcam	ab21603
Nestin	Nestin	mouse	ICC	1:500	Millipore	MAB353
Oct4	Oct4 (POU5F1)	rabbit	ICC	1:100	Cell Signaling	2840
Otx2	Otx2	goat	ICC	1:10	R&D Systems	AF1979
Pax6	Pax6	mouse	ICC	1:500	DSHB	Pax6
pS396	Tau pS396	rabbit	WB	1:5000	Invitrogen	44752G
Sox2	Sox2	rabbit	ICC	1:750	abcam	ab15830
Stella	Stella	rabbit	ICC	1:200	Santa Cruz	sc-67249
Synaptophysin	Synaptophysin	mouse	WB	1:1000	Calbiochem	573822
Tuj1	beta III Tubulin	rabbit	ICC	1:400	abcam	ab18207
			WB	1:50.000		
VGLUT2	VGLUT2	guinea pig	WB	1:1000	Millipore	ab2251

[1)] WB, Western Blot; ICC, Immunocytochemistry

5.6.2 Secondary Antibodies

Name	Conjugate	Host	Use[1)]	Dilution	Provider	Catalog Nr.
anti-rabbit	Alexa Fluor® 488	donkey	ICC	1:500	Invitrogen	A21206
anit-goat	Alexa Fluor® 488	donkey	ICC	1:500	Invitrogen	A11055
anti-mouse	Alexa Fluor® 594	donkey	ICC	1:500	Invitrogen	A21203
anti-rabbit	Alexa Fluor® 594	donkey	ICC	1:500	Invitrogen	A21207
anti-mouse	peroxidase	goat	WB	1:5000	Dianova	115-065-020
anti-rabbit	peroxidase	goat	WB	1:5000	Dianova	111-035-003
anti-guinea pig	peroxidase	donkey	WB	1:5000	Dianova	706-035-148

[1)] WB, Western Blot; ICC, Immunocytochemistry

5.7 Plasmids

Name	Description
pCAG-C31 OE-bpa	C31 Integrase expression vector with codon optimized sequence
pCAG-C31-bpa	C31 Integrase expression vector
pCAG-creER(T2)-bpA SS1	$CreER^{T2}$ expression vector
pCS2+_hAPPswe	Contains human cDNA of APPswe (APP mutation K670N/M671L)
pCS2-venus	Contains cDNA of Venus-protein
pEx-CAGstop-bpa	Contains a CAG promoter followed by a floxed stop cassette
pNG2htau40/P301L	Contains human cDNA of Tau^{P301L}
pPgk-hygro	Contains a hygromycin resistance driven by Pgk promoter
pPgk-neo-bpA	Contains a neomycin resistance driven by Pgk promoter
pReproII-attB	Doxycycline-controlled expression of Oct4, Sox2, cMyc and Klf4. Contains an attB site for genomic integration via C31 integrase.
pReproII-attB-shp53	Doxycycline-controlled expression of Oct4, Sox2, cMyc, Klf4 and a shRNA against p53. Contains an attB site for genomic integration via C31 integrase.

5.8 Oligonucleotides

5.8.1 Oligonucleotides for Genotyping

Name	Sequence (5' - 3')	Conditions	Size of Product
huAPP-1 huAPP-2	GGTGAGTTTGTAAGTGATGCC TCTTCTTCTTCCACCTCAGC	94°C 30 sec 53°C 30 sec 35 x 72°C 1 min	Tg APP: 300 bp
PS1-K13 PS1-K15	CACACGCACACTCTGACATGCACAGGC AGGCAGGAAGATCACGTGTTCCAAGTAC	94°C 40 sec 62°C 40 sec 35 x 72°C 1 min	550 bp, WT: 550 bp*, het: 550 + 300 + 250 bp* hom: 300 + 250 bp*
5tauRev APPinternal Thy12.4	TCCAAAGTTCACCTGATAGT GCTTGCACCAGTTCTGGATGG GAGGTATTCAGTCATGTGCT	94°C 30 sec 53°C 30 sec 25 x 72°C 1 min	Tg APP: 500 bp Tg Tau: 350 bp

P301S F P301S R	GGGGACACGTCTCCACGGCATCTCAGCAATGTCTCC TCCCCCAGCCTAGACCACGAGAAT	94°C 40 sec 57°C 40 sec 35 x 72°C 1 min	Tg Tau: 350 bp
Ctrl 2 F Ctrl 2 R	CAAATGTTGCTTGTCTGGTG GTCAGTCGAGTGCACAGTTT	94°C 30 sec 57°C 1 min 1 35 x 72°C min	Internal control: 200 bp
GFP F GFP R	AAGTTCATCTGCACCACCG TGCTCAGGTAGTGGTTGTCG	94°C 30 sec 62°C 1 min 1 35 x 72°C min	Tg GFP: 475 bp
Ctrl 1 F Ctrl 1 R	CTCAGCATCCCACCTGTAAC CCAGTTGTGTATGTCCACCC	94°C 30 sec 62°C 1 min 1 35 x 72°C min	Internal control: 187 bp
pTAV 1F pTAV 1R	GAGATCGTGTACAAGTCGCC TGAATCCCACTTCCCATTCTG	94°C 30 sec 60°C 1 min 1 35 x 72°C min	pTAV vector: 370 bp
SeqCAG CreERT2 Rev	GCTAACCATGTTCATGCCTTCTTC CATTGCTGTCACTTGGTCGT	94°C 30 sec 60°C 1 min 1 35 x 72°C min	pHC vector: 409 bp

* after BstEII digestion: 30 µl PCR product, 5 µl NEBuffer 3 (10x), 0.6 µl BstEII, 14.4 µl H_2O; 2 h incubation at 37°C

5.8.2 Oligonucleotides for Cloning

Name	Sequence (5' - 3')	Application
hTAU F NruI Kozak	GATCTCGCGAGCCACCATGGCTGAGCCCCGCCAGGAG	see section 6.2.2.2 for details
hTAU R T2A	TCCTCCACGTCACCGCATGTTAGAAGACTTCCTCTGCCCTCCAA-ACCCTGCTTGGCCAGG	
hAPP F T2A	AAGTCTTCTAACATGCGGTGACGTGGAGGAGAATCCCGGCCCT-ATGCTGCCCGGTTTGGCAC	see section 6.2.2.2 for details
hAPP R P2A	TCAACATCTCCTGCTTGCTTTAACAGAGAGAAGTTCGTGGCGT-TCTGCATCTGCTCAAAGAACT	
Venus F P2A	TCTCTGTTAAAGCAAGCAGGAGATGTTGAAGAAAACCCCGGGC-CTATGGTGAGCAAGGGCGAGGAG	see section 6.2.2.2 for details
Venus R AsiSI	GACTGCGATCGCTTACTTGTACAGCTCGTCCATG	
attB1	GGCCCCGCGGTGCGGGTGCCAGGGCGTGCCCTTGGGCTCCCCGG-GCGCGTACTCCAC	see section 6.2.2.3 for details
attB2	GGCCGTGGAGTACGCGCCCGGGGAGCCCAAGGGCACGCCCTGGC-ACCCGCACCGCGG	

5.8.3 Oligonucleotides for Neuronal Identity Detection by RT-PCR

Gene	Forward (F) and Reverse (R) Primer (5' - 3')		T_m / °C	Size of product (bp)	Reference
BF1	**F**	CTGACGCTCAATGGCATCTA	55	438	Abranches *et al.* 2009
	R	TTTGAGTCAACACGGAGCTG			
Brn2	**F**	AACAGCATCAACAGCAACAG	55	594	self-designed
	R	CACATGTTCTTGAAGCTCAG			
ChAT	**F**	GCTGAAACATATGATGACAGG	55	270	self-designed
	R	GTAAAGCCTGTAGTAAGCCA			
Ctip2	**F**	ATCGTCGGAACATTCCTCTG	55	400	Ideguchi *et al.* 2010
	R	GTGTTTCTCCAGGGTGCTGT			
Cux2	**F**	TCAAGACGAACACCGTCATC	61	400	Ideguchi *et al.* 2010
	R	GCCAGCTCTGAGAGGTCACT			
Emx1	**F**	GAGCCTTTGAGAAGAATCAC	55	248	Hack *et al.* 2004
	R	CTAGTCATTGGAGGTGACAT			
Emx2	**F**	CACCTTCTACCCCTGGCTCA	58	522	Gaspard *et al.* 2009
	R	TTCTCGGTGGATGTGTGTGC			
En1	**F**	GACAGTGGCGGTGGTAGTG	55	568	Ideguchi *et al.* 2010
	R	GAGGAGCCTGGAGGTGGC			
Fezf2	**F**	TCCATACCCAGGAAAAACCA	55	395	Ideguchi *et al.* 2010
	R	TGTCCTGGCTAGGTCCTTTG			
Gad1	**F**	GAAGTGGTAGACATACTCCTC	61	525	self-designed
	R	TGGAATAGTGACTGTGTTCTG			
GAPDH	**F**	ATTCAACGGCACAGTCAAGG	55-61	466	Abranches *et al.* 2009
	R	TGGATGCAGGGATGATGTTC			
Gli3	**F**	GAGCCTGAAGTCATCTACGA	58	410	self-designed
	R	GCATACATACGGTTTCTCATTGG			
Gsh2	**F**	CCTTTGCTCAAAAGCCAGTT	58	112	Hack *et al.* 2004
	R	GGTGATGGTGATGATGATGC			
HB9	**F**	GTTGGAGCTGGAACACCAGT	55	400	Ideguchi *et al.* 2010
	R	CTCAGATGAGCAGTCGGATG			
Irx3	**F**	CTGGGTCCCTATCCAATGTG	58	538	Okada *et al.* 2004
	R	CGTTTGCTCTCTTCCTCGTC			
Isl1	**F**	GCAACCCAACGACAAAACTA	58	120	Hack *et al.* 2004
	R	GGCTGGTAACTTTGCACCTC			
Lhx6	**F**	TAGAGCCTCCCCATGTACGCC	55	723	Gaspard *et al.* 2009
	R	TGCTGCGGTGTATGCTTTTT			
Lhx8	**F**	AAGTGGAGAACGGTAATGGGA	58	277	self-designed
	R	GGCTGAGGAAGAATGGTTGG			
Lim1	**F**	TTACGGAGATTACCAGAGTGAG	58	323	self-designed
	R	CCATTGACCGACAGAGATGAG			
Mash1	**F**	AGATGAGCAAGGTGGAGACG	55	137	Abranches *et al.* 2009
	R	TGGAGTAGTTGGGGGAGATG			
Nkx2.1	**F**	GTGCCGGTCCTAGTCAAAGAC	55	292	Ideguchi *et al.* 2010
	R	AGTCCGAGCCCGAGGAGTTCAG			

Gene	Forward (F) and Reverse (R) Primer (5' - 3')		T_m / °C	Size of product (bp)	Reference
Nkx2.2	**F**	GCTGACCAACACAAAAGACG	58	102	Hack *et al.* 2004
	R	CTCTCCTCCTCTGGCCCTTC			
Nkx6.1	**F**	TCAGGTCAAGGTCTGGTTCC	55	212	Okada *et al.* 2004
	R	CGATTTGTGCTTTTTCAGCA			
Otx1	**F**	ACCTTCACGCGCTCACAG	55	378	Ideguchi *et al.* 2010
	R	GCTCAGAGAGGACGCTGCT			
Otx2	**F**	ACAAGTGGCCAGTTCAGTCC	58	347	Abranches *et al.* 2009
	R	CTGGGTGGAAAGAGAAGCTG			
Pax2	**F**	AAGATTGCCGAATACAAGCGAC	58	405	self-designed
	R	CCTCAGACACATCTCTTAAAGTCC			
Pax6	**F**	AGGGGGAGAGAACACCAACT	58	249	Abranches *et al.* 2009
	R	CATTTGGCCCTTCGATTAGA			
Pax7	**F**	AATGGCCTGTCTCCTCAGGT	58	164	Okada *et al.* 2004
	R	TCTCCTGGCTTGATGGAGTC			
Phox2b	**F**	CCTCAATTCCTCTGCCTACG	58	374	Okada *et al.* 2004
	R	GTGCTAGCTCTTCCCTGGTG			
Satb2	**F**	CGTGGGAGGTTTGATGATTCC	58	454	self-designed
	R	CAATGGATGAAATCATACTCTGGG			
Six3	**F**	AAGAACAGGCTCCAGCATCAG	58	476	self-designed
	R	TGGATGTTACTCCTCAAACGGTG			
Tbr1	**F**	GTCACCGCCTACCAGAACAC	55	120	Ideguchi *et al.* 2010
	R	GGTCAAGCGGTCCATGTC			
TH	**F**	AAATCCACCACTTAGAGACC	55	380	self-designed
	R	TATACCTCCTTCCAGGTAGC			
VGlut1	**F**	CTAAACATGTTGATCCCTTCAG	61	409	self-designed
	R	GTGTTAAACTTCGTAACAGGG			
VGlut2	**F**	CACCTCTACCCTCAATATGC	61	280	self-designed
	R	ATGCCAAAGCTTCCATACAC			

5.8.4 Oligonucleotides for Tau Isoform Detection by RT-PCR

Name	Sequence (5' - 3')	Tm / °C	Size of Product	Application
hTAU Ex10 F	AAGTCGCCGTCTTCCGCCAAG	60°C	3R Tau: 288 bp 4R Tau: 381 bp	Tau isoform detection
hTAU Ex10 R	GTCCAGGGACCCAATCTTCGA			
Tau Ex1-F	ATGGCTGAGCCCCGCCAGGAG	60°C	0N Tau: 393 bp 1N Tau: 480 bp 2N Tau: 567 bp	Tau isoform detection
Tau Ex4-R	TGGAGGTTCACCAGAGCTGGG			
huGAPDH F	CCATGGCACCGTCAAGGCTGA	60°C	350 bp	Internal control: human GAPDH
huGAPDH R	GCCAGTAGAGGCAGGGATGAT			
mGAPDH F	ATTCAACGGCACAGTCAAGG	60°C	466 bp	Internal control: mouse GAPDH
mGAPDH R	TGGATGCAGGGATGATGTTC			

5.9 Mouse Lines

Abbrevation in this work	Genetic description	Characteristics	Provider / Reference
BL6	C57BL/6J	Wild type inbred mouse line	Helmholtz Zentrum München
BL6 C3	B6 C3 F1/J	WT control line for JX008169	JAX® Mice, stock JX100010
BL6/129	C57BL/6J*129-Rosa26.10	The modified *Rosa* locus contains a pgk-promoter-driven hygromycin resistance and attP sites*.	Ralf Kühn (Helmholtz Zentrum München)
3xTg AD	B6;129-*Psen1* ^{tm1Mpm} -Tg(APP^{Swe},Tau^{P301L})1 Lfa/J	PS1^{M146V} Knock-In, transgenic APP- and Tau-pathology related gene variants of APP and Tau, expression of transgenes controlled by Thy1.2 promoter. 6-8 fold overexpression of transgenes in cortex and hippocampus, age related and progressive Tau and Aß pathology, cognitive impairment.	Thomas Floss (Helmholtz Zentrum München); also available from JAX® Mice as stock JX004807; published by Oddo *et al.* (2003)
Tau^{P301S}	B6;C3-Tg(Prnp-MAPT*P301S)PS19Vle/J	Prion-promoter drives 5 fold overexpression of transgenic mutant Tau in the CNS resulting in Tau tangles in cortex and hippocampus at 5 month. Synaptic and neuronal loss occurs by 8 to 9 month, median life span is ~9 month.	JAX® Mice, stock JX008169, published by Yoshiyama *et al*. (2007)
hTAU	B6.Cg-*Mapt* $^{tm1(GFP)Klt}$ -Tg(MAPT)8cPdav/J	Expression of all six isoforms of transgenic human WT Tau is driven by human MAPT promoter resulting in Tau overexpression in neurons. Insertion of EGFP cDNA into exon one of endogenous Tau results in mouse Tau knockout and neuron-specific EGFP expression. Tau hyperphosphorylation appears at 6 month, aggregated Tau at 9 month.	JAX® Mice, stock JX005491, published by Andorfer *et al.* (2003)

* The Rosa26.10 locus was intended to be used for a side project that in the end was not realized. As these mice were only used in the generation of ESC lines and the ESC lines used in this study were tested negative for the Rosa26.10 locus by PCR (data not shown), it is not mentioned further in the text.

5.10 Cell Lines

Abbrevation in this work	Genetic description	Characteristics	Provider
JM8	BI6 (C57BL/6)	Wild type mouse ES cell line	Ralf Kühn (Helmholtz Zentrum München)
E14	129 (129P2/Ola)	Wild type mouse ES cell line	Ralf Kühn (Helmholtz Zentrum München)
IDG3.2	BI6*129 (C57BL/6J*129S6/SvEvTac)	Wild type mouse ES cell line	Ralf Kühn (Helmholtz Zentrum München)

5.11 Common Solutions

Ampicillin selection agar		LB agar with 100 µg/mL ampicillin
Ampicillin selection medium		LB medium with 50 µg/mL ampicillin
Blocking Solution (Immunocytochemistry)	1%	BSA
	0,5%	Triton X 100
		in PBS
Cyclopamine stock solution	400 mg/ml	Cyclopamine in absloute ethanol
		store at -20°C, use 1:1000
DAPI stock solution (immunocytochemistry)	5 mg/ml	DAPI in Dimethylformamide
		store at -20°C, use 1:25.000 in PBS with 0.5% Triton X 100
DAPI stock solution (karyotyping)	5 mg/ml	DAPI in Dimethylformamide
		store at -20°C, use 1:25.000 in PBS
Doxycycline stock solution	1 mg/ml	Doxycycline in H_2O
		store at -20°C, use 1:1000
Gelatin solution (cell culture)	0.1%	Gelatin in H_2O
LB agar	98.5 %	LB-Medium
	1.5 %	Bacto agar
LB medium	10 g	Bacto peptone
	5 g	yeast extract
	5 g	NaCl
	ad 1 L	H_2O
loading buffer for agarose gels	15%	Ficoll 400
	200 mM	EDTA
	0.001%	Bromphenolblue
Lysis Buffer (DNA Extraction 96-well plate)	10 mM	Tris, pH 7.5
	10 mM	EDTA
	10 mM	NaCl
	0.5%	Sarcosyl
	0.4 mg/ml	Proteinase K (freshly added)
paraformaldehyde solution (PFA, 4 %)	4%	PFA w/v in PBS
Poly-DL-Ornithin stock solution	0.5 mg/ml	Poly-DL-ornithine hydrobromide
	150 mM	Borat
		in H_2O, pH 8.3
		store at -20°C, use 1:5 in H_2O
Retinoic acid stock solution	5 mM	Retinoic acid in DMSO
		protect from light, store at -20°C, use 1:1000
TBS-T (1x)	25 mM	Tris-HCl pH 7.5
	137 mM	NaCl
	0.05 %	Tween 20
TE (Tris-EDTA)	10 mM	Tris-HCl pH 7.5
	1 mM	EDTA
Tris-HCl	1 M	Tris base
		pH 7.5

Valproic acid (VPA) stock solution	1 M	Valproic acid in H_2O *store at -20°C, use 1:500*
Vitamin C (VitC) stock solution	1 mg/ml	Vitamin C in H_2O *store at -20°C, use 1:1000*

5.12 Solutions for Western Blot

Blocking solution (non-phospho antibodies)	5%	skim milk powder in TBS-T
Blocking solution (phospho antibodies)	5%	BSA in TBS-T
Lämmli Buffer (1x)	150 mM	NaCl
	50 mM	Tris pH 6.8
	50 mM	DTT
	10%	Glycerol
	2%	SDS
	1x	Complete® Mini (protease inhibitors)
	1x	PhosSTOP (phosphatase inhibitors)
Lämmli Loading Buffer (1x)	1x	Lämmli Buffer
	0.001%	Bromphenolblue
Stripping Buffer, harsh	2%	SDS
	65 mM	1M Tris-HCl, pH 6.8
	100 mM	ß-Me (freshly added)
Stripping Buffer, mild	1.5 %	Glycine
	0.1 %	SDS
	1%	Tween 20
		pH 2.2
Transfer Buffer	1x	NuPAGE® Transfer Buffer (20x)
	10%	Methanol

5.13 Cell Culture Media

Embryonic stem cells	**Blastocyst medium**	50 µM	MEK inhibitor
		15%	PAN FCS
		3 mM	L-Glutamine
		0.1 mM	MEM Non essential amino acids
		0.1 mM	ß-Mercaptoethanol
		1500 U/ml	LIF
		1x	Penicillin - Streptomycin (100x)
			in DMEM
	ES F1 medium	15%	PAN FCS
		3 mM	L-Glutamine
		0.1 mM	MEM Non essential amino acids
		0.1 mM	ß-Mercaptoethanol
		1500 U/ml	LIF
			in Knock Out DMEM
Primary ear fibroblasts	**PEF Medium**	10%	PAA FCS
		2 mM	L-Glutamine
		0.1 mM	MEM Non essential amino acids
		0.1 mM	ß-Mercaptoethanol
		3x	Penicillin - Streptomycin (100x)
			in DMEM
Primary cortical neurons	**Dissection medium**	10 mM	HEPES
		12 mM	$MgSO_4$
		1x	PenStrep
			in HBSS
	Culture medium	1x	B27
		0.5 mM	L-Glutamine
		1x	PenStrep
			in Neurobasal medium
Neuronal Differentiation via Bibel & Barde protocol	**EB medium**	10%	PAN FCS
		2 mM	L-Glutamine
		0.1 mM	MEM Non essential amino acids
		0.1 mM	ß-Mercaptoethanol
			in Knock Out DMEM
	N2 medium	1x	N2-supplement (100x)
		0.1 mM	ß-Mercaptoethanol
			in DMEM/F-12, GlutaMAX™
			use within 1 week
	B27 medium	1x	B27-supplement
		2 mM	L-Glutamine
		3 µM	AraC
		0.1 mM	ß-Mercaptoethanol
			in Neurobasal
			use within 1 week

Neuronal Differentiation via Gaspard & Vanderhaeghen protocol	**DDM Medium**	1x	N2-supplement (100x)
		0.1 mM	MEM Non essential amino acids
		1 mM	Sodium Pyruvat
		0.5 mg/ml	BSA
		0.1 mM	ß-Mercaptoethanol
			in DMEM/F-12, GlutaMAX™
			use within 1 week
	B27 Medium	1x	B27-supplement (minus vitaminA)
		2 mM	L-Glutamine
			in Neurobasal medium
			use within 1 week
	N2/B27 Medium	50%	DDM medium
		50%	B27 medium
			use within 1 week

6 Methods

6.1 Mouse Husbandry

All mice were kept and bred in facilities of the Helmholtz Zentrum München according to national and institutional guidelines under standard conditions: 12 hours light/dark cycle, temperature of 22 ± 2 °C, relative humidity of 55 ± 5 %, food and water *ad libitum*. For breeding, one male was paired with one or two females. Pups were weaned at the age of 3 weeks, separated by sex and tail clips were taken for genotyping.

6.2 DNA Works

6.2.1 Extraction of Genomic DNA

Genomic DNA from mouse tail clips and from cultured cells grown in 24-well or larger plates was extracted using the Promega Wizard genomic DNA purification kit following manufacturer's instructions. For isolation of genomic DNA from cells grown on gelatin-coated 96-well plates, the following protocol was used. Plates were washed twice with PBS, afterwards 50 µl lysis buffer were pipetted in each well. After overnight incubation in a moist chamber at 56°C, plates were cooled down to RT and lysis buffer was replaced by 100 µl of 100% ethanol. After 1 h incubation at 4°C, in which the DNA precipitated, plates were washed thrice with 70% ethanol. Plates were dried and the DNA was solved in 50 µl TE-buffer.

6.2.2 Cloning and Work with Plasmid DNA

6.2.2.1 *General Methods*

For all cloning steps electro competent bacteria of *E. coli* strain DH5α (Invitrogen) were used. Bacteria were grown at 37°C using LB medium and LB agar, both containing ampicillin. Plasmid DNA was prepared from overnight cultures of 2-5 ml and 200 ml with the Qiagen MiniPrep and Plasmid Maxi Kit, respectively. For digestion of plasmid DNA, restriction enzymes were used and heat-inactivated according to manufacturer's instructions. Klenow fragment of DNA polymerase I was used for blunt end generation and free vector ends were dephosphorylated with alkaline phosphatase (CIP), following the manuals. Restriction digests were analyzed on a 0.9% agarose gel prepared with TAE buffer and containing ethidiumbromide. For isolation of DNA fragments for further cloning, DNA was visualized with UV light of a wavelength of 366 nm to minimize DNA

damage. Gel slices containing the DNA fragment of interest were cut out and subjected to DNA purification with the Qiagen Gel Extraction Kit. Cloneable DNA fragments were also obtained from a hybridization reaction in which 2 complementary oligonucleotides attB1/2 (1 µg of each) were annealed in 100 µl TE by incubation at 100°C for 5 min and subsequent slow cooling down to RT. Fragments were ligated into linearized vector with T4 Ligase in a 15 µl over night reaction at 16°C. Typically 1 µl of ligation reaction was used for transformation. After transformation, cells were plated on ampicillin-containing LB agar plates and grown over night. MiniPrep cultures were inoculated with picked colonies and analyzed by restriction analysis or sequencing (GATC Biotech AG, Konstanz). Confirmed clones were used for Plasmid Maxi preparation which was used directly for further cloning or for transfection after sterilization.

6.2.2.2 *Construction of pNeo-CAG-Tau^{P301L}/APP^{swe}/Venus-attB vector*

A vector for the constitutive expression of Tau^{P301L}, APP^{swe} and Venus under the control of CAG promoter was constructed. A neomycin resistance gene as selection marker and an attB site for integration by C31 integrase were included (section 3.4.1). The cDNAs of Tau^{P301L}, APP^{swe} and Venus were obtained by single PCR reactions using the plasmids pNG2htau40/P301L, pCS2+_hAPPswe and pCS2-venus as templates and the correspondent primer pairs indicated in **Fig. 6.1**.

Primer design enabled for fusion of the PCR fragments in 2 consecutive fusion PCR reactions as the fragments included an overlap of 30 bp. In the first part of the fusion PCR, fragments were fused by performing 5 cycles (1. 10s at 98°C, 2. 20s at 63°C, 3. 80s at 72°C) in a PCR reaction mix without primers. Upon addition of the outer primers the fusion fragment was amplified in 25 cycles (1. 10s at 98°C, 2. 2 min at 72°C). Due to the primer design, in the final 4.3 kb PCR fragment (termed TAV) the cDNAs of Tau^{P301L}, APP^{swe} and Venus were linked by a T2A and a P2A site and flanked by a NruI and an AsiSI restriction site (**Fig. 6.1 A**). After NruI/AsiSI digestion the fragment was ready for ligation. The vector for insertion of the TAV PCR fragment was obtained as following: Vector pEx-CAG-stop-bpa was opened with SgrDI, blunted and digested with EcoRI (**Fig. 6.1 B**). The such prepared vector was ligated with the blunted 1.6 kb NotI/EcoRI fragment from vector pPGK-neo-bpa which contained a PGK-driven neomycin resistance. The resulting vector pNeo-CAG-stop-attB was digested with NruI/AsiSI and ligated with the 4.3 kb NruI/AsiSI digested TAV PCR fragment (**Fig. 6.1 C**). As the resulting vector pNeo-CAG-stop-Tau^{P301L}-T2A-APP^{swe}-P2A-Venus-attB contained a loxP site flanked stop cassette, the vector was incubated with Cre recombinase for removal of the stop cassette (**Fig. 6.1 D**). Non-recombined plasmids were removed by SalI digestion. The thus activated vector pNeo-CAG-

Tau^{P301L}-T2A-APP^{swe}-P2A-Venus-attB (abbreviated as pTAV, **Fig. 6.1 E**) was used for transfection into ES cells as described in section 3.4.2.

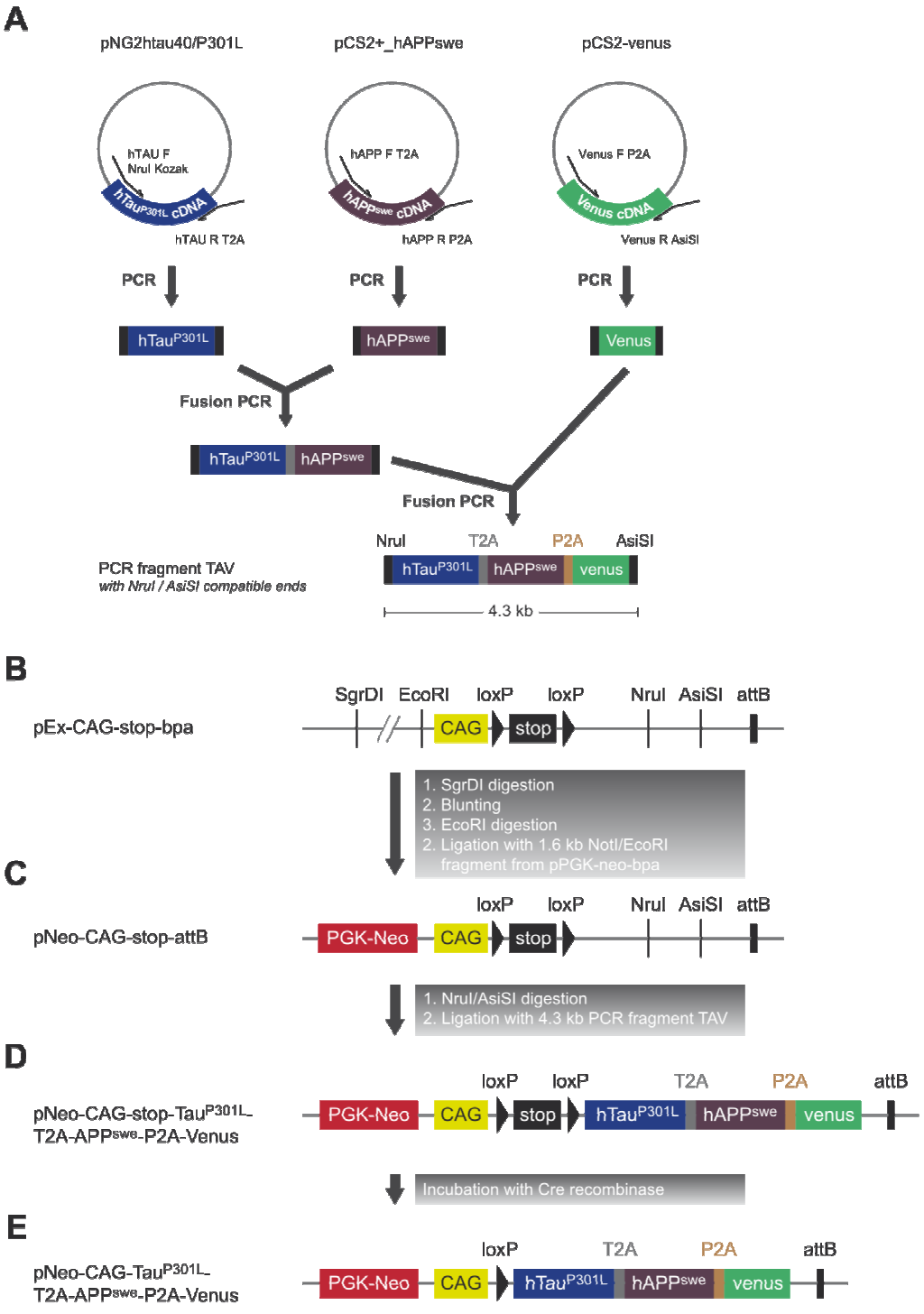

Fig. 6.1: Construction of vector pNeo-CAG-Tau^{P301L}-T2A-APP^{swe}-P2A-Venus-attB (pTAV)
(**A**) Generation of the cloneable fragment Tau^{P301L}-T2A-APP^{swe}-P2A-Venus (TAV) by fusion PCR. The cDNAs of Tau^{P301L}, APP^{swe} and Venus were amplified from plasmids with the indicated primer

Fig. 6.1 continued:
pairs. Primer design enabled for fusion of the PCR fragments in 2 consecutive fusion PCR reactions as the fragments included an overlap of 30 bp. In the resulting 4.3 kb PCR fragment (TAV) the cDNAs of Tau^{P301L}, APP^{swe} and Venus were linked by a T2A and a P2A site and flanked by a NruI and an AsiSI restriction site. (**B**) A fragment from vector pPGK-neo-bpa containing a PGK promoter-driven neomycin resistance was inserted into vector pEx-CAG-stop-bpa. (**C**) The resulting vector pNeo-CAG-stop-attB was opened and ligated with the Nru/AsiSI digested PCR fragment TAV from (**A**) which resulted in the vector pNeo-CAG-stop-Tau^{P301L}-T2A-APP^{swe}-P2A-Venus-attB. (**D**) The vector was incubated with Cre which removed the stop cassette by recombination of the flanking loxP sites. (**E**) The thus activated vector pNeo-CAG-Tau^{P301L}-T2A-APP^{swe}-P2A-Venus-attB was used for transfection.

6.2.2.3 *Construction of pHygro-CAG-$CreER^{T2}$-attB vector*

A vector was constructed that enabled for constitutive expression of $CreER^{T2}$ driven by CAG promoter (**Fig. 6.2 C**). The vector further contained a hygromycin resistance and an attB site for integration by C31 integrase (see section 3.4.1). First, vector pCAG-CreERT2-bpa SS1 was digested with EcoRI, blunted and ligated with the blunted 1.8 kb BglII fragment from vector pPGK-hygro, containing a hygromycin resistance (**Fig. 6.2 A**). The generated vector pHygro-CAG-$CreER^{T2}$ was opened with NotI. Hybridization of oligonucleotides attB1 and attB2 resulted in a cloneable doublestranded DNA fragment with NotI specific overhangs which was ligated into NotI-digested vector pHygro-CAG-CreERT2 (**Fig. 6.2 B**). The resulting vector pHygro-CAG-CreERT2-attB (abbreviated as pHC, **Fig. 6.2 C**) was used for transfection into ES cells as described in section 3.4.2.

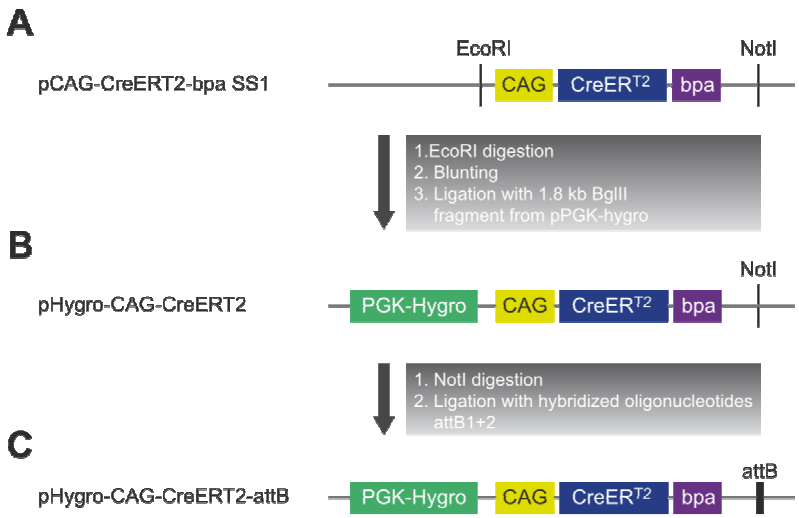

Fig. 6.2: Construction of vector pHygro-CAG-CreERT2
(**A**) A fragment from vector pPGK-hygro containing a PGK promoter-driven hygromycin resistance was inserted into vector pCAG-CreERT2-bpa SS1. (**B**) The generated vector pHygro-CAG-CreERT2 was opened with NotI and ligated with a cloneable doublestranded DNA fragment with NotI specific overhangs resulting from hybridization of oligonucleotides attB1 and attB2. (**C**) The resulting vector pHygro-CAG-CreERT2-attB was used for transfection.

6.2.3 Sterilization of Plasmid DNA

Plasmid DNA was sterilized before using for transfection by the following steps. A mix of plasmid DNA, 1/10 volume of 3 M sodium acetate (pH 5.3) and 2.5 volumes of 100% ethanol was incubated for 2 h to overnight at -20°C. After pelleting the DNA by centrifugation and washing with 70% ethanol, the DNA pellet was dissolved in sterile water to a final concentration of 1 µg/µl while working under a sterile flow. After verification of the DNA concentration the plasmid DNA was used for transfection.

6.2.4 Polymerase Chain Reaction (PCR)

Unless stated otherwise a typical PCR reaction consisted of 5 Prime Master Mix (1x), primers (10 µM), 50-500 ng DNA and water, added to an end volume of 25 µl. The PCR cycling conditions are given for each pair of oligonucleotides individually in section 5.8. Where sequence correctness was required for further cloning steps, Herculase polymerase was used with the reaction setup adjusted to manufacturer's instructions. Amplicons with a size above 300 bp were analyzed on a 1.5% agarose gel; when sizes were below 300 bp, a 2% agarose gel was used.

6.3 RNA Works

6.3.1 Extraction of RNA and Reverse Transcription

Samples for RNA isolation were stored at -80°C to minimize degradation of RNA. To that same end, RNAse-free consumables were used, as well as tools and working place were cleaned with RNaseZAP®.

For isolation of RNA from adult brains, mice were asphyxiated, decapitated, and the brains were dissected by removal of bones and meninges. RNA from embryonic brains was isolated by pooling 3-4 heads from embryos prepared as described in section 6.4.4. Tissues were homogenized in a glass homogenizer in 10-20 volumes of Tri Reagent. After centrifugation at 13.000 rpm for 10 min at 4°C and transfer of the supernatant to a new cup, 200 µl chloroform were added per 1 ml Tri Reagent. The samples were vortexed for 15 sec and incubated for 10 min at RT. After centrifugation at 14.000 rpm for 15 min at 4°C, the upper, clear phase was transferred to a new cup. Upon addition of 530 µl 100% ethanol per 1 ml Tri Reagent, samples were vortexed shortly and incubated for 10 min at RT. The such treated samples were transferred to a column of the RNeasy Mini Kit (Qiagen) and processed following manufacturer's instructions. RNA from cultured cells was isolated by lysing the cells directly on the dish

with Tri Reagent. These cell lysates were treated as described for the brain samples after the first centrifugation step.

The RNA concentration was determined on a NanoDrop spectrophotometer. For transcription of total RNA into cDNA the High Capacity cDNA Reverse Transcription Kit (Applied Biosystems) was used. The yielded concentration of cDNA was determined on an Eppendorf spectrophotometer.

6.3.2 Primer Design and Conditions for RT-PCR

Primer sequences for analysis of gene expression by RT-PCR were taken from literature (Hack *et al.* 2004; Okada *et al.* 2004; Abranches *et al.* 2009; Gaspard *et al.* 2009; Ideguchi *et al.* 2010) or designed with the PerlPrimer software (http://perlprimer.sourceforge.net/), as indicated in section 8.1. Care was taken to use primer pairs, in which at least one primer lies across an intron/exon boundary in order to assure the amplification of only cDNA and no genomic DNA. All RT-PCR reactions consisted of 5 Prime Master Mix (1x), primers (10 µM), 50-500 ng DNA and water, added to an end volume of 25 µl. The general RT-PCR program was: 1. 95°C, 5 min; 2. 95°C, 30 sec; 3. $\mathbf{T_m}$, 1 min; 4. 72°C, 1 min; repeat step 2.-4. 35x; 5. 72°C, 10 min. Individual melting temperatures ($\mathbf{T_m}$) are listed for each primer pair in sections 5.8.3 and 5.8.4.

6.4 Cell Culture Work

6.4.1 Generation and Culture of Embryonic Stem Cell Lines

6.4.1.1 *General Culture Techniques for Embryonic Stem Cells*

In general, ESC were cultured at 37°C and 7.5% CO_2 in ES F1 medium containing LIF and FCS for maintenance of pluripotency. Culture plates were coated with mitotically inactivated primary mouse embryo fibroblasts (MMC-treated MEF), as for maintenance of a homogenous, pluripotent ESC population over many passages culture on MEFs is mandatory. Therefore ESC were only transferred to gelatin-coated plates (0.1% gelatin in water, 5 min coating time) when cells were to be submitted to neuronal differentiation, immunostaining or DNA extraction. As a rule, medium was changed daily and cells were split every second day in ratios of 1:4 to 1:6. Cells were split by washing once with PBS, incubation with Trypsin for 4 min at 37°C, inactivation of Trypsin by addition of medium, pelleting the cells by centrifugation (1.200 rpm, 4 min), resuspension of the pellet in medium and subsequent distribution of the cell suspension to new plates. For well sizes smaller than 6-well, the centrifugation step was omitted due to the small

amount of cells. In that case, the residual Trypsin was diluted with medium minimum 1:4. Cells for cryoconservation were trypsinized, pelleted, resuspended in freezing medium (ES F1 medium with 10% DMSO) and stored in liquid nitrogen using cryovials. For thawing, the cryovials were warmed in a water bath at 37°C until their content was liquid. The cell suspension was washed in medium for removal of DMSO. The pelleted cells were resuspended in medium and plated. In the case of a 96-well plate, cells were trypsinized in 50 µl Trypsin to which 50 µl of 2 x freezing medium (containing 20% DMSO) were added directly. After sealing, plates could be stored at -80°C for up to 2 months. Upon thawing, cells were recovered by centrifugation and subsequent resuspension in medium.

For transfection of a vector into ESC by electroporation, typically 5-10 x 10^6 cells were used for one transfection. The vector contained one of the selection markers Neomycin- or Hygromycin resistance, for which can be selected by supplying the culture medium with G418 or Hygromycin, respectively. Cells were trypsinized, washed with PBS and resuspended in 800 µl PBS containing 25 µg of sterile vector pTAV or pHC and 25 µg of the vector pCAG-C31-bpa for transient expression of C31 Integrase (see section 3.4.1). Upon transfer of this suspension to a 4 mm electroporation cuvette cells were electroporated at 300 V for 2 ms, time constant. After an incubation of 5 min at room temperature cells were plated in non-selection medium on 1-2 10 cm dishes coated with feeders, resistant against the used selecting agent. After 24 h (day 1 after transfection) cells were supplied with non-selection medium. From day 2 to day 8 cells were supplied daily with fresh medium containing the selecting agent (final concentrations in medium: G418 140 µg/ml, hygromycin 125 U/ml) for selection of resistant, and thus vector-containing cells. On day 9 after transfection colonies were picked, transferred to a 96-well with 50 µl Trypsin using one colony per well and incubated for 5 min at 37°C. After addition of 50 µl medium and dissociation of the colony by repeated pipetting, the cell suspension was transferred to a MEF-coated 96-well containing 100 µl medium. The clones were expanded in selection medium on feeders for freezing and on gelatin for DNA isolation.

6.4.1.2 *Generation of Embryonic Stem Cell Lines*

For the matings for blastocyst production 3xTg AD mice were introduced into the mouse facility by *in vitro* fertilization (IVF) and further bred with BL6/129 (see note in section 5.9) mice resulting in heterozygous 3xTg AD mice. In the matings, only superovulated, pre-puberty BL6 females (i.e. 3-6 weeks old) were used. For superovulation, females were injected i.p. 7.5 units of PMSG 2 days before the mating and 7.5 units of HCG at the mating day, defined as d0. Mating pairs were separated at

d1. At d 3.5 females were asphyxiated and uteri were dissected and transferred to a 10 cm Petri dish with M2-medium (containing 1 x Pen-Strep). Under a stereo microscope, blastocysts were flushed out of the uteri into a 6 cm Petri dish with M2-medium using a syringe with a gauge needle. Blastocysts were collected with a mouth controlled, drawn-out Pasteur pipette and transferred to 30 µl drops of M2-medium covered by light mineral oil. Blastocysts were washed twice by transferring to drops of blastocyst-medium. Blastocyst medium contained 50 µM MEK-Inhibitor for maintenance of pluripotency and Pen-Strep for inhibition of microbial growth. Subsequently, blastocysts were transferred to a MEF-coated 96-well plate with 200 µl blastocyst-medium using one blastocyst per well to achieve clonal conditions. After 3 days, the upper half of the medium was carefully replaced with fresh medium. 5 days after blastocyst preparation, the ICM was set free and dispersed by dissociation of the blastocysts: After washing with PBS, blastocysts were incubated in 30 µl PBS for 10 min at 37°C, followed by addition of 30 µl Trypsin and another incubation of 10 min at 37°C. Upon addition of 160 µl blastocyst medium, blastocysts were dissociated by repeated pipetting before the cell suspension was transferred to a new MEF-coated 96-well. Complete medium change the next day was followed by medium change every 1-2 days while appearance of ESC colonies was monitored daily. When ESC colonies filled at least 50% of the 96-well, cells were and transferred to a MEF-coated 24-well. After the transfer to the 24-well, MEK-inhibitor and Pen-Strep were omitted, which is equivalent to the usage of standard ES F1 medium. The ESC were expanded further until two MEF-coated 6-wells could be used for freezing and one gelatin-coated 6-well could be used for extraction of genomic DNA and genotyping. All generated ESC lines were tested for Mycoplasma contamination as an in-house service by EUCOMM as described previously (Uphoff & Drexler 2002).

6.4.2 Generation of Induced Pluripotent Stem Cell Lines

6.4.2.1 *Culture of Adult Primary Ear Fibroblasts*

Induced Pluripotent stem cell (iPSC) lines were derived from adult primary ear fibroblasts. The latter were cultured by the following protocol, established by inspirations from different publications (Thompson *et al.* 1994; Shao *et al.* 1999; Wiktor-Brown *et al.* 2008). The ear was washed with 80% ethanol and 1/3 part of it was dissected and transferred to a tube with PBS. After transfer to a 6-well containing 1 ml PBS with 2 mg/ml Collagenase/Dispase (Roche 10 269 638 001), the ear was minced with scissors. The suspension was filled into a 1.5 ml Eppendorf cup and incubated for 1 h at 37°C with shaking at 500 rpm on a thermomixer. The cells were triturated by

pipetting and pelleted by centrifugation for 5 min at 1.200 rpm. The pellet was resuspended in PEF medium (adult primary ear fibroblast medium) and the cells were plated on 1-2 24-wells coated with gelatin. The next day, the medium was changed while avoiding the removal of floating pieces as they might contain cells that attach later. In the following, medium was changed every 2-5 days, depending on cell growth. After 1-2 weeks, cells were confluent and therefore split 1:3 to 1:5. After that, cells were passaged when confluent again, usually meaning every 5 days. The adult primary ear fibroblasts were expanded until they could be cryoconserved or directly used for reprogramming (see section 6.4.1.1 for splitting and freezing techniques). After passage 2-3, the PenStrep in the PEF medium was reduced from 3 fold to 1 fold concentration.

6.4.2.2 *Reprogramming Procedure*

For generation of iPSC lines, adult primary ear fibroblasts were reprogrammed with the vector pReproII-attB-shP53 that in the presence of Doxycycline (DOX) expresses Oct4, Sox2, cMyc, Klf4 and a shRNA against p53 (section 3.2.1, **Fig. 3.5**). The vectors pCAG-C31-bpa or pCAG-C31 OE-bpa were used for transient expression of C31 Integrase, mediating genomic integration of vector pReproII-attB-shP53 via attB sites. The Amaxa MEF Nucleofector Kit was used for nucleofection. For one nucleofection, 2-5x10^6 fibroblasts were trypsinized, pelleted, washed with PBS, pelleted again and resuspended in 100 µl Nucleofector solution. Upon addition of 5 µg of both vectors, cells were transferred to a cuvette and nucleofected in an Amaxa Nucleofector, set for protocol T020. The cells were plated on 1-2 gelatin-coated 10 cm dishes in ES F1 medium containing 1 µg/ml Doxycycline. On day 1 after nucleofection, cells were supplied with fresh ES F1 medium containing 1µg/ml DOX. On day 2, cells were split on MEF-coated 10 cm plates and on 8-well ibidi-slides using ES F1 medium with 1 µg/ml DOX or additionally 25 µg/ml Vitamin C (VitC) and 2 mM Valproic acid (VPA) (see sections 3.2.1 and 3.3.1). Per 10 cm dish ~8x10^5 cells were plated. For one well of an ibidi-slide 100-200 µl of this plating suspension were used. Medium was changed every 1-2 days, at day 4 the cells on the ibidi-slides were immunostained for Oct4. After d10, VPA and after colony picking, also VitC was omitted from the medium. Colonies were picked after 2-3 weeks and clones were expanded as described for ESC in section 6.4.1.1. At passage 5 after colony picking, also Dox was omitted from the culture medium. All generated iPSC lines were tested for Mycoplasma contamination as an in-house service by EUCOMM as described previously (Uphoff & Drexler 2002).

6.4.2.3 *Characterization of Generated iPSC Lines*

The generated iPSC lines were characterized in regard to expression of pluripotency markers by immunostainings and alkaline phosphatase (AP) staining and in regard to correct karyotype by chromosome counting. Immunostainings were performed as described in section 6.5.2, and AP staining was done with the AP Staining Kit (System Biosciences) following manufacturer's instructions. The workflow of karyotyping is given in the following section.

For karyotyping, cells of maximum passage number 10 were used. Cells were cultured on gelatin-coated plates in a highly proliferative state. Colcemid, which arrests dividing cells in the metaphase, was added to the medium to a final concentration of 0.2 µg/ml when cells where ~50% confluent. After incubation of 2-3 h, cells where washed twice with PBS, trypsinized, centrifuged and the pellet was resuspended in 0.5 ml medium. 10 ml of 75 mM KCl solution were added drop wise and the suspension was incubated for 10 min at RT. After centrifugation for 10 min at 1.100 rpm, the pellet was resuspended in 15 ml fixative (methanol : acetic acid, 3:1). After a second centrifugation for 10 min at 1.000 rpm the cells were resuspended in 2-3 ml fixative and stored at -20°C or processed directly. The cells were burst open and spread on an object slide in the same step by pipetting 20 µl of the cell suspension an object slide previously wetted with tab water. After drying for 24 h at RT, the samples were incubated for 1 h at RT with DAPI staining solution (0.2µg/ml DAPI in PBS). After washing with tab water, slides were dried and the chromosome numbers of 30 metaphases were determined for each iPSC line on a fluorescence microscope at 100x magnification.

6.4.3 Neuronal Differentiation Protocols

6.4.3.1 *Feeder-Free Culture of ESC and iPSC*

For the derivation of neurons from ESC and iPSC (together termed PSC), the interfering feeder cells were removed from the cultures by the following protocol, adapted from (Gaspard *et al.* 2009). Both on feeders and on gelatin, the PSC were kept in a highly proliferative state by culturing them in high density and splitting them every second day in ratios of 1:2-1:4. For removal of feeders, PSC were pelleted after trypsinization, resuspended in 10 ml medium and transferred to a gelatin-coated 10 cm dish. During an incubation of maximum 30 min, the attachment of the feeder cells could be monitored easily every 5-10 min, as feeder cells are 3-4 times bigger than PSC and attach before them. When most of the feeder cells had attached, the floating cells were removed carefully and split to gelatin-coated dishes. As in general the first passage to

gelatin and in special the described protocol results in the loss of some PSC, the splitting ratio was increased by factor 1.5-2. For example, cells were split 1:2 instead of 1:3. After a second passage in which residual feeder cells were removed in the same manner, PSC cultures were virtually feeder-free and could be submitted to neuronal differentiation protocols.

6.4.3.2 *Bibel & Barde Protocol*

The Bibel & Barde embryoid body-based protocol was adapted with slight modifications from (Bibel *et al.* 2004; Bibel *et al.* 2007). For neuronal cultures, 12-well plates were coated for Western Blot- and RNA-samples and 24-well plates containing a cover slip for immunostaining-samples. Cover slips were pre-treated by boiling in 30 ml 100% ethanol containing 1 drop HCl, followed by washing 3 times with 80% ethanol and subsequent drying. After autoclaving, the cover slips were transferred to the 24-wells with a sterile Pasteur pipette connected to a vacuum pump. For coating, a volume of 1 ml and 0.5 ml coating solution was used for a 12-well and a 24-well, respectively. First, plates were coated with Poly-DL-Ornithin (PORN) and incubated overnight. Then plates were washed thrice with H_2O and coated with Laminin (2 µg/ml Laminin in PBS) overnight. After washing once with PBS while avoiding Laminin to dry out, plates were ready for seeding of neuronal progenitors.

PSC cultured feeder-free on gelatin were trypsinized, pelleted, resuspended in EB-medium (Embryoid Body-medium) and counted. 4 x 10^6 PSC were plated as suspension culture on non-coated, non-adhesive 10 cm bacterial dishes (Greiner Bio-One) in 15 ml EB-medium. The medium was changed on day 2 after EB formation. Therefore, the EBs were collected in the center of the dish by slow circular movements and transferred to a 50 ml tube with a 25 ml pipette. After 3-5 min, the EBs had settled down so that the medium could be replaced with 15 ml fresh EB medium and the EB suspension could be transferred to a fresh dish. The medium was changed in the same way on day 4 and day 6, but was supplied with 5 µM retinoic acid. On day 8, the EBs were dissociated by washing once with PBS in a 50 ml tube as described for EB medium change and then trypsinized by incubation in TrypLE™ Express (Gibco) for 5 min at 37°C. Per dissociated EB dish 2-4 ml of TrypLE™ Express were used. After 5 to 10 min the EBs were dissociated to a single cell suspension by gentle pipetting and 10 ml EB medium were added. The cell suspension was passed through a 40 µm cell strainer (BD Falcon) and centrifuged at 1050 rpm for 4 min. The pelleted cells were resuspended in N2 medium and seeded on the PORN/Laminin-coated plates. For a 24-well 20 x 10^4 cells and for a 12-well 40 x 10^4 cells were used. 2 h and 24 h after the EB dissociation cells were supplied with fresh N2 medium. On day 2 after EB dissociation,

N2 medium was replaced with B27 medium. Subsequently half of the medium was replaced twice a week.

Note: In many EB dissociations the cells formed clumps, which was equivalent with the loss of a great deal of cells or had a negative impact on the quality of the resulting neuronal culture. This problem could be largely overcome by supplying the TrypLE™ Express freshly before use with 200 U/ml DNaseI (Roche).

6.4.3.3 *Gaspard & Vanderhaeghen Protocol*

The Gaspard & Vanderhaeghen monolayer protocol was performed as described in (Gaspard *et al.* 2009) with minor modifications. For neuronal cultures, 12-well plates were coated for Western Blot- and RNA-samples and 24-well plates containing a pre-treated cover slip (see 6.4.3.2) for immunostaining-samples. For coating, a volume of 1 ml and 0.5 ml coating solution was used for a 12-well and a 24-well, respectively. Plates were coated with PBS containing 38.5 µg/ml Poly-D-Lysine (PDL) and 3 µg/ml Laminin, incubated overnight and washed twice with PBS before usage.

PSC cultured feeder-free on gelatin were trypsinized, pelleted, resuspended in ES F1-medium to a single-cell suspension and counted. Cells were plated on gelatin-coated 6-wells using 5 – 80 x 10^4 cells per well. On d0, plates were washed once with PBS and supplied with DDM medium. Subsequently, medium was changed every second day until d10. On d4, d6 and d8 the DDM medium was supplied with 0.4 µg/ml cyclopamine, on d2 and d10, cyclopamine-free DDM medium was used. On d12, DDM medium was replaced with N2/B27 medium. After 1 h, cells were washed once with PBS and then trypsinized for 1-2 min. Cells were resuspended and again upon addition of PBS containing 10% FCS. After centrifugation, the cells were resuspended in N2/B27 medium, counted and seeded on the PDL/Laminin-coated plates. For a 24-well 20 x 10^4 cells and for a 12-well 40 x 10^4 cells were used. Subsequently N2/B27 medium was refreshed every second day.

6.4.3.4 *Treatments of Neuronal Cultures*

Neuronal cultures were treated with BSO (100 µM, 24 h) for generation of oxidative stress conditions and with okadaic acid (1 µM, 3 h) for phosphatase inhibition. See section 3.3.4 for more details.

6.4.4 Culture of Embryonic Primary Neurons

For the culture of embryonic primary neurons (E16.5) only 6-well plates coated with Poly-D-Lysine were used. Therefore the plates were incubated with Poly-D-Lysine overnight and were ready for using after being washed 3 times with water. Pregnant females were asphyxiated at dpc 16.5 and embryo-containing uteri were dissected and transferred to ice-cold dissection medium. Cortex and hippocampus were prepared and transferred to dissection medium. After washing the tissue with dissection medium, it was trypsinized for 15 min at 37°C followed by 3 washing steps with culture medium. Using a fire-polished Pasteur pipette, the tissue was triturated. The cell concentration of the suspension was determined by a Neubauer counting chamber and 5 x 10^5 cells were plated per 6-well. Half of the medium was replaced with fresh medium at day 3 after preparation, followed by weekly replacement of half of the medium.

6.5 Protein Analysis Methods

6.5.1 Western Blot

6.5.1.1 *Sample Preparation*

Samples for Western Blot analysis were kept on ice and lysed with buffer supplied with protease and phosphatase inhibitors to minimize protein degradation and dephosphorylation. Cultured cells to be analyzed by Western Blot were washed with PBS and then lysed directly on the dish by adding ice-cold Lämmli buffer; e.g. 100 µl for a 12-well. After an incubation of 0.5-1 min, the cell lysate was scratched off with a bent 200 µl pipette tip and transferred to an Eppendorf cup on ice. The lysate was incubated for 7 min at 99°C, chilled down on ice and spun down for 10 min at 13.000 rpm. The supernatant was used for measurement of protein concentration with the Pierce BCA Protein Assay Kit following manufacturer's instructions.

For preparation of adult brain samples, mice were asphyxiated with CO2, decapitated, and the brains were dissected by removal of bones and meninges. After homogenization in a glass homogenizer using typically 2 ml ice-cold Lämmli buffer for one hemisphere, the homogenate was incubated for 7 min at 99°C, chilled down on ice and spun down for 10 min at 13.000 rpm. The supernatant was used for measurement of protein concentration with the Pierce BCA Protein Assay Kit following manufacturer's instructions.

Embryonic brain samples were obtained from embryos prepared as described in section 6.4.4. Dissected brains were homogenized in 0.5 ml ice-cold Lämmli buffer and subsequently treated as described for adult brains.

6.5.1.2 *Western Blot Procedure*

For each sample, a volume corresponding to 10-50 µg of total protein was mixed with a volume of Lämmli loading buffer (1x), resulting in an end volume of 20 µl. After incubation for 5 min at 99°C and subsequent chilling on ice, samples were loaded on precast NuPAGE Bis-Tris gels of 10% and 4-12% polyacrylamide by Invitrogen. Gel run and blotting was performed on the Invitrogen system Xcell SureLock™ Mini-Cell. A standard gel run consisted of a 10% gel run for 1.5 h at 200 V using MES running buffer. When clearer separation of proteins between 50 and 70 kDa was required, protein samples were loaded on a 4-12% gel that was run with MOPS running buffer for 3-4 h at 200 V. To analyze varied sized Tau variants and isoforms as a single band, protein samples were loaded on a 10% gel that was run for 15 min at 200 V with MES running buffer. After the gel run, the proteins were transferred to a PVDF membrane that had been activated by incubation in 100% methanol for 1 min. This blotting process was performed for 1 h at 30 V in transfer buffer. Subsequently the membrane was blocked for 1 h in blocking solution (5 % skim milk in TBS-T in general, 5% BSA in TBS-T for phospho-antibodies) at RT and incubated with the primary antibody in blocking solution over night at 4°C. After washing 3 times for 5 min with TBS-T, the membrane was incubated with the secondary, horseradish-peroxidase-conjugated antibody in blocking solution for 1 h at RT followed by 3 washing steps of 5 min incubation in TBS-T. The membrane was moistened with ECL detection reagent, incubated for 1 min and then transferred to a film cassette. Chemiluminescent film was exposed for 5 sec to 15 min, according to signal intensity. Afterwards the exposed films were developed with a developing machine. Antibodies for Western Blot and their usage conditions are given in section 5.6.

When reprobing of the membrane with one or more antibodies was required, the membrane was stripped by mild or harsh stripping according to the affinity properties of the bound antibody. The protocol for mild stripping was: 3 x 5 min TBS-T, 2 x 10 min mild stripping buffer, 2 x 10 min PBS, 2 x 5 min TBS-T, with all steps executed at RT. The protocol for harsh stripping was: 4 x 5 min TBS-T at RT, 1.5 h incubation in harsh stripping buffer at 50°C, 6 x 5 min TBS-T at RT. After stripping, the membranes were blocked again and then reprobed as described above.

6.5.2 Immunocytochemistry

Neuronal cells for analysis by immunocytochemistry were grown in 24-wells on coated coverslips and washed once with PBS before fixation. After fixation with 4% PFA in PBS for 10 min, cells were washed thrice with PBS. Fixed cells were immunostained directly or stored at 4°C for up to 1 week before analysis. Incubation with the primary antibody in blocking solution overnight at 4°C was followed by 3 washing steps with PBS. Afterwards, a fluorescence dye labeled secondary antibody was incubated for 2 h at RT, followed by 3 washing steps with PBS. Cells were stained with the DNA-marker DAPI for 10 min at RT and washed once with PBS. The coverslips were mounted on Superfrost Plus slides with Aqua- Polymount mounting medium. After drying for 24 h at 4°C, the samples were ready for analysis on a Zeiss Axioplan 2 fluorescence microscope.

All other cell types were grown on ibidi-slides and immunostained as described for neuronal cells. Antibodies for immunocytochemistry and their usage conditions are given in section 5.6.

7 Zusammenfassung

Unser Verständnis von neurodegenerativen Krankheiten und die Entwicklung entsprechender Therapien werden stark eingeschränkt durch den Umstand, dass keine lebenden Nervenzellen von Patienten analysiert werden können und dass keine Modellsysteme zur Verfügung stehen, die alle Aspekte der sporadischen Krankheitsform rekapitulieren. Diese Einschränkungen könnten möglicherweise durch die Verwendung von Patienten-iPS-Zellen als unerschöpfliche Quelle zur Erzeugung analysierbarer Neurone überwunden werden. In den bereits publizierten Studien konnten jedoch nicht alle Krankheitsaspekte nachvollzogen werden, und es ist noch ungeklärt ob ein Symptom, das in einer späten Lebensphase auftritt, in „jungen“, von iPS Zellen abgeleiteten Nervenzellen rekapituliert werden kann.

Um zu analysieren, ob von pluripotenten Stammzellen abgeleitete Neurone dazu geeignet sind, das sich spät manifestierende Symptom der Tau Pathologie zu analysieren, habe ich in dieser Arbeit iPS Zelllinien aus den Tau Pathologie Mausmodellen 3xTg AD, Tau^{P301S} und hTau erzeugt. Darüber hinaus habe ich die transgene Tau^{P301S}/APP^{Swe}/Venus ES Zelllinie konstruiert. Alle vier Zelllinien wurden nach dem Bibel & Barde Protokoll in Neuronen differenziert. Obwohl somit laut der Originalpublikation eine homogene Population voll-ausgereifter kortikaler Neurone erzeugt wird, ergab eine detaillierte Analyse unerwarteter weise, dass die in dieser Arbeit aus pluripotenten Stammzellen abgeleiteten Nervenzellen unreif waren und sehr heterogene neuronale Identitäten aufwiesen. Die vier Promotor-Systeme wurden durch diese Eigenschaften in ihrer Aktivität stark beeinflusst und erwiesen sich somit als unterschiedlich gut dafür geeignet um Transgene in durch *in vitro* Differenzierung erzeugten Neuronen zu überexprimieren. Der humane MAPT Promoter erzeugte eine starke, und der Prionen Promotor eine mittlere bis schwache Transgen Expression. Der Thy1.2 Promotor war völlig inaktiv und der CAG Promotor erwies sich als ungeeignet aufgrund einer starken Abhängigkeit vom Integrationsort. Von Tau^{P301S} und hTau iPS Zellen abgeleitete Neurone wiesen weder unter Standardbedingungen noch unter oxidativem Stress eine Tau Hyperphosphorylierung auf. Die Tau^{P301S} und hTau Nervenzellen zeigten auch keine stärkere Reaktion auf die Phosphatasen Inhibierung als Wildtyp Zellen. Demnach spiegelte sich in den *in vitro* Neuronen nicht die Tau Pathologie Symptomatik wieder, die sich *in vivo* in den Gehirn-Neuronen der entsprechenden transgenen Maus manifestiert.

Insgesamt konnte ich in dieser Arbeit zeigen, dass Tau Pathologie in aus pluripotenten Stammzellen abgeleiteten Neuronen untersucht werden kann. Allerdings unterschieden sich die Nervenzellen, die aus Tau^{P301S} und hTau iPS Zellen abgeleitet wurden so stark von den Nervenzellen im Gehirn der transgenen Maus, dass sie unter

Standard-Bedingungen die Tau Pathologie nicht reproduzierten. Somit konnten in dieser Arbeit wertvolle Erkenntnisse darüber gewonnen werden, wie von pluripotenten Stammzellen abgeleitete Neurone dazu verwendet werden können um *in vitro* Modellsysteme von neurodegenerativen Krankheiten zu entwickeln und welche Probleme dabei noch überwunden werden müssen. Die Ergebnisse dieser Arbeit bringen eine aussagekräftige Analyse von neurodegenerativen Krankheiten in Neuronen, die aus Patienten-iPS-Zellen erzeugt wurden, demnach einen wichtigen Schritt näher. Somit stellt diese Arbeit einen Beitrag zum besseren Verständnis von neurodegenerativen Krankheiten und der Entwicklung entsprechender kausaler Therapien dar.

8 Appendix

8.1 Expression patterns of neuronal identity marker genes

Gene	Correlated neuronal identity	Reference
BF1	forebrain	Watanabe *et al.* 2005
Brn2	cortical layer 2-5	Hevner *et al.* 2003
ChAT	cholinergic neurons	Hartikka & Hefti 1988
Ctip2	cortical layer 5+6	Eiraku *et al.* 2008, Gaspard *et al.* 2009, Molyneaux et al. 2007
Cux2	cortical layer 2-4	Molyneaux *et al.* 2007
Emx1	dorsal forebrain	Nat & Dechant 2011
Emx2	dorsal forebrain	Hevner *et al.* 2006
En1	mid-hindbrain	Koch *et al.* 2009
Fezf2	cortical layer 5+6	Molyneaux *et al.* 2007
Gad1	GABAergic	Abe *et al.* 2003
Gli3	dorsal forebrain	Nat & Dechant 2011
Gsh2	ventral forebrain	Schuurmans & Guillemot 2002, Watanabe *et al.* 2005
HB9	motor neurons	Okada *et al.* 2004
Irx3	forebrain (caudal to ZLI) and midbrain	Echevarria *et al.* 2003
Isl1	ventral forebrain	Gaspard *et al.* 2009
Lhx6	ventral forebrain GABAergic neurons	Nat & Dechant 2011
Lhx8	ventral forebrain cholinergic neurons	Nat & Dechant 2011
Lim1	midbrain GABAergic neurons	Kala *et al.* 2009
Mash1	ventral forebrain	Nat & Dechant 2011
Nkx2.1	ventral forebrain	Gaspard *et al.* 2009, Watanabe *et al* . 2005
Nkx2.2	ventral forebrain	Gaspard *et al.* 2009, Koch *et al.* 2009
Nkx6.1	ventral hindbrain	Koch *et al.* 2009
Otx1	forebrain and midbrain	Gaspard *et al.* 2009, Watanabe *et al* . 2005
Otx2	forebrain and midbrain	Gaspard *et al.* 2009, Watanabe *et al* . 2005
Pax2	mid-hindbrain and spinal cord	Watanabe *et al.* 2005
Pax6	cortex and thalamus	Gaspard *et al.* 2009, Watanabe *et al* . 2005
Pax7	dorsal identity	Koch *et al.* 2009
Phox2b	hindbrain motor neurons	Okada *et al.* 2004, Koch *et al.* 2009
Satb2	cortical layer 2-5	Gaspard *et al.* 2009
Six3	forebrain (rostral to ZLI)	Echevarria *et al.* 2003, Nat & Dechant 2011
Tbr1	cortical layer 2/3+6	Molyneaux *et al.* 2007
TH	dopaminergic neurons	Kawasaki *et al.* 2000
VGlut1	glutamatergic neurons (mainly cortex and hippocampus)	Fremeau Jr *et al.* 2004, Wojcik *et al.* 2004
VGlut2	glutamatergic neurons (mainly thalamus and brainstem)	Fremeau Jr *et al.* 2004, Wojcik *et al.* 2004

8.2 Abbreviations

AD	Alzheimer's disease
AP	alkaline phosphatase
BSO	buthionine sulfoximine
CNS	central nervous system
DAPI	4′,6-Diamidin-2-phenylindol
DMSO	dimethyl sulfoxide
DOX	doxycycline
dpc	days post coitum
E15.5	15.5 days of embryonic age = 15.5 days post coitum
ESC	embryonic stem cells
fAD	familial Alzheimer's disease
FCS	fetal calf serum
GSH	glutathione
HCG	human chorionic gonadotropin
HDAC	histone deacetylase
Het	heterozygous
i.p.	intraperitoneal
ICM	inner cell mass
iPSC	induced pluripotent stem cells
IVF	*in vitro* fertilization
KCl	potassium chloride
kDa	kilodalton
LIF	leukemia inhibitory factor
MEF	mouse embryonic fibroblasts
MMC	mitomycin C
NDD	neurodegenerative disease
NSC	neural stem cells
OA	okadaic acid
P6	postnatal day 6
PCR	polymerase chain reaction
PDL	Poly-D-Lysine
PEF medium	primary adult ear fibroblast medium
PFA	paraformaldehyde
pHC	pHygro-CAG-CreER^{T2}-attB
PMSG	pregnant mare's serum gonadotropin
PORN	Poly-DL-Ornithin
PSC	pluripotent stem cells (iPSC and ESC)

pTAV	pNeo-CAG-Tau^{P301L}/APP^{swe}/Venus-attB
RA	retinoic acid
ROS	reactive oxygen species
rpm	revolutions per minute
RT	room temperature
RT-PCR	reverse transcription polymerase chain reaction
VitC	vitamin C
VPA	valproic acid
WT	wild type
ZLI	zona limitans intrathalamica

8.3 Danksagungen

Mein besonderer Dank richtet sich an Herrn Prof. Dr. Wolfgang Wurst für die Möglichkeit, meine Promotionsarbeit am Institut für Entwicklungsgenetik durchzuführen sowie für die hilfreichen Ideen zur Ausrichtung des Projekts.

Herrn Dr. Ralf Kühn möchte ich für die direkte Betreuung der Arbeit, die wissenschaftlichen Diskussionen und die praktischen Tipps und Tricks danken.

Den Mitgliedern meines Thesis-Committees, Prof. Dr. Wolfgang Wurst, Prof. Dr. Angelika Schnieke, Dr. Ralf Kühn und Dr. Nilima Prakash möchte ich für die hilfreichen Diskussionen und Anregungen danken.

Ein herzliches Dankeschön an alle Kollegen aus dem Labor und dem Institut für ihre Hilfsbereitschaft und die angenehme Atmosphäre. Sie werden die Zeit in schöner Erinnerung bleiben lassen.

Im Speziellen möchte ich danken:

- Adrianne Tasdemir, Susanne Weidemann, Regina Kneuttinger und Claudia Arndt für die technische Unterstützung bei der Blastozysten-Entnahme, der Betreuung meiner Mauslinien und verschiedenen anderen Projekten.
- Helga Grunert für die Bereitstellung der 3xTg AD Fibroblasten.
- Dem EUCOMM Team für die Durchführung der Mycoplasmen-PCRs.
- Benedikt Wefers, Miriam Homburg, Florian Giesert und Florian Meier für die Erklärung von Techniken.
- Dominik Paquet, Susanne Bourier, Irina Rodionova, Dr. Saida Zoubaa, Karina Kloos, Dr. Anna Pertek und AG Lie für die Bereitstellung von Material.
- Dr. Joel Schick für hilfreiche wissenschaftliche Diskussion.
- Dr. Michael Willem für hilfreiche wissenschaftliche Diskussion und Materialbereitstellung.
- Den Mitarbeitern des Oktogons und des C-Streifens für die Betreuung meiner Mauslinien.

9 References

Abe, Y., K. Kouyama, T. Tomita, Y. Tomita, N. Ban, M. Nawa, M. Matsuoka, T. Niikura, S. Aiso, Y. Kita, T. Iwatsubo and I. Nishimoto (2003). "Analysis of Neurons Created from Wild-Type and Alzheimer's Mutation Knock-In Embryonic Stem Cells by a Highly Efficient Differentiation Protocol " The Journal of Neuroscience **23** (24): 8513-8525

Abranches, E., M. Silva, L. Pradier, H. Schulz, O. Hummel, D. Henrique and E. Bekman (2009). "Neural Differentiation of Embryonic Stem Cells *In Vitro*: A Road Map to Neurogenesis in the Embryo." PLoS ONE **4** (7): e6286 EP.

ADI (2010). World Alzheimer Report 2010: The Global Economic Impact of Dementia. Alzheimer's Disease International (ADI).

Alonso, A. d. C., A. Mederlyova, M. Novak, I. Grundke-Iqbal and K. Iqbal (2004). "Promotion of Hyperphosphorylation by Frontotemporal Dementia Tau Mutations." Journal of Biological Chemistry **279** (33): 34873-34881.

Andorfer, C., Y. Kress, M. Espinoza, R. De Silva, K. L. Tucker, Y.-A. Barde, K. Duff and P. Davies (2003). "Hyperphosphorylation and aggregation of tau in mice expressing normal human tau isoforms." Journal of Neurochemistry **86** (3): 582-590.

Baas, P. W. and L. Qiang (2005). "Neuronal microtubules: when the MAP is the roadblock." Trends in Cell Biology **15** (4): 183-187.

Ballatore, C., V. M.-Y. Lee and J. Q. Trojanowski (2007). "Tau-mediated neurodegeneration in Alzheimer's disease and related disorders." Nat Rev Neurosci **8** (9): 663-672.

Batlle-Morera, L., A. Smith and J. Nichols (2008). "Parameters influencing derivation of embryonic stem cells from murine embryos." Genesis **46** (12): 758-767.

Bibel, M., J. Richter, E. Lacroix and Y.-A. Barde (2007). "Generation of a defined and uniform population of CNS progenitors and neurons from mouse embryonic stem cells." Nature Protocols **2** (5): 1034-1043.

Bibel, M., J. Richter, K. Schrenk, K. L. Tucker, V. Staiger, M. Korte, M. Goetz and Y.-A. Barde (2004). "Differentiation of mouse embryonic stem cells into a defined neuronal lineage." Nature Neuroscience **7** (9): 1003-1009.

Borchelt, D. R., J. Davis, M. Fischer, M. K. Lee, H. H. Slunt, T. Ratovitsky, J. Regard, N. G. Copeland, N. A. Jenkins, S. S. Sisodia and D. L. Price (1996). "A vector for expressing foreign genes in the brains and hearts of transgenic mice." Genetic Analysis: Biomolecular Engineering **13** (6): 159-163.

Borghese, L., D. Dolezalova, T. Opitz, S. Haupt, A. Leinhaas, B. Steinfarz, P. Koch, F. Edenhofer, A. Hampl and O. Brüstle (2010). "Inhibition of Notch Signaling in Human Embryonic Stem Cell-Derived Neural Stem Cells Delays G1/S Phase Transition and Accelerates Neuronal Differentiation In Vitro and In Vivo." STEM CELLS **28** (5): 955-964.

Brandt, R., M. Hundelt and N. Shahani (2005). "Tau alteration and neuronal degeneration in tauopathies: mechanisms and models." Biochimica et Biophysica Acta (BBA) - Molecular Basis of Disease **1739**: 331-354.

Buee, L., T. Bussiere, V. Buee-Scherrer, A. Delacourte and P. R. Hof (2000). "Tau protein isoforms, phosphorylation and role in neurodegenerative disorders." Brain Research Reviews **33** (1): 95-130.

Cai, C. and L. Grabel (2007). "Directing the differentiation of embryonic stem cells to neural stem cells." Dev. Dyn. **236** (12): 3255-3266.

Campisi, J. and F. d'Adda di Fagagna (2007). "Cellular senescence: when bad things happen to good cells." Nat Rev Mol Cell Biol **8** (9): 729-740.

Caroni, P. (1997). "Overexpression of growth-associated proteins in the neurons of adult transgenic mice." Journal of Neuroscience Methods **71** (1): 3-9.

Chambers, S. M., C. A. Fasano, E. P. Papapetrou, M. Tomishima, M. Sadelain and L. Studer (2009). "Highly efficient neural conversion of human ES and iPS cells by dual inhibition of SMAD signaling." Nat Biotech **27** (3): 275-280.

Chen, C.-m., J. Krohn, S. Bhattacharya and B. Davies (2011). "A Comparison of Exogenous Promoter Activity at the ROSA26 Locus Using a PhiC31 Integrase Mediated Cassette Exchange Approach in Mouse ES Cells." PLoS ONE **6** (8): e23376 EP.

Chen, H., Y.-C. Tung, B. Li, K. Iqbal and I. Grundke-Iqbal (2007). "Trophic factors counteract elevated FGF-2-induced inhibition of adult neurogenesis." Neurobiology of Aging **28** (8): 1148-1162.

Citron, M. (2010). "Alzheimer's disease: strategies for disease modification." Nat Rev Drug Discov **9** (5): 387-398.

Cohen, E. and A. Dillin (2008). "The insulin paradox: aging, proteotoxicity and neurodegeneration." Nat Rev Neurosci **9** (10): 759-767.

Crawford, T. Q. and H. Roelink (2007). "The Notch response inhibitor DAPT enhances neuronal differentiation in embryonic stem cell-derived embryoid bodies independently of sonic hedgehog signaling." Dev. Dyn. **236** (3): 886-892.

Devine, M. J., M. Ryten, P. Vodicka, A. J. Thomson, T. Burdon, H. Houlden, F. Cavaleri, M. Nagano, N. J. Drummond, J.-W. Taanman, A. H. Schapira, K. Gwinn, J. Hardy, P. A. Lewis and T. Kunath (2011). "Parkinson's disease induced pluripotent stem cells with triplication of the alpha-synuclein locus." Nat Commun **2**: 440.

Doetschman, T. (2009). Influence of Genetic Background on Genetically Engineered Mouse Phenotypes: Gene Knockout Protocols. W. Wurst and R. Kühn, Humana Press. **530:** 423-433.

Dolmetsch, R. and D. H. Geschwind (2011). "The Human Brain in a Dish: The Promise of iPSC-Derived Neurons." Cell **145** (6): 831-834.

Echevarria, D., C. Vieira, L. Gimeno and S. Martinez (2003). "Neuroepithelial secondary organizers and cell fate specification in the developing brain." Brain Research Reviews **43** (2): 179-191.

Eckermann, K., M.-M. Mocanu, I. Khlistunova, J. Biernat, A. Nissen, A. Hofmann, K. Schönig, H. Bujard, A. Haemisch, E. Mandelkow, L. Zhou, G. Rune and E.-M. Mandelkow (2007). "The beta-Propensity of Tau Determines Aggregation and Synaptic Loss in Inducible Mouse Models of Tauopathy." Journal of Biological Chemistry **282** (43): 31755-31765.

Eiraku, M., K. Watanabe, M. Matsuo-Takasaki, M. Kawada, S. Yonemura, M. Matsumura, T. Wataya, A. Nishiyama, K. Muguruma and Y. Sasai (2008). "Self-Organized Formation of Polarized Cortical Tissues from ESCs and Its Active Manipulation by Extrinsic Signals." Cell Stem Cell **3** (5): 519-532.

Esteban, M. A., T. Wang, B. Qin, J. Yang, D. Qin, J. Cai, W. Li, Z. Weng, J. Chen, S. Ni, K. Chen, Y. Li, X. Liu, J. Xu, S. Zhang, F. Li, W. He, K. Labuda, Y. Song, A. Peterbauer, S. Wolbank, H. Redl, M. Zhong, D. Cai, L. Zeng and D. Pei (2010). "Vitamin C Enhances the Generation of Mouse and Human Induced Pluripotent Stem Cells." Cell Stem Cell **6** (1): 71-79.

Feng, B., J.-H. Ng, J.-C. D. Heng and H.-H. Ng (2009). "Molecules that Promote or Enhance Reprogramming of Somatic Cells to Induced Pluripotent Stem Cells." Cell Stem Cell **4** (4): 301-312.

Fraga, M. F. and M. Esteller (2007). "Epigenetics and aging: the targets and the marks." Trends in Genetics **23** (8): 413-418.

Fremeau Jr, R. T., S. Voglmaier, R. P. Seal and R. H. Edwards (2004). "VGLUTs define subsets of excitatory neurons and suggest novel roles for glutamate." Trends in Neurosciences **27** (2): 98-103.

Gaspard, N., T. Bouschet, A. Herpoel, G. Naeije, J. van den Ameele and P. Vanderhaeghen (2009). "Generation of cortical neurons from mouse embryonic stem cells." Nat. Protocols **4** (10): 1454-1463.

Gaspard, N., T. Bouschet, R. Hourez, J. Dimidschstein, G. Naeije, J. van den Ameele, I. Espuny-Camacho, A. Herpoel, L. Passante, S. N. Schiffmann, A. Gaillard and P. Vanderhaeghen (2008). "An intrinsic mechanism of corticogenesis from embryonic stem cells." Nature **455** (7211): 351-357.

Gaulden, J. and J. F. Reiter (2008). "Neur-ons and neur-offs: regulators of neural induction in vertebrate embryos and embryonic stem cells." Human Molecular Genetics **17** (R1): R60-R66.

Germain, N. l., E. Banda and L. Grabel (2010). "Embryonic stem cell neurogenesis and neural specification." J. Cell. Biochem. **111** (3): 535-542.

Glaser, T. and O. Brüstle (2005). "Retinoic acid induction of ES-cell-derived neurons: the radial glia connection." Trends in Neurosciences **28** (8): 397-400.

Goedert, M. and R. Jakes (1990). "Expression of seperate isoforms of human tau protein: correlation with the tau pattern in brain and effects on tubulin polimerization." Embo J. **9**: 4225-4230.

Gonzalez, F., S. Boue and J. C. Belmonte (2011). "Methods for making induced pluripotent stem cells: reprogramming a la carte." Nat Rev Genet **12** (4): 231-242.

Götz, J., N. Deters, A. Doldissen, L. Bokhari, Y. Ke, A. Wiesner, N. Schonrock and L. M. Ittner (2007). "A Decade of Tau Transgenic Animal Models and Beyond." Brain Pathology **17** (1): 91-103.

Götz, J., A. Gladbach, L. Pennanen, J. van Eersel, A. Schild, D. David and L. M. Ittner (2010). "Animal models reveal role for tau phosphorylation in human disease." Biochimica et Biophysica Acta (BBA) - Molecular Basis of Disease **1802** (10): 860-871.

Götz, J. and L. M. Ittner (2008). "Animal models of Alzheimer's disease and frontotemporal dementia." Nat Rev Neurosci **9** (7): 532-544.

Haass, C. and D. J. Selkoe (2007). "Soluble protein oligomers in neurodegeneration: lessons from the Alzheimer's amyloid [beta]-peptide." Nat Rev Mol Cell Biol **8** (2): 101-112.

Hack, M. A., M. Sugimori, C. Lundberg, M. Nakafuku and M. Götz (2004). "Regionalization and fate specification in neurospheres: the role of Olig2 and Pax6." Molecular and Cellular Neuroscience **25** (4): 664-678.

Hall, G. F. and J. Yao (2005). "Modeling tauopathy: a range of complementary approaches." Biochimica et Biophysica Acta (BBA) - Molecular Basis of Disease **1739** (2): 224-239.

Han, S. S. W., L. A. Williams and K. C. Eggan (2011). "Constructing and Deconstructing Stem Cell Models of Neurological Disease." Neuron **70** (4): 626-644.

Hanna, J. H., K. Saha and R. Jaenisch (2010). "Pluripotency and Cellular Reprogramming: Facts, Hypotheses, Unresolved Issues." Cell **143** (4): 508-525.

Hartikka, J. and F. Hefti (1988). "Development of septal cholinergic neurons in culture: plating density and glial cells modulate effects of NGF on survival, fiber growth, and expression of transmitter-specific enzymes " The Journal of Neuroscience **8** (8): 2967-2985

Haupt, S., F. Edenhofer, M. Peitz, A. Leinhaas and O. Brüstle (2007). "Stage-Specific Conditional Mutagenesis in Mouse Embryonic Stem Cell-Derived Neural Cells and Postmitotic Neurons by Direct Delivery of Biologically Active Cre Recombinase." STEM CELLS **25** (1): 181-188.

Hayashi, K., S. M. C. d. S. Lopes, F. Tang and M. A. Surani (2008). "Dynamic Equilibrium and Heterogeneity of Mouse Pluripotent Stem Cells with Distinct Functional and Epigenetic States." Cell Stem Cell **3** (4): 391-401.

Hevner, R. F., R. A. M. Daza, J. L. R. Rubenstein, H. Stunnenberg, J. F. Olavarria and C. Englund (2003). "Beyond Laminar Fate: Toward a Molecular Classification of Cortical Projection/Pyramidal Neurons." Dev Neurosci **25** (2-4): 139-151.

Hevner, R. F., R. D. Hodge, R. A. M. Daza and C. Englund (2006). "Transcription factors in glutamatergic neurogenesis: Conserved programs in neocortex, cerebellum, and adult hippocampus." Neuroscience Research **55** (3): 223-233.

Hitoshi, N., Y. Ken-ichi and M. Jun-ichi (1991). "Efficient selection for high-expression transfectants with a novel eukaryotic vector." Gene **108** (2): 193-199.

Hu, B.-Y., J. P. Weick, J. Yu, L.-X. Ma, X.-Q. Zhang, J. A. Thomson and S.-C. Zhang (2010). "Neural differentiation of human induced pluripotent stem cells follows developmental principles but with variable potency." Proceedings of the National Academy of Sciences **107** (9): 4335-4340.

Huangfu, D., R. Maehr, W. Guo, A. Eijkelenboom, M. Snitow, A. E. Chen and D. A. Melton (2008). "Induction of pluripotent stem cells by defined factors is greatly improved by small-molecule compounds." Nat Biotech **26** (7): 795-797.

Hughes, E., Y. Qu, S. Genik, R. Lyons, C. Pacheco, A. Lieberman, L. Samuelson, I. Nasonkin, S. Camper, M. Van Keuren and T. Saunders (2007). Genetic variation in C57BL/6 ES cell lines and genetic instability in the Bruce4 C57BL/6 ES cell line. Mammalian Genome, Springer New York. **18:** 549-558.

Ideguchi, M., T. D. Palmer, L. D. Recht and J. M. Weimann (2010). "Murine Embryonic Stem Cell-Derived Pyramidal Neurons Integrate into the Cerebral Cortex and Appropriately Project Axons to Subcortical Targets." The Journal of Neuroscience **30** (3): 894-904.

Iovino, M., R. Patani, C. Watts, S. Chandran and M. G. Spillantini (2010). "Human Stem Cell-Derived Neurons: A System to Study Human Tau Function and Dysfunction." PLoS ONE **5** (11): e13947 EP -.

Iqbal, K., F. Liu, C.-X. Gong, A. Alonso and I. Grundke-Iqbal (2009). Mechanisms of tau-induced neurodegeneration. Acta Neuropathologica, Springer Berlin / Heidelberg. **118:** 53-69.

Israel, M. A., S. H. Yuan, C. Bardy, S. M. Reyna, Y. Mu, C. Herrera, M. P. Hefferan, S. Van Gorp, K. L. Nazor, F. S. Boscolo, C. T. Carson, L. C. Laurent, M. Marsala, F. H. Gage, A. M. Remes, E. H. Koo and L. S. B. Goldstein (2012). "Probing sporadic and familial Alzheimer/'s disease using induced pluripotent stem cells." Nature **advance online publication**.

Jin, M., N. Shepardson, T. Yang, G. Chen, D. Walsh and D. J. Selkoe (2011). "Soluble amyloid beta-protein dimers isolated from Alzheimer cortex directly induce Tau hyperphosphorylation and neuritic degeneration." Proceedings of the National Academy of Sciences **108** (14): 5819-5824.

Kala, K., M. Haugas, K. Lillevai, J. Guimera, W. Wurst, M. Salminen and J. Partanen (2009). "Gata2 is a tissue-specific post-mitotic selector gene for midbrain GABAergic neurons." Development **136** (2): 253-262.

Kampers, T., M. Pangalos, H. Geerts, H. Wiech and E. Mandelkow (1999). "Assembly of paired helical filaments from mouse tau: implications for the neurofibrillary pathology in transgenic mouse models for Alzheimer's disease." FEBS Letters **451** (1): 39-44.

Kawasaki, H., K. Mizuseki, S. Nishikawa, S. Kaneko, Y. Kuwana, S. Nakanishi, S.-I. Nishikawa and Y. Sasai (2000). "Induction of Midbrain Dopaminergic Neurons from ES Cells by Stromal Cells-Derived Inducing Activity." Neuron **28** (1): 31-40.

Kenyon, C. J. (2010). "The genetics of ageing." Nature **464** (7288): 504-512.

Kim, D.-S., J. Lee, J. Leem, Y. Huh, J. Kim, H.-S. Kim, I.-H. Park, G. Daley, D.-Y. Hwang and D.-W. Kim (2010a). Robust Enhancement of Neural Differentiation from Human ES and iPS Cells Regardless of their Innate Difference in Differentiation Propensity. Stem Cell Reviews and Reports, Humana Press Inc. **6:** 270-281.

Kim, K., A. Doi, B. Wen, K. Ng, R. Zhao, P. Cahan, J. Kim, M. J. Aryee, H. Ji, L. I. R. Ehrlich, A. Yabuuchi, A. Takeuchi, K. C. Cunniff, H. Hongguang, S. Mckinney-Freeman, O. Naveiras, T. J. Yoon, R. A. Irizarry, N. Jung, J. Seita, J. Hanna, P. Murakami, R. Jaenisch, R. Weissleder, S. H. Orkin, I. L. Weissman, A. P. Feinberg and G. Q. Daley (2010). "Epigenetic memory in induced pluripotent stem cells." **467** (7313): 285-290.

Kim, M., A. Habiba, J. M. Doherty, J. C. Mills, R. W. Mercer and J. E. Huettner (2009). "Regulation of mouse embryonic stem cell neural differentiation by retinoic acid." Developmental Biology **328** (2): 456-471.

Koch, P., T. Opitz, J. A. Steinbeck, J. Ladewig and O. Brüstle (2009). "A rosette-type, self-renewing human ES cell-derived neural stem cell with potential for in vitro instruction and synaptic integration." Proceedings of the National Academy of Sciences **106** (9): 3225-3230.

Liu, L., G.-Z. Luo, W. Yang, X. Zhao, Q. Zheng, Z. Lv, W. Li, H.-J. Wu, L. Wang, X.-J. Wang and Q. Zhou (2010). "Activation of the Imprinted Dlk1-Dio3 Region Correlates with Pluripotency Levels of Mouse Stem Cells." Journal of Biological Chemistry **285** (25): 19483-19490.

Liu, X., H. Wu, J. Loring, S. Hormuzdi, C. M. Disteche, P. Bornstein and R. Jaenisch (1997). "Trisomy eight in ES cells is a common potential problem in gene targeting and interferes with germ line transmission." Dev. Dyn. **209** (1): 85-91.

Louvi, A. and S. Artavanis-Tsakonas (2006). "Notch signalling in vertebrate neural development." Nat Rev Neurosci **7** (2): 93-102.

Maden, M. (2007). "Retinoic acid in the development, regeneration and maintenance of the nervous system." Nat Rev Neurosci **8** (10): 755-765.

Malatesta, P., M. A. Hack, E. Hartfuss, H. Kettenmann, W. Klinkert, F. Kirchhoff and M. Götz (2003). "Neuronal or Glial Progeny: Regional Differences in Radial Glia Fate." Neuron **37** (5): 751-764.

Mandelkow, E., M. Von Bergen, J. Biernat and E.-M. Mandelkow (2007). "Structural Principles of Tau and the Paired Helical Filaments of Alzheimer's Disease." Brain Pathology **17** (1): 83-90.

Marion, R. M., K. Strati, H. Li, M. Murga, R. Blanco, S. Ortega, O. Fernandez-Capetillo, M. Serrano and M. A. Blasco (2009). "A p53-mediated DNA damage response limits reprogramming to ensure iPS cell genomic integrity." Nature **460** (7259): 1149-1153.

Marques, S. C. F., C. R. Oliveira, C. M. F. Pereira and T. F. Outeiro (2011). "Epigenetics in neurodegeneration: A new layer of complexity." Progress in Neuro-Psychopharmacology and Biological Psychiatry **35** (2): 348-355.

Martinez, Y., F. Bena, S. Gimelli, D. Tirefort, M. Dubois-Dauphin, K.-H. Krause and O. Preynat-Seauve (2012). "Cellular diversity within embryonic stem cells: pluripotent clonal sublines show distinct differentiation potential." Journal of Cellular and Molecular Medicine **16** (3): 456-467.

Mattson, M. P. and T. Magnus (2006). "Ageing and neuronal vulnerability." Nature Reviews Neuroscience **7** (4): 278-294.

McGowan, E., J. Eriksen and M. Hutton (2006). "A decade of modeling Alzheimer's disease in transgenic mice." Trends in Genetics **22** (5): 281-289.

McMillan, P., E. Korvatska, P. Poorkaj, Z. Evstafjeva, L. Robinson, L. Greenup, J. Leverenz, G. D. Schellenberg and I. D'Souza (2008). "Tau isoform regulation is region- and cell-specific in mouse brain." J. Comp. Neurol. **511** (6): 788-803.

Ming, G.-L., O. Brüstle, A. Muotri, L. Studer, M. Wernig and K. M. Christian (2011). "Cellular Reprogramming: Recent Advances in Modeling Neurological Diseases." The Journal of Neuroscience **31** (45): 16070-16075.

Molyneaux, B. J., P. Arlotta, J. R. L. Menezes and J. D. Macklis (2007). "Neuronal subtype specification in the cerebral cortex." Nat Rev Neurosci **8** (6): 427-437.

Mori, T., K. Tanaka, A. Buffo, W. Wurst, R. Kühn and M. Götz (2006). "Inducible gene deletion in astroglia and radial glia: A valuable tool for functional and lineage analysis." Glia **54** (1): 21-34.

Morris, M., S. Maeda, K. Vossel and L. Mucke (2011). "The Many Faces of Tau." Neuron **70** (3): 410-426.

Nat, R. and G. Dechant (2011). "Milestones of Directed Differentiation of Mouse and Human Embryonic Stem Cells into Telencephalic Neurons Based on Neural Development In Vivo." Stem Cells and Development **20** (6): 947-958.

Nguyen, H. N., B. Byers, B. Cord, A. Shcheglovitov, J. Byrne, P. Gujar, K. Kee, B. Schüle, R. E. Dolmetsch, W. Langston, T. D. Palmer and R. R. Pera (2011). "LRRK2 Mutant iPSC-Derived DA Neurons Demonstrate Increased Susceptibility to Oxidative Stress." Cell Stem Cell **8** (3): 267-280.

Novak, A., C. Guo, W. Yang, A. Nagy and C. G. Lobe (2000). "Z/EG, a double reporter mouse line that expresses enhanced green fluorescent protein upon cre-mediated excision." Genesis **28** (3-4): 147-155.

Oddo, S., A. Caccamo, J. D. Shepherd, M. P. Murphy, T. E. Golde, R. Kayed, R. Metherate, M. P. Mattson, Y. Akbari and F. M. LaFerla (2003). "Triple-Transgenic Model of Alzheimer's Disease with Plaques and Tangles: Intracellular A beta and Synaptic Dysfunction." Neuron **39** (3): 409-421.

Okabe, M., M. Ikawa, K. Kominami, T. Nakanishi and Y. Nishimune (1997). "`Green mice' as a source of ubiquitous green cells." FEBS Letters **407** (3): 313-319.

Okada, Y., T. Shimazaki, G. Sobue and H. Okano (2004). "Retinoic-acid-concentration-dependent acquisition of neural cell identity during in vitro differentiation of mouse embryonic stem cells." Developmental Biology **275** (1): 124-142.

Osafune, K., L. Caron, M. Borowiak, R. J. Martinez, C. S. Fitz-Gerald, Y. Sato, C. A. Cowan, K. R. Chien and D. A. Melton (2008). "Marked differences in differentiation propensity among human embryonic stem cell lines." Nat Biotech **26** (3): 313-315.

Osborn, M. J., A. Panoskaltsis-Mortari, R. T. McElmurry, S. K. Bell, D. A. A. Vignali, M. D. Ryan, A. C. Wilber, R. S. McIvor, J. Tolar and B. R. Blazar (2005). "A picornaviral 2A-like Sequence-based Tricistronic Vector Allowing for High-level Therapeutic Gene Expression Coupled to a Dual-Reporter System." Mol Ther **12** (3): 569-574.

Pratt, T., L. Sharp, J. Nichols, D. J. Price and J. O. Mason (2000). "Embryonic Stem Cells and Transgenic Mice Ubiquitously Expressing a Tau-Tagged Green Fluorescent Protein." Developmental Biology **228** (1): 19-28.

Przedborski, S., M. Vila and V. Jackson-Lewis (2003). "Series Introduction: Neurodegeneration: What is it and where are we?" J Clin Invest **111** (1): 3-10.

Raymond, C. S. and P. Soriano (2007). "High-Efficiency FLP and C31 Site-Specific Recombination in Mammalian Cells." PLoS ONE **2** (1): e162 EP.

Sachlos, E. and D. T. Auguste (2008). "Embryoid body morphology influences diffusive transport of inductive biochemicals: A strategy for stem cell differentiation." Biomaterials **29** (34): 4471-4480.

Saha, K. and R. Jaenisch (2009). "Technical Challenges in Using Human Induced Pluripotent Stem Cells to Model Disease." Cell Stem Cell **5** (6): 584-595.

Saxena, S. and P. Caroni (2011). "Selective Neuronal Vulnerability in Neurodegenerative Diseases: from Stressor Thresholds to Degeneration." Neuron **71** (1): 35-48.

Schuurmans, C. and F. o. Guillemot (2002). "Molecular mechanisms underlying cell fate specification in the developing telencephalon." Current Opinion in Neurobiology **12** (1): 26-34.

Selkoe, D. J. (2011). "Resolving controversies on the path to Alzheimer's therapeutics." Nat Med **17** (9): 1060-1065.

Shao, C., L. Deng, O. Henegariu, L. Liang, N. Raikwar, A. Sahota, P. J. Stambrook and J. A. Tischfield (1999). "Mitotic recombination produces the majority of recessive fibroblast variants in heterozygous mice." Proceedings of the National Academy of Sciences **96** (16): 9230-9235.

Smith, I. F., B. Hitt, K. N. Green, S. Oddo and F. M. LaFerla (2005). "Enhanced caffeine-induced Ca2+ release in the 3xTg-AD mouse model of Alzheimer's disease." Journal of Neurochemistry **94** (6): 1711-1718.

Spires-Jones, T. L., W. H. Stoothoff, A. de Calignon, P. B. Jones and B. T. Hyman (2009). "Tau pathophysiology in neurodegeneration: a tangled issue." Trends in Neurosciences **32** (3): 150-159.

Stadtfeld, M., E. Apostolou, H. Akutsu, A. Fukuda, P. Follett, S. Natesan, T. Kono, T. Shioda and K. Hochedlinger (2010). "Aberrant silencing of imprinted genes on chromosome 12qF1 in mouse induced pluripotent stem cells." Nature **465** (7295): 175-181.

Su, B., X. Wang, H.-g. Lee, M. Tabaton, G. Perry, M. A. Smith and X. Zhu (2010). "Chronic oxidative stress causes increased tau phosphorylation in M17 neuroblastoma cells." Neuroscience Letters **468** (3): 267-271.

Takahashi, K. and S. Yamanaka (2006). "Induction of Pluripotent Stem Cells from Mouse Embryonic and Adult Fibroblast Cultures by Defined Factors." Cell **126** (4): 663-676.

Takuma, H., S. Arawaka and H. Mori (2003). "Isoforms changes of tau protein during development in various species." Developmental Brain Research **142** (2): 121-127.

Taylor, J. P., J. Hardy and K. H. Fischbeck (2002). "Toxic Proteins in Neurodegenerative Disease." Science **296** (5575): 1991-1995.

Thompson, E. M., E. Christians, M. G. Stinnakre and J. P. Renard (1994). "Scaffold attachment regions stimulate HSP70.1 expression in mouse preimplantation embryos but not in differentiated tissues." Molecular and Cellular Biology **14** (7): 4694-4703.

Thyagarajan, B., E. C. Olivares, R. P. Hollis, D. S. Ginsburg and M. P. Calos (2001). "Site-Specific Genomic Integration in Mammalian Cells Mediated by Phage phiC31 Integrase." Molecular and Cellular Biology **21** (12): 3926-3934.

Tremblay, P., E. Bouzamondo-Bernstein, C. Heinrich, S. B. Prusiner and S. J. DeArmond (2007). "Developmental expression of PrP in the post-implantation embryo." Brain Research **1139** (0): 60-67.

Uphoff, C. and H. Drexler (2002). Comparative PCR analysis for detection of mycoplasma infections in continuous cell lines. In Vitro Cellular & Developmental Biology - Animal, Springer Berlin / Heidelberg. **38:** 79-85.

Vale, C., E. Alonso, J. Rubiolo, M. Vieytes, F. LaFerla, L. Gimenez-Llort and L. Botana (2010). Profile for Amyloid-beta and Tau Expression in Primary Cortical Cultures from 3xTg-AD Mice. Cellular and Molecular Neurobiology, Springer Netherlands. **30:** 577-590.

Wallace, H., R. Ansell, J. Clark and J. McWhir (2000). "Pre-selection of integration sites imparts repeatable transgene expression." Nucleic Acids Research **28** (6): 1455-1464.

Wang, Y. P., J. Biernat, M. Pickhardt, E. Mandelkow and E.-M. Mandelkow (2007). "Stepwise proteolysis liberates tau fragments that nucleate the Alzheimer-like aggregation of full-length tau in a neuronal cell model." Proceedings of the National Academy of Sciences **104** (24): 10252-10257.

Watanabe, K., D. Kamiya, A. Nishiyama, T. Katayama, S. Nozaki, H. Kawasaki, Y. Watanabe, K. Mizuseki and Y. Sasai (2005). "Directed differentiation of telencephalic precursors from embryonic stem cells." Nat Neurosci **8** (3): 288-296.

Wernig, M., K. L. Tucker, V. Gornik, A. Schneiders, R. Buschwald, O. D. Wiestler, Y.-A. Barde and O. Brüstle (2002). "Tau EGFP embryonic stem cells: An efficient tool for neuronal lineage selection and transplantation." J. Neurosci. Res. **69** (6): 918-924.

Wichterle, H. and S. Przedborski (2010). "What can pluripotent stem cells teach us about neurodegenerative diseases." **13** (7): 800-804.

Wiktor-Brown, D. M., W. Olipitz, C. A. Hendricks, R. E. Rugo and B. P. Engelward (2008). "Tissue-specific differences in the accumulation of sequence rearrangements with age." DNA Repair **7** (5): 694-703.

Wojcik, S. M., J. S. Rhee, E. Herzog, A. Sigler, R. Jahn, S. Takamori, N. Brose and C. Rosenmund (2004). "An essential role for vesicular glutamate transporter 1 (VGLUT1) in postnatal development and control of quantal size." Proceedings of the National Academy of Sciences of the United States of America **101** (18): 7158-7163.

Ye, L., J. C. Chang, C. Lin, Z. Qi, J. Yu and Y. W. Kan (2010). "Generation of induced pluripotent stem cells using site-specific integration with phage integrase." Proceedings of the National Academy of Sciences **107** (45): 19467-19472.

Ying, Q.-L., J. Wray, J. Nichols, L. Batlle-Morera, B. Doble, J. Woodgett, P. Cohen and A. Smith (2008). "The ground state of embryonic stem cell self-renewal." **453** (7194): 519-523.

Yoshiyama, Y., M. Higuchi, B. Zhang, S.-M. Huang, N. Iwata, T. C. Saido, J. Maeda, T. Suhara, J. Q. Trojanowski and V. M.-Y. Lee (2007). "Synapse Loss and Microglial Activation Precede Tangles in a P301S Tauopathy Mouse Model." Neuron **53** (3): 337-351.

Zhang, J.-Q., X.-B. Yu, B.-F. Ma, W.-H. Yu, A.-X. Zhang, G. Huang, F. F. Mao, X.-M. Zhang, Z.-C. Wang, S.-N. Li, B. T. Lahn and A. P. Xiang (2006). "Neural differentiation of embryonic stem cells induced by conditioned medium from neural stem cell." NeuroReport **17** (10): 981-986.

Zhao, X.-y., W. Li, Z. Lv, L. Liu, M. Tong, T. Hai, J. Hao, C.-l. Guo, Q.-w. Ma, L. Wang, F. Zeng and Q. Zhou (2009). "iPS cells produce viable mice through tetraploid complementation." Nature **461** (7260): 86-90.

Zhao, Y., X. Yin, H. Qin, F. Zhu, H. Liu, W. Yang, Q. Zhang, C. Xiang, P. Hou, Z. Song, Y. Liu, J. Yong, P. Zhang, J. Cai, M. Liu, H. Li, Y. Li, X. Qu, K. Cui, W. Zhang, T. Xiang, Y. Wu, Y. Zhao, C. Liu, C. Yu, K. Yuan, J. Lou, M. Ding and H. Deng (2008). "Two Supporting Factors Greatly Improve the Efficiency of Human iPSC Generation." Cell Stem Cell **3** (5): 475-479.